NTNU – Trondheim
Norwegian University of
Science and Technology

Rate of Hydrate Inhibitor in Long Subsea Pipelines

Håkon Eidem Christiansen

Earth Sciences and Petroleum Engineering
Submission date: June 2012
Supervisor: Jon Steinar Gudmundsson, IPT

Norwegian University of Science and Technology
Department of Petroleum Engineering and Applied Geophysics

Abstract

This thesis is divided into several parts. The first part deals with hydrate theory and where hydrates form in the gas-and oil-dominated systems. A review of how hydrate plugs is formed and a method for removing hydrate plugs safely is also included.

Simplified HYSYS models of the upstream part of Ormen Lange and Snøhvit gas fields on the Norwegian Continental Shelf constituted the basis for answering the second part of the task. Data from private conversations, reports, slide presentations, and other documents were used to create the models.

Based on the models, calculations were made on the injection rate and storage capacity of mono ethylene glycol (MEG) on Ormen Lange and Snøhvit. The same models and calculation methods were used to determine injection rates for both methanol (MeOH) and MEG on the same fields. All the results combined with literature were then used to compare the inhibitors' properties to determine which one was best suited for use on the current fields. During rate calculations several cases were made to determine which factors have the greatest impact on the amount of inhibitor needed.

It was found that hydrates are formed on the pipe wall in gas dominated pipelines, while they are formed in the bulk flow in oil-dominated systems. The heat transfer coefficient and the seabed temperature have great influence on the amount of inhibitor needed. MEG-rate and storage capacity on Snøhvit are very large. Ormen Lange needs a larger inhibitor injection rate than Snøhvit. MEG is better suited than MeOH as an inhibitor of long-distance multi-phase tie-backs such as Ormen Lange and Snøhvit.

Sammendrag

Denne masteroppgaven er delt opp i flere deler. Der den første delen tar for seg hydratteori og hvor hydrater dannes i gass/ og oljedominerte systemer. Det er også inkludert en gjennomgang om hvordan hydratplugger dannes og en metode for å fjerne hydratplugger trygt.

Forenklede HYSYS-modeller av oppstrøms Ormen Lange og Snøhvit utgjorde grunnlaget for besvarelsen av den andre delen av oppgaven. Data fra lysarkpresentasjoner, private samtaler, rapporter og andre dokument ble brukt for å lage mest mulig virkelighetstro modeller.

Ut ifra modellene ble det gjort beregninger på injeksjonsraten og largringskapasiteten av monoetylenglykol (MEG) på Ormen Lange og Snøhvit. De samme modellene og beregningsmetodene ble brukt til å finne injeksjonsrater for både metanol (MeOH) og MEG. Alle resultatene kombinert med litteratur ble så brukt til å sammenligne inhibitorene for å finne ut hvilken som passet best til bruk på gjeldene felt. Under rate beregningene ble det laget flere caser for å finne ut hvilke faktorer som har størst påvirkning for mengden inhibitor som trengs.

Det ble funnet ut at hydrater dannes på rørveggen i gassdominerte rørledninger, mens de dannes i bulk strømingen i oljedominerte systemer. Varmeoverføringskoeffisenten og havbunnstemperaturen har stor påvirkning på mengden inhibitor som trengs. MEG-raten og lagringskapasiteten på Snøhvit er veldig stor. Ormen Lange trenger større inhibitor injeksjonsrate enn Snøhvit. MEG egner seg bedre som inhibitor på langdistanse multifasen tie-backs som Ormen Lange og Snøhvit.

Acknowledgement

Trondheim, June, 2012.

The topic of this Master thesis was developed in collaboration with Professor Jon Steinar Gudmundsson at the Department of Petroleum Engineering and Applied Geophysics at NTNU.

I would like to thank Professor Jon Steinar Gudmundsson, for his help and guidance throughout the process. His commitment and contribution has been a good help for performing this thesis.

I would also like to thank Baard Kaasa, Morten Svenning, and Xiaoyun Li at Statoil for providing me with helpful data.

The author of this work hereby declares that the work in this thesis is made independently and in accordance to the rules set down by Examination regulations at the Norwegian University of Science and Technology (NTNU), Trondheim.

Table of content

1 Introduction 1

2 Introduction to Hydrates 3

2.1 Introduction to the Hydrate Chapter 3

2.2 Water and Hydrogen Bonds 4

2.3 Host and Guest Molecules 5

2.4 Hydrate Forming Conditions 6

2.5 Hydrate Types and Formers 7

2.6 Chemical Properties of Potential Guest Molecules 9

2.7 Liquid Hydrate Formers 9

2.8 Hydrates and Natural Gas Mixtures 10

2.9 Azeotropy 11

3 Inhibitors 13

4 Locations of Hydrate Formation 15

4.1 Hydrate Plugs in Industrial Equipment 15

4.2 Case Study: 1 16

4.3 Oil Dominated Pipelines 17

4.4 Gas Dominated Pipelines 18

5 Hydrate Prevention 19

5.1 How to Prevent Hydrate Plug Formations 19

5.2 Case Study: 2 19

6 Hydrate Plug Removal 21

6.1 Review of a Hydrate Plug Remediation Process 21

6.2 Recommended Actions 24

6.3 Safety and Hydrate Plug Removal 24

6.4 Case Study: 3 25
6.5 Summary 26
7 HYSYS 27
7.1 HYSYS Process Simulator 27
7.2 Introduction to the Model 27
7.3 The Ormen Lange Model 28
7.4 The Snøhvit Model 31
8 Calculations 33
8.1 Procedure for Calculating Inhibitor Injection 35
8.2 Hydrate Calculations Ormen Lange 42
8.3 Hydrate Calculation Snøhvit 46
9 Methanol versus MEG 51
9.1 Comparison Based on Literature 52
9.2 Comparison Based on Own Calculations 54
10 Discussion 57
11 Conclusion 61
12 Nomenclature 63
13 References 65
14 Tables 71
15 Figures 87
16 Equations 107

List of Tables

TABLE 1: COMPARISON OF TYPE 1, TYPE 2 AND TYPE H HYDRATES (CARROLL, 2003) 71
TABLE 2: HYDRATE FORMING CONDITIONS METHANE 72
TABLE 3: PHYSICAL PROPERTIES AND HYDRATE FORMATION OF SOME COMMON NATURAL GAS COMPONENTS (CARROLL, 2003) 73
TABLE 4: PROPERTIES OF COMMON CHEMICAL INHIBITORS (CARROLL, 2003) 73
TABLE 5: ORMEN LANGE WELL TEMPERATURE PROFILE 74
TABLE 6: GAS COMPOSITION ORMEN LANGE (VALBERG, 2005) 74
TABLE 7: HYSYS MODEL DATA 75
TABLE 8: HYSYS MODEL DATA REFERENCE TABLE 76
TABLE 9: PIPELINE DIAMETER TABLE 77
TABLE 10: SNØHVIT WELL TEMPERATURE PROFILE 78
TABLE 11: GAS COMPOSITION SNØHVIT (GUDMUNDSSON, 2012) 78
TABLE 12: THE SUMMARY OF THE MOST ACCURATE METHOD 79
TABLE 13: ORMEN LANGE CASE COMPARISON 79
TABLE 14: WHY HYDRATE PLUGS MAY FORM, AND WHERE 79
TABLE 15: INFLECTION POINT DATA FROM BASE CASE SNØHVIT 79
TABLE 16: SNØHVIT CASE COMPARISON 80
TABLE 17: SNØHVIT BASE CASE EXTREME POINT WITH SF 80
TABLE 18: EFFECTS OF INHIBITOR INJECTION ON OUTLET TEMPERATURE 81
TABLE 19: UPSTREAM FIELD VOLUME INHIBITOR SNØHVIT 82
TABLE 20: CALCULATED VALUES OF DEPRESSION OF HYDRATE POINT (°C) FOR VARIOUS THERMODYNAMIC INHIBITORS (KELLAND, 2000) 83
TABLE 21: ROUGH COSTS FOR COMMON THERMODYNAMIC INHIBITORS (BRUSTAD, ET AL., 2005) 83
TABLE 22: SUMMARY OF INHIBITOR COMPARISON FROM ORMEN LANGE AND SNØHVIT 84
TABLE 23: SNØHVIT 60 WT% MEG 84
TABLE 24: SNØHVIT BASE CASE INCLUDING SAFETY FACTOR=5% 85
TABLE 25: SNØHVIT BASE CASE 85
TABLE 26: ORMEN LANGE SHUT-IN CASE (60 WT% MEG) 85
TABLE 27: ORMEN LANGE BASE CASE INCLUDING SAFETY FACTOR=5% 86
TABLE 28: ORMEN LANGE BASE CASE 86
TABLE 29 86

List of Figures

FIGURE 1: THE SHAPE OF THE WATER MOLECULE 87
FIGURE 2: COMPARISON OF GUEST SIZE, HYDRATE TYPE, AND CAVITIES OCCUPIED FOR VARIOUS HYDRATE FORMERS (MODIFIED FROM THE ORIGINAL BY (VON STACKELBERG, 1949)) 88
FIGURE 3: HYDRATE LOCI FOR SEVERAL COMPOUNDS FOUND IN NATURAL GAS (CARROLL, 2003) 89
FIGURE 4: HYDRATE FORMATION MAP FOR A MIXTURE OF ETHANE AND PROPANE (BASE ON HOLDER AND HANDS)(HOLDER & HAND, 1982) 90
FIGURE 5: EXPANSION OF TWO GASES INTO HYDRATE FORMATION REGION (SLOAN & KOH, 2008) 91
FIGURE 6: 1ST LAW OF THERMODYNAMICS (SLOAN & KOH, 2008) 91
FIGURE 7: CONCEPTUAL FIGURE OF HYDRATE FORMATION IN AN OIL-DOMINATED SYSTEM (SLOAN & KOH, 2008) 92
FIGURE 8: HYDRATE BLOCKAGE FORMATION (BOTTOM) AND CORRESPONDING PRESSURE BUILDUP (TOP) IN A GAS-DOMINATED PIPELINE (SLOAN & KOH, 2008) 92
FIGURE 9: PRESSURE DISSOCIATION (SLOAN & KOH, 2008) 93
FIGURE 10: RADIAL DISSOCIATION OF HYDRATE PLUGS IN THREE EXPERIMENTS (PETERS, 1999) 93
FIGURE 11: TWO WAYS A HYDRATE PLUG CAN RUPTURE A PIPE (SLOAN & KOH, 2008) 94
FIGURE 12: ORMEN LANGE FLOWLINE ELEVATION PROFILE (BIØRNSTAD, 2006) 94
FIGURE 13: RESERVOIR GAS 95
FIGURE 14: ORMEN LANGE WELL 95
FIGURE 15: INFLOW PERFORMANCE AND TUBING PERFORMANCE 96
FIGURE 16: LIQUID LOADING VS RATE AND PRODUCTION RATE 96
FIGURE 17: ORMEN LANGE WELL ELEVATION PROFILE 97
FIGURE 18: NETWORK HIERARCHY, SNØHVIT FIELD DEVELOPMENT (PETTERSEN, 2011) 97
FIGURE 19: SNØHVIT FLOWLINE ELEVATION PROFILE 98
FIGURE 20: WATER CONTENT CHART (HESKESTAD, 2004) 99
FIGURE 21: ORMEN LANGE NORMAL OPERATION U=20 100
FIGURE 22: ORMEN LANGE CASE COMPARISON 100
FIGURE 23: ORMEN LANGE SHUT-IN TEMPERATURE DEVELOPMENT 101
FIGURE 24: ORMEN LANGE EXTREME CASE 101
FIGURE 25: ITERATION PROCESS FOR FINDING THE WELL HEAD PRESSURE AT SHUT-IN CONDITIONS 102
FIGURE 26: MOST LIKELY HYDRATE FORMATION LOCATIONS 103
FIGURE 27: SNØHVIT NORMAL OPERATION 103
FIGURE 28: SNØHVIT CASE COMPARISON 104
FIGURE 29: SNØHVIT HYDRATE CURVES 104
FIGURE 30: MEOH/MEG CORRELATION 105

List of Equations

EQUATION 1: INFLOW PRESSURE EQUATION 107
EQUATION 2 107
EQUATION 3 107
EQUATION 4 107
EQUATION 5 107
EQUATION 6: SHUT-IN TEMPERATURE EQUATION (GUDMUNDSSON, 2011) 107
EQUATION 7: GAS WELL PRESSURE EQUATION 107
EQUATION 8: GAS WELL PRESSURE EQUATION (WELL PROPERTIES) 107
EQUATION 9: GAS WELL PRESSURE EQUATION (GAS PROPERTIES) 107
EQUATION 10: PUMP EFFECT EQUATION 107

1 Introduction

Hydrates have long been the biggest problem in flow assurance for the petroleum industry (Macintosh, 2000). And as new resources are often smaller and located in areas with more extreme conditions, hydrates remain a major obstacle for the further supply of hydrocarbons.

Hydrate plugs can block the production systems. The consequences of this can be both economic and safety-related. In extreme cases the owners may be forced to abandon the pipeline, and perhaps close down production. Hydrates may also cause danger to human lifes and the environment.

It is very useful for production engineers that shall design production systems to be able to predict whether hydrates could be a problem. And if conditions are favorable for hydrate formation, the engineer must be able to calculate the amount of inhibitor required to remove the hydrate threat.

It is also interesting to identify which factors have the greatest impact on the amount of inhibitor needed to prevent hydrate formation. It is mainly the combination of temperature and pressure with water that allows for hydrate formation. And it is the factors that affect this composition that will be identified in this task.

There have been written many books on the subject of hydrates. Among them are Clathrate Hydrates of Natural Gases (Sloan & Koh, 2008), and Natural Gas Hydrates (Carroll, 2003). Sloan has also written a book on the inhibition of systems to prevent hydrate formation called Hydrate Engineering (Sloan, 2000). There have also been conducted studies with focus on MeOH and MEG as inhibitors (Brustad, et al., 2005).

This thesis focuses on hydrates and thermodynamic inhibitors. First there is a theory section that deals with the technical details of the hydrates. Details such as the composition of hydrates, the hydrate structure, types of hydrates, at which conditions they are formed, how and where they are formed. At the end of the theory section I get into the various inhibitors that exist. And then there is a quick review of plug formation, and methods to remove hydrate plugs.

The problem is divided into several parts. One of the tasks is to describe two situations in which hydrates are formed in a pipeline. One is in a pipeline where water condenses out, and the other is an oil pipeline with associate gas and a water cut.

The other sub-task is to create HYSYS models of Ormen Lange and Snøhvit. The models will be used to obtain data that can be used to calculate the injection rate and storage capacity of MEG. Then the models are extended to both MeOH and MEG injection. These two inhibitors are compared, and results from HYSYS and the literature are used to determine the advantages and disadvantages of each one.

On the matter of the thesis' task, it was not specified any specific problem statements in cooperation with my professor. Only a general description of a possible task was formulated to get me started. That is why this thesis may not cover all of the subjects declared in the problem statement.

2 Introduction to Hydrates

2.1 Introduction to the Hydrate Chapter

In the oil and gas industry hydrates are comprised of small molecules and water. Hydrates are crystalline solid compounds formed from water and smaller molecules. They are a subset of compounds known as clathrates or inclusion compounds. A clathrate is a compound where a molecule of one substance is inclosed in a structure built from molecules of another substance.

Sir Humphrey Davy is credited for discovering hydrates; chlorine in the early 19th century. Faraday, his assistant, reported the composition of chlorine hydrate in 1823 (Carroll, 2003). Hydrates became an intellectual curiosity in the 18 hundreds, and a lot of work was done on the subject.

In this report natural gas means reservoir gas. It consists mainly of light alkanes, hydrocarbons, like methane, ethane, propane, butane and so on. Other components often found in the natural gas mixture are non-hydrocarbons like carbon dioxide, hydrogen, nitrogen, sulfur and water.

Natural gas is a valuable resource and is mostly used for heating, cooking and electric power production. Because of high focus on the emissions of green house gases like carbon dioxide, it has become more common to use natural gas as fuel in cars, buses and boats/ships. It burns much cleaner than oil, releasing less carbon dioxide, nitrogen and sulfur into the atmosphere. Natural gas is also being made in to consumer products like methanol and plastic in chemical plants.

Oil and gas companies have to add or remove components to/from their natural gas to meet the sales specifications. Natural gas that contains sulfur is considered sour. To get the right specifications the gas can be treated in a refinery or mixed with another type of natural gas. To make sure that the costumers are getting quality gas they have certain criteria that have to be met. There are limitations on the amount of impurity it can contain, heating value, hydrocarbon dewpoint and more. Water is considered an impurity. It is also the main building block in hydrates. That is why the gas has to be properly processed and dried prior to export.

2.2 Water and Hydrogen Bonds

When natural gas and free water together are subjected to high pressures and relatively low temperatures hydrates may form. In the early days of the gas industry this was not known. Not until the natural gas expansion in the 20th century, when the gas was transported under high pressures that the first experience with hydrates in pipes and processing equipment was made. Hammerschmidt demonstrated in the 1930s that the ice found blocking pipes actually was gas hydrates. His argument was that the temperature was not sufficiently low for water to freeze (Carroll, 2003).

"*In the petroleum industry, the term hydrate is reserved for substances that are usually gaseous at room temperature. These include methane, ethane, carbon dioxide, and hydrogen sulfide. This leads to the term gas hydrates and to one of the popular misconceptions regarding these compounds. It is commonly believed that non-aqueous liquids do not form hydrates. However, liquids may also form hydrates. An example of a compound that is liquid at room conditions, yet forms a hydrate, is dichlorodifluoromethane* (Freon 12)."(Carroll, 2003).

It is the structure of the water molecule that creates the foundation for hydrate formation. The water molecule consists of one oxygen atom and two hydrogen atoms. It is polar and has four electrons, but only two of these are shared with the hydrogen atoms. Consider a point in the room with four lines sticking straight out of it. The angle between each line would be 109.5°, like the case is for the methane molecule, CH4. The water molecule has two free electrons on the opposite side of where the hydrogen atoms are connected. And the angle between the hydrogen atoms is only 104.5°.

The induced charges on the water molecule that result in hydrogen bonding and the angle between the hydrogen atoms are showed in Figure 1 (Carroll, 2003). This can be explained in a simplified way as that the pair of free electrons repulses each other and the hydrogen atoms with a larger force than the hydrogen atoms repulse each other. The free electrons induce a negative charge on the oxygen molecule and a weak positive charge on the hydrogen atoms (Granger, u.d.).

The hydrogen atoms share electrons with the oxygen atoms. These binding forces are very strong and are called covalent bonds. Since the water molecule is polar, the negative side

will be attracted to another water molecules positive side. This causes each of the hydrogen atoms to attract a new water molecule. These bonds are called hydrogen bonds and are stronger than van der Waals forces, which connects regular un-polar molecules.

Hydrogen bonds are electro static forces. They are strong and explain the special properties of water compared to other molecules that consist of elements from the same place in the periodic table. Elements that possess similar properties are organized together in the periodic table. The water molecule stands out from the other with its high boiling temperature. It also requires much more energy to break up the net of water molecules when the water is boiled.

Another special feature of water is that it expands when it turn into a solid. When the water molecules come together they form a hexagonal structure. With lower temperature the movement of the water molecules stops and the water freezes to form symmetrical ice crystals. Water molecules form lattices when water freezes, and this increases the distance between each molecule. The water expands when it freezes, and is the reason why ice has lower density than liquid water.

2.3 Host and Guest Molecules

Hydrogen bonds are the reason that water can form hydrates. Hydrogen bonds cause the water molecules to organize in specific patterns. The presence of some particulate compounds can cause these structures to stabilize and cause solids to precipitate.

The water molecules are often referred to as the host molecules, while the stabilizing compounds are called guest molecules. The guest molecules are in addition frequently called the forming -molecule. The water molecules form three dimensional cages with complex geometry and room for guest molecules.

Van der Waals forces between the guest molecule and the water molecules are thought to stabilize the cage. Van der Waals forces are attraction between molecules caused by other things than electro static forces. The guest molecule is not tied to the host molecules, and has space to rotate freely inside the cage. That is why these components are best described as solid-solution.

2.4 Hydrate Forming Conditions

The formation of hydrates requires the combination of three critical criteria; (1) the right combination of pressure and temperature (High pressure and low temperature), (2) the presence of hydrate formers (for example methane, ethane and carbon dioxide), (3) and the presence of a sufficient amount water (not too much, not too little).

The hydrate formation temperature is very dependent on the gas composition, but is larger than the freezing point of water, 0°C. Due to the requirement mentioned above it may seem trivial to avoid hydrate formation. Remove one of them and hydrates will not form, but in reality it is not that easy. The hydrate formers are the gas that the energy companies are after. The focus in the natural gas industry is therefore on the other two conditions.

Two phenomena that enhance the growth of hydrates are turbulence and nucleation sites. Two factors play an important role affecting the turbulence, high velocity and agitation. Hydrates forms more rapidly in places of high velocity like choke valves. The diameter reduction in the valve causes the gas to accelerate. Mixing of water and hydro carbons in flowlines, process vessels, heat exchangers, etc, increase the rate of hydrate formation.

Nucleation sites can in general terms be described as a point where phase transition is favored. In the case of hydrates; the formation of a solid from a fluid phase. An example of a nucleation site is the potatoes that are fried in a deep fryer to make French fries. Before the potatoes are put into the hot oil nothing happens. But as they are lowered into the fryer, the oil forcefully boils because the potatoes provide an excellent nucleation site.

Fine nucleation sites for hydrate formation comprise of an imperfection in the flowline, a weld spot, or a flowline fitting (elbow, tee, valve, etc.). In addition silt, scale and sand all make good nucleation sites. The presence of free water increases hydrate formation. The gas-water transition provides a good nucleation site as well. The points above are not required for hydrate formation, but will increase speed of the establishment.

The accumulation of hydrates does not necessarily occur at the same place as they are formed. Hydrates may be carried along with liquid phase. They tend to accumulate at same locations as the liquid. A typical place is at the bottom of a v-shapes pipe. This can block the

pipe and cause damage to equipment and endanger the safety of humans and the environment.

A way to avoid formation of hydrate plugs is to inject an inhibitor to lower the hydrate formation temperature. Another way is to pig the flowline to remove deposits, like hydrates, wax, scale, salt, etc., and liquid accumulations. A pig, flowline investigation gauge, is a cylinder shaped tool that hugs the wall inside the flowline. Its outer diameter is almost the same as the flowlines inner diameter. The pig is transported through the flowline from high to low pressure where it cleans the pipe along the way. Modern pigs are advanced diagnostic tools. It is important not to let the pig intervals become too large. The deposits in deposits accumulate over time, and may become too large for the pig to transport. The result is a stuck pig, and this may lead to the abandonment of the flowline.

A reservoir gas will always be saturated with water vapor. Pressure and temperature changes in the production system may cause water to condensate. When producing at a high rate or from an aging field, it is common to produce formation water together with the gas. Water is often involved in processing of natural gas. The process to sweeten natural gas (that is to remove carbon dioxide and hydrogen sulfide, known as the “acid gases”) often employs aqueous solutions. The resulting sweet gas is then saturated with water. There are a lot of different ways to dry the gas, but they will not be further reviewed her.

2.5 Hydrate Types and Formers

There are three different types of hydrates; type 1, type 2 and type H. They are classified by how the water molecules are arranged in the lattice/crystal. In the oil and gas industry it is most common to see hydrates of type 1 and Type 2. Table 1 shows a comparison of the different hydrate types. The focus of this chapter is going to be on type 1 and type 2 hydrates.

The simplest hydrate structure is Type 1. It is composed of two types of cages: (1) Dodecahedron, a twelve sided polyhedron where each surface is a regular pentagon, and (2) Tetrakaidecahedron, a fourteen sided polyhedron with twelve pentagonal surfaces and two hexagonal surfaces. The dodecahedron cages are often referred to as the small cages because they are smaller than the tetrakaidecahedron cages. For the opposite reason the tetrakaidecahedron cages are called the big cages.

Type 1 hydrates consist of 46 water molecules. The theoretical formula for the number of water molecules in a type 1 hydrate is X×5 3/4 H2O, where X is the guest molecule (Carroll, 2003). Hydrates are non-stoichiometric, that means that not all the cages need to have a guest molecule to make the hydrate stabile. The saturation amount is a function of pressure and temperature. This means that the real hydrate composition is not equal to the theoretical. Methane, ethane, carbon dioxide and hydrogen sulfide are common type 1 formers. With the exception of ethane, which can only occupy large cages, the other ones can occupy both cages.

The structure of type 2 hydrates is much more complex than of that of type 1. It consists of two cage types: (1) Dodacahedron and (2) Hexakaidecahedron, a sixteen sided polyhedron with twelve pentagonal sides and four hexagonal sides. Type 2 consists of 136 water molecules. The theoretical formula for the maximum number of water molecules is X×5 2/3 H2O. If only the large cages are filled then the formula is X×17 H2O. Nor this hydrate type is stoichiometric, and the real composition will deviate from the theoretical. Common type 2 formers are isobutane, nitrogen and propane. Nitrogen can occupy both the small and large cages, while isobutane and propane can only occupy the large cages.

Von Stackelberg discovered that there is a relationship between the size of the guest molecule and type of hydrate formed (von Stackelberg, 1949). He made an overview that shows which hydrate type are formed by guest molecules of increasing size (Figure 2). The molecule size is given in Ångstrøm: 1 Å = 1E-10 meter).

Molecules with smaller diameter than 3.8 Å do not form hydrates. Molecules with diameters between 3.8 and 4.2 are small enough to enter both small and large cages and form type 2 hydrates. In the next section molecules with diameter between 4.4 Å and 5.4 Å are located. Carbon dioxide, hydrogen sulfide and methane are found in this region. They form hydrates of type 1 and are small enough to occupy both cage sizes. The subsequent region is quite small and extends from 5.6 Å to 5.8 Å. Ethane is the most important molecule and forms type 1, but can only fit the large cages. The following region is larger. It contains molecules with diameter from 6.0 Å to 6.9 Å, like isobutane and propane. They form type 2 hydrates, and can similarly to the other molecules in this region only fit inside the large cages.

" Eventually a limited is reached. Molecules larger than about 7 Å do not form either a Type I or Type II hydrate. Therefore, molecules such as pentane, hexane, and larger paraffin hydrocarbons are non-formers. From the chart, we can see that cyclopropane (c-C 3 H 8) and n-butane are in the hatched regions. These special components are discussed in more detail later in this chapter. Slightly larger molecules can form Type H hydrates, but the maximum size for these compounds to form a hydrate is about 9 Å." (Carroll, 2003).

N-butane is a transition molecule. Molecules larger than n-butane do not form type 1 and type 2 hydrates, but smaller once do. What make n-butane so special is that is does not form hydrates alone, but in the presence of another hydrate former n-butane can occupy cages/a cage.

There are other types of hydrocarbon that are sufficiently small to form hydrates. Compounds like acethylene, ethylene, propylene, and propyne are hydrate formers. Cyclopropane can form both type 1 and type 2 hydrates. Which hydrate it forms is dependent on pressure and temperature.

2.6 Chemical Properties of Potential Guest Molecules

Just to have the right size is not adequate for a molecule to be hydrate former. It has to possess the right chemical properties. Components easily soluble in water usually do not form hydrates. Carbon dioxide and hydrogen sulfide are fairly soluble in water and form hydrates. These molecules can, as a rule of thumb, be thought of as being in the transition when it comes to solubility in water. Molecules as ammonia and hydrogen chloride fits into a hydrate cage, but are very soluble in water and do not for hydrates.

Hydrates will not form if the molecule interferes with the hydrogen bond. The small molecule methanol is an example of this. Its own hydrogen bond interferes with the hydrogen bond in the water molecules. Methanol is also very soluble in water. Methanol plays an important role in the oil and gas industry's hydrate issues.

2.7 Liquid Hydrate Formers

Hydrates can also be formed by liquid hydrocarbons. The only thing that matters is whether or not the three hydrate forming factors are present; hydrate formers, sufficient amount of water, and the right combination of pressure and temperature. The component's phase is

not a limiting factor. It is most often referred to as gas hydrates, which may lead one to think that hydrates can only form from gas molecules. The confusion may be because hydrates only form from light components which there are a lot of in natural gas.

There have been done experiments with all the common components in natural gas to find out when they are forming hydrates. Sloan has collected all the results in a book (Sloan, 1998). A pressure-temperature table for methane has been included here to give an example (Table 2). Tables for other natural gas components can be found in chapter 2.12.1 in Natural Gas Hydrates (Carroll, 2003).

The tableh as been limited to 30 °C, possibly because the hydrate formation pressure at this temperature is 85.9 MPa. A pressure not normally exceeded in regular petroleum operations. From experiments in a laboratory it has been found that methane can form hydrates at higher pressures. The values in the table are among others presented in a plot shown in Figure 3. In every case, the three-phase loci involving two liquid phases are very steep. That means small changes in temperature have dramatic effect on the pressure. It is also seen from the figure that methane does not have such a locus.

For the purpose of comparing, there have been made a common data base for several hydrate formers. The temperature variable was eliminated by using the hydrate pressure at 0 °C as reference. Carroll has presented the hydrate pressure for multiple components at 0 °C together with several of their physical properties in Table 3. More information on the calculation methods can be found at the same reference.

2.8 Hydrates and Natural Gas Mixtures

For people in the oil and gas industry it is more interesting to look at how a mixture of pure components behaves with respect to hydrate formation. How do non-formers affect the equilibrium locus? Which hydrate types are formed when pure components are mixed in different ratios? We already know that n-butene does not form hydrates alone, but may in the presence of another hydrate former.

A rule of thumb says that if the mixture only consists of guest molecules that form the same type of hydrate, that hydrate type will be formed. A mixture of carbon dioxide, hydrogen

sulfide and methane, all type 1 formers, will for type 1 hydrate. However the hydrates behavior may be both complex and surprising.

Which type of hydrate will form in the mixture consists of type 1 and type 2 formers? From a thermodynamic point of view one would predict whatever hydrate type which minimizes the system's free energy. In other words, the hydrate type formed from the mixture is thermodynamically stabile. It turns out there is no set of fixed rules applicable to every incident. The only way to know for sure is to investigate every incident.

(Holder & Hand, 1982) studied the hydrate forming conditions for a mixture of ethane (type 1) and propane (type 2). They made a chart, reproduced in Figure 4. The chart shows within which region every hydrate type will form. From their results a statement on what the mixture ratio of the two components can be made. As an approximation a mixture of less than 80% ethane will form type 2 hydrates, and if it is more than 80% ethane type 1 hydrates will form. For comparison a mixture of methane (type 1) and propane (type 2) will only form type 1 hydrates when the methane content is very high (99%).

2.9 Azeotropy

A very interesting phenomenon is azeotropic hydrates. These forms either at lower or higher pressure compared to the pure components. An example from Natural Gas Hydrates (Carroll, 2003) is the hydrate that is formed from a mixture of hydrogen sulfide and propane. This mixture forms hydrates at lower pressure than the pure components. From calculations with a software called CSMHYD the hydrate pressure of hydrogen sulfide and propane at 3 °C is found to be 145 kPa and 318 kPa. On the other hand, for an equimolar mixture of these components the hydrate pressure is 64 kPa at the same temperature. This is much lower than for the pure components. Hydrogen sulfide and propane shows azeotrope in the traditional way, vapor-liquid, as well (Carroll, 2003).

3 Inhibitors

As mentioned earlier the formation of hydrates in the natural gas industry is a very serious problem. This part is dedicated to find ways to stop hydrate formation with chemicals. The next part is looking closer at how hydrates form in pipes and process equipment. Subsequently different strategies for removing hydrate plugs are presented.

Since people first started to live in cold places, they have learned to cope with the problems caused by the cold weather. In modern times it is common to salt highways to prevent ice from forming. On airports they spray the aircraft wings with a glycol solution to prevent ice from accumulating. Both glycol and salt lowers the freezing temperature of water. That is in principle the same thing what is done in the oil and gas industry.

Compounds that have the property of inhibiting hydrates are often polar solutions like alcohol, and glycol, and ionic salt(s). The supply of an inhibitor does not prevent the formation of hydrates at any condition. Dependent on the type of inhibitor and its concentration in the water phase, it lowers the temperature, or increases the pressure for hydrate formation. An inhibitor has to be present in a minimum concentration to have an effect.

The most ordinary inhibitors are methanol (MeOH), monoethylene glycol (MEG), and triethylene glycol (TEG). The properties of some common polar components used as inhibitors are displayed in Table 4. It is worth noting that every component has some kind of hydrogen bonding. Thus are able to interfere with the hydrogen bonding in the water molecules.

Ionic salt also inhibits hydrate formation. It lowers the freezing temperature of water as well, but is not used in the industry. As a rule the produced formation water is salt. This may contribute to the inhibiting, but in addition includes various unwanted features.

Salt tends to concentrate in MEG phase during regeneration because water is more volatile than MEG. If not removed, the salt concentration will increase in each cycle. Accumulation of salt can cause precipitation and plugging problems in the system. The salt should be removed after regeneration to avoid salt related problems.

4 Locations of Hydrate Formation

Some of the content in section 0, 0 and 0 is a summary of the contents in chapter 8 in Clathrates Hydrates of Natural Gases written by Sloan(Sloan & Koh, 2008). This book gives a very thorough review of hydrate formation and case studies from real events. Hydrate Engineering (Sloan, 2000) by Sloan has even more case studies on hydrate plug formation and hydrate plug remediation methods. I have tried to extract the most important information, and write it in an understandable fashion.

4.1 Hydrate Plugs in Industrial Equipment

To begin with there are certain criteria that has to be fulfilled by the system to make it possible for hydrates to form. There has to be a sufficient amount of water present, a guest molecule has to be there (often a natural gas component), and the there has to be the right combination of pressure and temperature (high pressure and low temperature, common subsea flowlines operation conditions).

During production of hydrocarbon removing either one of these is very unpractical. The natural gas is the whole reason for operations. The reservoir gas is always saturated with water and it condenses at low temperatures. High pressure is needed to transport the hydrocarbons from the reservoir to the process installation, and to make it possible to produce at economical rates. Lower pressure results in lower density and less gas per volume produced.

Hydrate plugs tend to form in water accumulations. Water tends to accumulate in downward v-shapes pipe sections, just before a riser and on the pipe wall. To reduce the risk of hydrate formation, the temperature could be controlled. Flowline insulation, by coating or burying the pipe, will reduce the heat exchange between the natural gas and the surroundings. Alternatively direct electrical heating could be used. Both insulation and heating are expensive.

Another way to avoid the formation of hydrates is by lowering the hydrate equilibrium temperature by using thermodynamic inhibitors. When an inhibitor is injected its hydrogen bonds are bonded to the water molecule's hydrogen bonds. This reduces the water activity and the result is that higher pressure and lower temperature is needed to form hydrates.

In 1999 flow assurance was ranked at the top of major technical problems during offshore developments by 110 energy companies (welling and associates, 1999) (Macintosh, 2000). The importance of flow assurance problems listed after decreasing significance: Hydrates, wax, scale, corrosion and asphaltenes. The level of importance varies over the world, but in the Gulf of Mexico (GoM) hydrates are a much larger concern than any of the other ones.

A production system is designed not to form hydrates during normal operations. Hydrate plugs are a result of one or several types of abnormal operations. For example like when the aqueous phase is not inhibited, as in the case when the inhibitor injection stop because of an error on the injection pump or the umbilical. At the time of system restart after emergency shut-downs, and there has been no possibility for inhibitor injection. Or because the flow has been cooled while passing a restriction (for example when wet gas flows through a valve).

4.2 Case Study: 1

Hydrate Formation Due to Expansion Through Restrictions or Valves

When wet gas flows through a valve or a flow restriction, it causes a rapid pressure drop. The expansion that occurs is adiabatic, that is that the change in enthalpy is equal to zero, $\Delta H = 0$. And for the enthalpy to remain the same on the other side of the valve the temperature must be reduced.

This is called the Joule-Thomson expansion. When the temperature decreases, the water condenses and the basis for hydrate formation is present. The expansion of two gases with gravity of 0.6 is showed in Figure 5. The reduction in pressure causes a temperature reduction that leads both gases into the hydrate region.

Generally the upstream pressure and temperature is known, and downstream pressure can be found if the pressure drop across the flow restriction is known. The cooling curves in Figure 5 are designed for constant enthalpy (Joule-Thomson) expansion. They are taken from the first law of thermodynamics for systems that flows in the steady-state Figure 6, where one disregards the change in kinetic and potential energy.

ΔH is the change in enthalpy across the restriction, Q is applied heat and Ws is the shaft work. Restrictions perform no shaft work, and because of rapid flow the operation approaches an adiabatic process (limited heat transfer), both Q and Ws are zero. Which

results in $\Delta H = 0$. As mentioned earlier, the temperature must be reduced to keep the enthalpy constant when the pressure drops.

4.3 Oil Dominated Pipelines

A conceptual illustration of the hydrate formation in an oil dominated system is shown in Figure 7. The figure is an expansion of a hypothesis first made by Norsk Hydro (Lingelem, et al., 1994) and has to some degree been accepted in the industry. The formation is depicted in six steps.

In the first stage the water phase emulsifies into the oil phase. As a rule there is less water than oil. This is not valid for mature fields in the Norwegian sector. But for the rest of the world it is common with water in oil emulsions. The water droplets are typically a couple of microns across.

In the second stage a thin hydrate starts to form on the outside of the water droplets (maybe even less than 6 microns thick). In the beginning the particles are very malleable. Whilst the particles still are malleable they form a diffusional barrier between the oil phase and the water phase. Usually the shell does not grow very thick, however they may if there is enough time for them to grow.

The droplets are drawn together by capillary forces. These forces have varying strength, which is dependent on the temperature. The magnitude of the forces is reduced when the temperature falls (measured by (Taylor, 2006)).

The accumulation of particles causes an increase in the apparent viscosity. Hydrate structures that breaks down can be identified as spikes in pressure drop measurements. In the end the accumulation of hydrate particles grows large, which results in a large pressure drop that will stop the flow. This is at this point the hydrate plug is located. With time the porosity and permeability of the plug is reduced due to particle growth and pressure exposure.

Agglomeration of hydrate particles is, indicated by the figure, the limiting factor for plug formation. This has made scientists wondering if it possible to prevent the particles from agglomerating. And the result of these ideas is anti-agglomerates, which make it possible for

the oil to transport the hydrate particles as slurry. In some Brazilian fields there are natural AAs in the oil.

4.4 Gas Dominated Pipelines

The amount of liquid hydrocarbons is much smaller in gas dominated systems. And for that reason the concept of water in oil emulsions is not valid for gas systems. Figure 8 is divided into two parts. The upper part is the depiction of the pressure drop reading upstream, before a hydrate plug is formed as a function of time. The pressure scale is semi-logarithmic. The lower part of the figure portrays stepwise the chain of events when a hydrate plug is formed in a gas dominated system. The upstream pressure response corresponding to each step is illustrated in the upper part of Figure 8

To make it easier to follow the description of the chain of events, each stage has been given a letter. Water in the flowline originates from the reservoir either as produced formation water, or as condensed vapor (point A). Hydrates are usually formed in water, condensed or splashed, at the pipe wall (B). In a hot gas stream the temperature falls radially from center of the pipe to the wall. The pipe wall has the lowest temperature due to heat exchange with surroundings. The inner pipe diameter is reduced when hydrates accumulates at the pipe wall (C). They are deposited unevenly on the wall, and this causes irregular pipe diameter and increased frictional pressure drop (D). Step (A) to (D) is marked “early” in the upper part.

After a while the hydrate accumulations breaks from the wall due to its own weight and the stress caused by passing flow (E). The event can be recognized as pressure reduction on the reading. With time the concentration of broken wall accumulations grows large in the liquid fraction. And the hydrates start to gather in lumps. Eventually they will plug the flow line (F). Corresponding pressure spikes can be found in the upper part, marked “final”.

5 Hydrate Prevention

5.1 How to Prevent Hydrate Plug Formations

Since the discovery of hydrate plugs in pipe in 1934, thermodynamic methods have been used exclusively for flow assurance. The majority of today's easy accessible hydrocarbon sources are running out. A lot of the new hydrocarbon reservoirs are at remote locations. Extreme conditions like high pressures, low temperatures and long distance multiphase flowlines, and sour gas are causing widespread thermodynamic methods of inhibition to become very expensive.

5.2 Case Study: 2

This case study is a summary of a similar case study found in Clathrates Hydrates of Natural Gases (Sloan & Koh, 2008).

Thermodynamic Inhibition at Canyon Express and Ormen Lange

This case study is included to give an understanding of how hydrate inhibition of subsea developments is commonly done in the Gulf of Mexico and on the Norwegian Continental Shelf. The Canyon Express held the record for deepest field development when production started in 2002. Three of the locations are at depths between 6500 ft-7200 ft (2000 m – 2200 m.

The extreme depths brought a need for large amounts of methanol injection. And this was just economical with a sophisticated processing plant to recycle inhibitor. Without methanol recovery the cost of inhibition at maximum design water production (1000 BPD), would have a cost of $ 1 million every 16th day (methanol price of U.S. $ 1/gal)

The Ormen Lange field in the Norwegian Sea (Wilson, et al., 2004), outside the coast of mid-Norway has two extreme factors that can lead to inhibition problems: (1) Because of ocean currents on the ocean floor the sea temperature can fall to -1.2 ° C, and (2) fluid flow in pipes with up to 26% inclination. The low ocean temperatures can cause the formation of ice plugs in the flowline as well as hydrates.

Pressure relief has no effect on the ice plugs. Therefore, they are much harder to get rid of than the hydrates. This leads to the need to take extra precautions when facing such a risk.

To keep the system inhibited, it is estimated that one needs a MEG injection of 26500 ft^3/D ~ 750 m^3/D. This enormous rate, and the volume of the transportation flowlines on the Ormen Lange, means that when the system is to be filled for the first time it will require 67% of the world's glycol production capacity (Sloan & Koh, 2008).

6 Hydrate Plug Removal

To get the feel of what a production engineer may do when a hydrate plug is blocking the system, a sequential routine for remediating the blockage is presented here. First the plug has to be located, and its size has to be determined. Then the safety risk must be evaluated carefully, and the decision on which of the four different hydrate plug remediation schemes to use has be made.

The established methods of remediation are based on four principles. Hydraulic method is pressure relief. Chemical method is injection of inhibitors or reactive chemicals which generate heat (Freitas, et al., 2002).Thermal methods involve direct electrical heating (Davies, et al., 2006). Mechanical methods are coiled tubing, drilling, etc.

6.1 Review of a Hydrate Plug Remediation Process

In this thesis only the alternative of pressure relief will be examined conceptually. Two sided pressure relief is the recommended method, both from a safety and technical point of view. It may be difficult to implement if the liquid head on the hydrate plug is larger than the dissociation pressure. Typical scenarios for this incident to happen are in ultra deep waters or in mountainous terrain. Then direct electrical heating can be a good option.

Normally the water temperature at the sea bed is above the freezing point of water. This excludes the possibility of ice plugs forming. When a hydrate plug is formed the system quickly cools down to the ambient temperature. Pressure and temperature conditions are illustrated in Figure 9. To the left of the three-phase line (Lw-H-V) hydrates can form, whilst on the right hand side only fluids can exist. The figure shows how rapid pressure relief may hurl the system further into the hydrate region.

Two different depressurization scenarios are depicted in Figure 9. Point 1 illustrates how the temperature drops when the gas is passing through a restriction like a valve. Rapid expansion, where $\Delta H=0$, will cool the gas quickly. In point 2 a large volume of gas is depressurized very slowly at a constant temperature. On the right in the figure it is shown that expanding gas may move from outside the hydrate region and into it due to expansion.

Generally the flowline may not be depressurized fast enough for the Joule-Thompson effect to occur. If the flowline is depressurized slowly it will be an isothermal process, and the

temperature will not change, ΔT=0. Most often an intermediate pressure relief causes the hydrate temperature to fall below the ambient temperature. This results in heat being transferred from the surroundings to the plug.

In the case of fast extreme depressurization, the hydrate temperature for methane hydrate depressurized to atmospheric conditions may sink below 0°C. Ice forming from the water from the hydrate plug dissociation will create a buffer for the temperature reduction at 0°C.

If ice is formed during dissociation on hydrate plugs, how fast will the ice plug melt compared to the hydrate plug? New experiments imply that the most effective way is to depressurize as rapidly as possible. The forming ice usually has lower temperature than the surroundings and higher thermal diffusivity than hydrates. This results in increased heat exchange towards the flow line, and faster melting.

From 1994 to 1997 there were completed field studies in a six inches flowline in Tommeliten Gamma field in the North Sea. Over twenty hydrate plugs were formed and removed. The plugs were found to be very porous (>50%) and permeable from tests done both in the laboratory and in the field. Porous and permeable plugs easily transmit gas pressure, while still stopping liquid flow. Then the pressure got reduced on both sides of a porous plug, the pressure quickly got reduced to a constant value across the whole plug.

A Plug's Dissociation Process

The melting temperature at the hydrate plug front is decided by the buffer capacity of the water freezing to ice. Depressurization causes the temperature to fall below ambient temperature. This results in radial heat transfer from the surroundings to the center of the flowline. That means that the temperature is at its highest at the flowline wall. And it causes melting along the entire plug length in contact with the wall.

Melting of a hydrate plug after one, two and three hours is displayed in Figure 10. The results displayed are from three independent experiments in the laboratory. Radial hydrate melting controls the plug removal in the flowline because the pipe diameter is at least on order of size smaller than the length of the plug. A plug is often more than 50 feet long.

The concept of melting due to radial heat transfer is in contrast with earlier longitudinal concepts of dissociation of non-porous hydrate plugs. They were based on that two sided

depressurization would cause dissociation progress on each end towards the middle of the plug (Yousif, et al., 1990).

How the heat flows radially towards the center of the plug when the hydrate temperature is less than ambient temperature is illustrated in Figure 10. And it causes dissociation along the entire length of the plug. Melting also occurs at the ends of the plug, just in a smaller tempo. It is the dissociation at the wall which controls the tempo of the plug removal.

On closer inspection of the picture after one hour, a change in the plug's peripheral morphology is observed. The reason is that when the hydrates are dissociated, the energy is drawn from the phase with the largest thermal diffusivity. In this case it is the water from the dissociated hydrates. In the first phase the hydrate plug is converted to an ice plug which later is melted to water.

The Dangers of a Partially Dissociated Plug

A partly dissociated plug may move down the flowline when the system is restarted. The partly dissociated plug may get stuck and form a new plug at pipe bend, valve or other flow restrictions. The stuck plug has most likely decreased porosity due to the momentum. A more compact plug may be harder to dissociate at a later time.

If the momentum is large enough it may make the plug more compact. In extreme incidents the plug may form a moving projectile, and be a serious safety concern. To avoid this, the flowline is normally pumped full of methanol when the annulus is large enough to allow for fluid flow past the plug. The methanol dissociates the rest of the hydrate plug.

The concept is the same for offshore and onshore flowlines. In the conceptual picture above, the wall temperature is assumed to be constant at 4 °C. An insulated flowline will experience less heat exchange with the surroundings. If the flowline is buried it may have higher temperature than the sea water, due to heating of the mud from the hot pipe flow.

(Austvik, et al., 1997) found an exception from the radial dissociation technique. Especially for hydrate plugs with low porosity and permeability, or very long plugs. (Berge, et al., 1998) showed that hydrate plugs consolidates after they are formed in the pipe. This causes dramatically reduced porosity and permeability. The amount of water converted to hydrates is very low. Between 2% and 4% because of the thin hydrate film, as shown in Figure 7.

6.2 Recommended Actions

Based on these arguments some recommendation can be made. A hydrate plug should be dissociated as soon as possible due to physical/chemical and economical reasons. Younger plugs have larger porosity and permeability, less hydrates. Hydrate plug depressurization should always be done carefully.

There are two main depressurization strategies, one-sided and two-sided depressurization. There are two arguments why to choose the second strategy. The first is that the risk of the hydrate plug turning into a projectile when it is detached from the pipe wall is eliminated by two-sided depressurization.

Hydrate projectiles creates a large safety risk, and can cause damage to equipment and humans. Joule-Thomson effect is avoided by two-sided depressurization. It can lead to cooling which may stabilize the plug's downstream end. The second argument is that two-sided depressurization can cause radial dissociation. This can reduce the down time by 50% compared to one-sided depressurization.

Another production flowline or umbilical should be used to depressurize upstream. Sometimes the liquid head on the hydrate plug may be too large to perform depressurization. In such events, direct electrical heating may be a good alternative.

6.3 Safety and Hydrate Plug Removal

There are several incidents where flowlines have ruptured and people have been seriously injured, or killed. Safety problems are caused by three types of characteristics. The density of hydrate is close to that of ice. Combined with a large upstream pressure gradient, a detached hydrate plug may reach very high velocity.

DeepStar Wyoming ran field test with plugs ranging from 8 m to 66 m. Plug velocities between approximately 20 m/s and 90 m/s were observed (Sloan & Koh, 2008). Statoil experiments have showed hydrate velocities can get even higher (Xiaoyun, 2012).Large mass at velocities of this magnitude creates adequate momentum to cause two types of flowline rupture.

The ruptures are most likely to happen at a flow restriction (orifice), obstruction (flange/valve), or by an immediate change in direction (bend, tee) as shown in Figure 11. As the hydrate projectile travels down the flowline the gas in front of it is being compressed and can lead to a burst. A direct impact could also cause the pipe to explode.

When it is discovered that the system is blocked by hydrates, it is not possible to know how many plugs there are. There is a risk that high pressure gradients are trapped between plugs. Hydrates contain approximately 164 Sm^3 gas per cubic meter hydrate. Hydrate plugs that are dissociated by heating release a lot of gas. If this gas is trapped between two plugs, there may be a rapid increase in the gas pressure. If the pressure gets to high the pipe may burst. For buried flowlines heating is almost never an option. The hydrate plugs are difficult to locate, and it is hard to heat an inaccessible flowline.

6.4 Case Study: 3

Hydrate Plug Incident Resulting In Loss of Life

When a hydrate plug is dissociated it is detached from the pipe wall. If it is exposed to a large pressure gradient at this moment, it may turn into a projectile. Hydrate plug projectiles is known to achieve high velocities, and may put equipment and human lives in danger.

At a large energy company in Alberta the foreman and an operator tried to remove a hydrate plug from a sour gas flowline. They bled the pressure downstream of the plug. They were standing near the pipeline when the plug came rushing up and destroyed it. The foreman was struck by a large portion of the pipeline and later died of his injuries. There were not discovered any pre-accident fault on the pipeline.

The Canadian Association of Petroleum Producers Hydrate Guidelines (King, et al., 1994) proposes three safety measures. (1) Always assume multiple plugs, (2) an attempt to move ice (hydrates) may rupture pipes and vessels, (3) even though heating seldom is an option for buried flowlines, all attempts should be done at the hydrate plug's ends. This way the gas is released, and does not build up a dangerous pressure.

6.5 Summary

An increasing part of newly developed fields produce from extreme conditions. Arctic climate and ultra-deepwater are examples with huge flow assurance problems. The development of gas/oil fields in such conditions is dependent on if problems like high pressure, low temperature, and sour gas are overcome. The costs of thermodynamic inhibitors will in some cases be the deciding factor if the project is accepted or not. Low dosage hydrate inhibitors may become more common.

A new and exciting technology may eliminate the flow assurance problems associated with multiphase transport. Subsea factories can make it possible to separate the different phases at the sea bed (Ree, 2012). Subsea compression can contribute to increase the recovery.

7 HYSYS

7.1 HYSYS Process Simulator

"*The process simulation program HYSYS is attributed Hyprotech, a subsidiary of Aspen Technology. The usability of the program is attributed to the following four key aspects of its design:*

• *Event driven operation*

• *Modular operations*

• *Multi-flowsheet Architecture*

• *Object oriented design*"(Heskestad, 2004).

7.2 Introduction to the Model

The task was to compare methanol (MeOH) and mono ethylene glycol (MEG) as inhibitors, both in general and how they matched the large, long-distance multiphase projects such as Ormen Lange and Snøhvit. Another goal for the task was to calculate the inhibitor amount needed in large pipelines. The task had to be solved by studying the literature on the subject, and by using computer programs such as MS Excel and HYSYS.

In Hydrate Engineering (Sloan, 2000) there is a lot of useful information about the use of both MeOH and MEG as inhibitors. There are many methods, both simpler and more advanced, to determine the amount of inhibitor needed for a given system. There is a chronological structure, starting with the first and simplest, hand calculation methods that actually have achieved great recognition in the industry. Then, more advanced methods are presented. Included with the book is a CD with the program Hydoff. This is developed by Sloan with colleagues at the Colorado School of Mines. Some of the simple methods are still used to make estimate calculations.

Before the inhibitor estimation could be started, the field models had to be created in HYSYS. HYSYS is a commercial process computer program that can be used to model processes and process plants. It includes the ability to model upstream activities, such as

transportation of hydrocarbons from the reservoir to the processing plant. This was exactly what the models had to contain.

To create a simplified model that can provide good and accurate data, HYSYS needs some input. Information on the gas composition, the multi-phase transport distance, the pipeline profile, the pipe diameter, the well head depth, the seabed temperature, the heat transfer coefficient of the pipeline, the reservoir depth, the reservoir temperature, well specifications, water production and gas rate is the minimum to form the basis for a model with a basis in reality.

Much information is available on Jon Steinar Gudmundsson's website (Gudmundsson, 2012). It has links to student assignments, subjects like Processing of Petroleum and Natural Gas, textbooks and articles and other external material. There are particularly many guest speakers from the industry in Natural Gas. It is common that each presenter uses a double lesson to give lectures about projects / technologies developed by their company. Delegates from Shell and Statoil have naturally enough, lectured on the Ormen Lange and the Snøhvit projects. All the material, with permission, from the lectures is available on the homepage

7.3 The Ormen Lange Model

The Ormen Lange field was the second largest gas field when it was discovered and put into operation on the Norwgian Continental Shelf. The field is located about 100 km northwest of Kristiansund, just outside the edge of the Storegga slide in the Norwegian Sea. The water depth is between 800 meters and 1100 meters, the extent is 40 km north-south, and 8 kilometers east-west. The reservoir is located approximately 2000 meters below the seabed. There are proven resources of at least 397 billion cubic meters of natural gas. More information can be found at Natural Gas's webpage (Gudmundsson, 2012)

I found that it was written a paper which contained a model of a well at Ormen Lange (Valberg, 2005). The model could not be attained, but a screenshot of the model showed the layout. Attached to the report was also information about the pressure loss in the well at full production, the well temperature profile (Table 5), the heat transfer coefficient, the internal diameter and the elevation profile (Figure 12). The simplified gas composition from the paper was also used and is showed Table 6. All data used in the model are presented in Table 7, and all the references to that data are gathered in

Table 8.

Data from slide presentations (Biørnstad, 2006) and from the reports mentioned above ((Heskestad, 2004)&(Valberg, 2005)) constituted the basis for the steady-state HYSYS model. All data used in the model represents the conditions at the very beginning when the production has become stable. In the first years no formation water production was expected. First, I replicated the well from Valberg (Valberg, 2005). And then I calibrated the model to the desired pressure losses was found. The friction factor used is typical for carbon steel pipes.

The first thing that had to be done was to ensure that the reservoir gas was saturated with water. This was done by combining the dry gas stream with a flow of water at reservoir conditions and separating the vapor phase by using a simple vertical two-phase separator. The setup is shown in Figure 13.

The well model that I used as a template for my own well model did not take into account the inflow pressure losses from the reservoir. The wells at Ormen Lange are a so-called big bore wells. That is, they have larger production tubing diameter than what is usual for such deep wells. This makes it able to produce gas at a very high rate (Figure 14).

The gas rate for each well was found by dividing the total field rate on the number of wells. But it was too large for the available inflow pressure loss equation for gas wells to be used (Equation 1). The pressure drop was thus estimated from a graph representing the assumed inflow performance of one of the wells on Ormen Lange (Figure 15).The figure is taken from Jon Steinar Gudmundsson's Alpha-field presentation (Gudmundsson, 2010). Equation 1 has no real theoretical back ground. It is an empirical equation made to fit the inflow performance of gas well.

The calibration consisted mostly of selecting the correct pipe flow correlation. The pipe flow correlation "HTFS Homogeneous flow" was chosen on the basis of that the gas phase dominated the flow portion of the well and that the well head pressure matched the real data. The other available pipeline correlations gave much greater pressure losses.

After calibrating the pressure loss in the well, a temperature profile had to be created. The temperature is very important in order to calculate the correct volume of the gas. There was

no available detailed information on this subject. Thus, it was decided to create a linear temperature profile from the reservoir to the seabed (Table 5). Both the reservoir temperature and the seabed temperature were known.

The HYSYS simulation made by Heskestad of Ormen Lange had four wells producing into one 30” transport flowline (Heskestad, 2004). The initial amount of wells was 8. They were assumed to be responsible for the total production of gas in the early years of the Ormen Lange field. It was decided by the field’s design engineers to have two identical 30” transport flowlines to reduce the liquid loading. The pressure loss and fluid volume in each pipeline with different production rates is illustrated in Figure 16.

Thus, it was an opportunity to simplify the model by halving the number of wells and pipelines. There was no other information about the wells. Therefore it was decided to use the first well to be a typical Ormen Lange well. Although not shown in Figure 14, there are four segments in the well. They can be seen Figure 17.

Next step was to design the 121 km long pipeline. The wells are located at 875 meters depth. And there is a very steep climb at the start of the transport stage, the Storegga slide edge, and then it levels out. The pipeline profile from the slide was copied and digitized to be used in HYSYS. The pipeline is not buried, and thus a typical heat transfer coefficient of submarine pipelines was used. The inner diameter was found in the slide Table 9 (Henriksson, et al., 2004).

The slug catcher pressure is set to a maximum of 90 bar. It will be produced against this pressure as long as possible, then it shall be reduced to 75 bar (Biørnstad, 2006). Thus, the pressure is controlled by a subsea choke. The appropriate subsea choke pressure was found by a "trial and error" method. There was no need to reduce the pressure from any of the wells because they had identical wellhead pressure, and in the model it is no distance between them.

After the basic model was completed, data from HYSYS was used to calculate the weight percentage (wt%) of inhibitor that was needed in the water phase. This figure was used, along with the gas rate and other data, to calculate the injection rate of inhibitor. Since the

inhibitor for the entire system would flow through one injection pipe, a splitter was installed ahead of the gas flow injection point to get the right amount in each flowline.

After this had been done it was time to design the inhibitor injection pipeline. At Ormen Lange there are two 6" injection pipelines, but one is a spare. For the most part, the same specifications were used on injection pipeline. Besides that the diameter was smaller and that the elevation profile had to be reversed. Peng-Robinson was used as pipe flow correlation because it was recommended for single phase flow.

At the entrance of the pipeline a pump was placed in order to ensure injection of the inhibitor. The static pressure head from the elevation difference is not enough to ensure inhibitor injection. To prevent backflow the ΔP pump (pump pressure) was calibrated in a way that would provide a one bar pressure difference over the injection valve subsea. The conditions upstream the injection pump was set at 15° C and 1 atm to represent the inhibitor from the storage tanks.

7.4 The Snøhvit Model

The Snøhvit model was made according to the Ormen Lange model and is slightly more complex. There was a lot of information on the website of Jon Steinar Gudmundsson (Gudmundsson, 2012). The Snøhvit field consisted initially of nine wells divided on three templates. Two of the templates (D and E) is located 3 km from PLEM, and the last (N) is located 11 km from PLEM. It required inhibitor injection at the wellheads. The whole network hierarchy is illustrated in Figure 18.

The well design was done in the same way as for the Ormen Lange wells. There was no detailed information available about the wells on Snøhvit. They were therefore assumed to be vertical and not be big bore wells (typical internal diameter). A similar external temperature profile was constructed (

Table 10), but there was no known seabed temperature and it had to be assumed (Gudmundsson, 2012). The gas composition is listed in Table 11. All data used in the model are presented in Table 7.

Gas rate for each well was also found in the same way as for the Ormen Lange (OL). This rate was of such magnitude that the normal inflow pressure loss equation (Equation 1) could be used. As there were no existing well data for Snøhvit to calibrate the well model after, the layout of the Ormen Lange was recreated as far as possible.

The multiphase pipeline to shore had an outer diameter of 26", and was 143 km long. The water depth is less on Snøhvit, but the terrain is very hilly. Just after passing 70 km the pipeline has to traverse a subsea mountain before it begins the climb up to the processing plant on land.

An elevation profile was available Pettersen's slides (Pettersen, 2011). This was digitized to be used in HYSYS (Figure 19). In order to meet the slug catcher pressure on Snøhvit a subsea choke had to be installed. All the information about the Snøhvit field is taken from the Statoil presentations (Pettersen, 2011), or from communication with professor (Gudmundsson, 2012).

A different challenge was met in the design of the Snøhvit model. It was assumed that all wellhead pressures were similar, but they were at different distances from the PLEM. Thus, it was necessary to use choke valves to prevent backflow where the pressure was lowest. The cluster pipes were designed to avoid that the gas velocity became too high, about 4.5 m/s.

The inhibitor pipeline at Snøhvit is 4", there is also a spare one. The same procedure for the elevation profile, the heat exchange coefficient and the injection pump was followed as was done in the Ormen Lange model. Inhibitor is being injected at each template. Thus the pump pressure (Δp) had to be set so that the pressure at the injection valve furthest away (at template N) was 1 bar above the production pressure. The other injection pressures were met by the use of choke valves. The conditions upstream injection pump was set to be 15 °C and 1 atm (Gudmundsson, 2012).

8 Calculations

In order to calculate the amount of inhibitor that was needed on both Ormen Lange and Snøhvit, I was not only dependent on accurate data, but also good methods. It was important that both the method of finding the equilibrium point of the gas mixture and the amount of inhibitor was recognized in the scientific community.

At a CD that had been attached in the book Hydrate Engineering by Sloan (JR., 2000), there were two recommended tools. One was a fairly accurate excel sheet that could be used to calculate the weigh percentage of inhibitor in the water phase that was needed at the given conditions. The second was Hydoff, a computer program.

Hydoff can be used to find the equilibrium pressure of a known gas composition at a given temperature. It can also be used to calculate the necessary weight percent (wt%) inhibitor in the water phase to inhibit the system. It is a bit cumbersome to use, and gives conservative values (Shuker, et al., 2011).

In Hydrate Engineering (JR., 2000) several methods that can transform the concentration of inhibitor in water phase to the injection rate is presented. One is more advanced, and takes into account the inhibitor loss to both vapor and liquid phase. It also includes graphs made from experimental data, to determine the losses to each phase. Exactly how it is done, I will come back to in the review of the calculations. An example of "The most Accurate" method with SI units are presented in 8.1.

The HYSYS models were used to find the conditions that required the largest amount of inhibition. Was it during an emergency stop when the hydrocarbon flow halted and cooled down to the ambient temperature? Was it because of cooling of the gas phase, as a result of the Joule-Thomson effect from the pressure reduction during the ascent towards the shore? Or would it be at a very different location in the system?

During an emergency shut-in the system will be cooled down to the temperature of the surroundings. Then there must be enough inhibitor present in order to prevent hydrate formation. These hydrates can come together and form a hydrate plug when the system is restarted. The most critical point is right after the wellhead, where the temperature is low

and the pressure is high. In extreme cases, the ocean temperature is below 0 °C. This is particularly problematic because ice is formed from the water in the pipeline.

To find the most extreme conditions many simulations for each model were carried out. Three different heat transfer coefficients for the pipelines on the seabed was tested (U = 15, 20 and 25) $W/m^2.C$. Which U gave the lowest temperature in the pipe? When the heat transfer coefficient was high, the sea water acted as a heating medium on the hydrocarbons when the temperature in the pipeline sank below the ocean temperature. The consequence was that a lower inhibitor concentration was needed.

The overall heat transfer coefficient (U) may vary with time. If the pipeline is covered by sediments, or sinks down in organic material this will help to isolate and reduce the U. But it can also increase if the pipeline is exposed to an ocean current of a few meters per second.

In cases where the seabed temperature is very low, the most extreme cases occur at an emergency shut-in of the system. To determine the amount of inhibitor necessary to prevent hydrate formation in such events, the shut-in well head pressure combined with the shut-in temperature must be known. When the flow halts, the inflow pressure loss and friction head loss in the well disappears. Then it is just the static column of hydrocarbons causing the pressure loss from the reservoir. Thus during a shut-in the well head pressure increases, and combined with very low temperatures it can have serious consequences.

Emergency Shut-in

During an emergency shut-in and / or a production stop the fluids movement stagnates. When the hot well flow stops, the system will be cooled by the sea until it reaches ambient temperature. All the pressure loss caused by fluid flow in pipes / well (friction pressure loss and inflow pressure loss) disappears. Then it is just the weight of the hydrocarbon column from the reservoir to the wellhead that is causing the pressure drop (static).

The consequence is that the wellhead pressure increases. And if the flow was large before shut-in, the pressure may increase a lot. This new combination of high pressure and low temperature can lead the pipeline conditions on the seabed into the hydrate region. It will form hydrates in the condensed water on the pipe wall, and / or in the transition between water phase and liquid hydrocarbons.

But the growth will not continue after the hydrocarbons that were in contact with water have formed hydrates, because there are no more mixing of fluids. When the system is restarted the fluids will be mixed up, and new hydrocarbons come in contact with cold water. This may lay the foundation for more growth, and the risk that it will form a / multiple hydrate plugs will increase.

This can be avoided by having a sufficient amount of inhibitor present in the water phase at any time. Any hydrate formation during shut-in will be dissolved by the inhibitor when the system is restarted. For planned shut-ins one can have the opportunity to inject inhibitor. It is not easy if the injection pipeline is not operational, which may be the case in an emergency shut-in.

With this in mind it is obvious that one must examine whether an emergency shut-in will cause the system to be insufficiently inhibited. To find this out, a combination of pressure and temperature which represented the most extreme combination that was likely in the production system was required.

The general assumption of oceanic temperature is that it is approximately 4 °C (Schnitker, 1980). It is at this temperature water has the highest density (Geerts, 2012), and thus it is collected at the seabed. Since the ocean is not an ideal place, where everything follows in according to established main rules, it is important to do thorough research. In some places, ocean currents can cause seawater to have below zero temperatures.

8.1 Procedure for Calculating Inhibitor Injection

Here is the procedure for the method to calculate inhibitor injection rate presented. The method is described as the most accurate in Hydrate Engineering. First, I have presented the equations that make it possible to perform the calculations. Next there is an example of the calculations made in this task with SI units. The example in Hydrate Engineering is in field units, and thus it is not easy to transfer the values commonly used on the Norwgian Continental Shelf directly. The calculations are summarized in Table 12.

Equations

Replacing MeOH with MEG in the aqueous phase is done by Equation 2. The solubility of MeOH in the gas is found with Equation 3. An estimation of the amount of dissolved MEG in

the vapor phase at 1000 psig from the data of Polderman is showed in Figure 2.11 (Sloan, 2000). The amount is very low, almost negligible. The solubility of MeOH and MEG in the condensate is found with Equation 4.

Calculation

Step 1: Calculate the concentration of MeOH and MEG in the water phase. Type in the gas composition in HYDOFF, and manually iterate the weight percent (wt%) MeOH in the water phase that is needed to meet the most severe hydrate forming pressure and temperature combination. Convert the amount of MeOH to MEG by using Equation 2.

Step 2: Calculate the mass of liquid H20/MMscf of natural gas:

i. For use in combination with HYSYS: Read the water rate from the outlet stream. Or use the water content chart in Figure 20 to calculate the water in vapor/MMscf. Use the inlet conditions to find how much water there is initially in the gas. Then use the outlet conditions to find how much water is left in the gas. The difference must be the water rate from the vapor in the pipeline. Calculate the mass of produced H20 flowing in the flowline. Convert the produced water rate from volume/time to mass/volume. No formation water is being produced in any of the cases investigated.
ii. When the condensed and produced water have the same basis they can be added together to give the total amount of water in the pipeline. If you have the water rate in kg/h you need to convert it to kg/MSm³ by multiplying it by 24 and dividing it by the gas rate in MSm³ per day.

Step 3: Calculate the rate of MeOH and MEG injection:
MeOH and MEG can exist in three phases. To provide the correct wt% in the aqueous phase, the amount of inhibitor in liquid hydrocarbon and vapor have to be calculated.

2. Calculate how much needed wt% MeOH in the water phase corresponds to in mass MeOH/volume water in the phase.

a. MeOH:

$$39.81\text{wt}\% = \frac{m_{MeOH}}{m_{MeOH} + 4267.2\left[\frac{kg}{MSm^3}\right]H_2O} \times 100\%$$

Calculation 1

b. solved for m_{MeOH} gives

$$m_{MeOH} = -\frac{4267.2\left[\frac{kg}{MSm^3}\right]H_2O \times 0.3981}{0.3981 - 1} = 2821.8\left[\frac{kg}{MSm^3}\right]$$

Calculation 2

c. MeOH in the water phase.

d. MEG:

$$60.00\text{wt}\% = \frac{m_{MEG}}{m_{MEG} + 4267.2\left[\frac{kg}{MSm^3}\right]H_2O} \times 100\%$$

Calculation 3

e. solved for m_{MEG} gives

$$m_{MEG} = -\frac{4267.2\left[\frac{kg}{MSm^3}\right]H_2O \times 0.6}{0.6 - 1} = 6400.5\left[\frac{kg}{MSm^3}\right]$$

Calculation 4

f. MEG in the water phase.

3. Calculate the amount of MeOH and MEG lost to the gas.
   a. MeOH lost to the vapor phase. Need to find the mole fraction MeOH in the free-water phase.

$$x_{MeOH} = \frac{2821.8\left[\frac{kg}{Sm^3}\right] / 32\left[\frac{kg}{kgmol\ MeOH}\right]}{\left[2821.8\left[\frac{kg}{Sm^3}\right] / 32\left[\frac{kg}{kgmol\ MeOH}\right] + 4267.2\left[\frac{kg}{Sm^3}\right] / 18\left[\frac{kg}{kgmol\ H_2O}\right]\right]} = 0.271$$

Calculation 5

The distribution constant of MeOH is the gas is calculated at -1.2 °C (489.53 °R) with Equation 3. [°F = °C × (9/5)+32], [°R = °F + 459.69]

$$\mathrm{K}_{MeOH}^{V} = \exp\left[5.706 - 5738 \times \{489.53\}^{-1}\right] = 2.44\mathrm{E}-03$$

Calculation 6

The mole fraction of MeOH in the vapor is

$$y_{MeOH} = K_{MeOH}^{V} \times x_{MeOh} = 2.44\mathrm{E}-03 \times 0.271 = 6.62\mathrm{E}-04$$

Calculation 7

The daily gas rate is $\frac{Q_g}{\left[\frac{\overline{M_g}}{\overline{\rho_g}}\right]} = \frac{35\left[\frac{MSm^3}{D}\right]}{\left[\frac{18.014\left(\frac{kg}{kgmol}\right)}{0.764\left(\frac{kg}{Sm^3}\right)}\right]} = 1.48\mathrm{E}+06\ \left[\frac{kgmol}{D}\right]$

Calculation 8

And the MeOH lost to the gas is

$$1.48\mathrm{E}+06\ \left(\frac{kgmol}{D}\right) \times 6.62\mathrm{E}-04 = 982.32\ \left(\frac{kgmol}{D}\right)$$

Calculation 9

which is

$$Q_{MeOH,\text{lost to vapor}} = 982.32\left(\frac{kgmol}{D}\right) \times 32\left(\frac{kg}{kgmol}\right) = 31434.22\left(\frac{kg}{D}\right)$$

Calculation 10

Because the basis for the calculation is 1 MSm³/D:

$$Q_{MeOH,\text{lost to vapor}} = \frac{31434.22\left(\frac{kg}{D}\right)}{35\left(\frac{Sm^3}{D}\right)} = 898.12\left(\frac{kg}{MSm^3}\right)$$

Calculation 11

b. MEG lost to gas. In Figure 2.11 (Sloan, 2000), use the 50 wt% line to determine that the MEG lost to the gas is 0.006 lbm/MMscf = 0.0593 kg/MSm³ at 38°F and 1000 psig, such an amount is negligible. Ng and Chen measured a negligible concentration of MEG in the gas phase at conditions similar to those in this problem (Ng & Robinson, 1983).

4. Calculate the amount of MeOH and MEG lost to the liquid hydrocarbon phase.

a. MeOH lost to the condensate. The distribution of MeOH in the liquid hydrocarbon phase is calculated with;

$$\mathrm{K}_{MeOH}^{L} = \exp\left[5.90 - 5404.5 \times \left\{489.53\right\}^{-1}\right] = 5.86\mathrm{E}-03$$

Calculation 12

b. the mole fraction MeOH in the liquid hydrocarbon phase is;

$$z_{MeOH} = K_{MeOH}^{L} \times x_{MeOH} = 5.86\mathrm{E}-03 \times 0.271 = 1.59\mathrm{E}-03$$

Calculation 13

c. the liquid hydrocarbon rate is;

$$\frac{Q_{condensate} \times \overline{\rho}_{condensate}}{Q_{gas} \times \overline{M}_{condensate}} = \frac{15\left(\frac{Sm^3}{D}\right) \times 511.23\left(\frac{kg}{Sm^3}\right)}{35\left(\frac{MSm^3}{D}\right) \times 47.09\left(\frac{kg}{kgmol}\right)} = 5\left(\frac{kgmol}{MSm^3}\right)$$

Calculation 14

d. The produced amount MeOH lost to liquid hydrocarbons per MSm³ gas produced is:

$$\frac{5\left(\frac{kgmol}{MSm^3}\right) \times z_{MeOH}}{1 - z_{MeOH}} = \frac{5\left(\frac{kgmol}{MSm^3}\right) - \left(1.59\mathrm{E}-03\right)}{1 - \left(1.59\mathrm{E}-03\right)} = 7.4\mathrm{E}-03\left(\frac{kgmol}{MSm^3}\right)$$

Calculation 15

e. which is

$$Q_{MeOH,\text{lost to the condensate}} = 7.4E-03\left(\frac{kgmol}{MSm^3}\right) \times M_{MeOH} = 7.4E-03 \times 32\left(\frac{kg}{kgmol}\right) = 2.4E-01\left(\frac{kg}{MSm^3}\right)$$

Calculation 16

b. MEG lost to condensate. The mole fraction of MEG in water is calculated as:

$$x_{MEG} = \frac{6400.5\left[\frac{kg}{Sm^3}\right]/62\left[\frac{kg}{kgmol\ MEG}\right]}{\left[6400.5\left[\frac{kg}{Sm^3}\right]/62\left[\frac{kg}{kgmol\ MEG}\right]+4267.2\left[\frac{kg}{Sm^3}\right]/18\left[\frac{kg}{kgmol\ H_2O}\right]\right]} = 3.03\text{E}-01$$

Calculation 17

The distribution between the aqueous liquid and the liquid hydrocarbon phase is:

$$\text{K}_{MEG}^{L} = \exp\left[4.20 - 7266.4 \times \{489.53\}^{-1}\right] = 2.39\text{E}-05$$

Calculation 18

The mole fraction of MEG in the liquid hydrocarbon phase is;

$$z_{MEG} = K_{MEG}^{L} \times x_{MEG} = 2.39\text{E}-05 \times 3.03\text{E}-01 = 7.24\text{E}-06$$

Calculation 19

$$Q_{MEG,\text{ lost to condensate}} = \frac{5\left(\frac{kgmol}{MSm^3}\right) \times z_{MEG}}{z_{MEG}} = \frac{5\left(\frac{kgmol}{MSm^3}\right) \times 7.24\text{E}-06}{7.24\text{E}-06} = 3.4\text{E}-05\left(\frac{kgmol}{MSm^3}\right)$$

Calculation 20

$$Q_{MEG,\text{ lost to condensate}} = Q_{MEG,\text{ lost to condensate}} \times M_{MEG} = 3.4\text{E}-05\left(\frac{kgmol}{MSm^3}\right) \times 62\left(\frac{kg}{kgmol}\right) = 2.1\text{E}-03\left(\frac{kg}{Sm^3}\right)$$

Calculation 21

All that is left is to put the values into a table and multiply with the gas rate

$$\text{Total}_{MeOH} = (2821.8+898.12+0.236)\left(\frac{kg}{MSm^3}\right) = 3720.1\left(\frac{kg}{MSm^3}\right)$$

Calculation 22

$$\text{Total}_{MeOH} = \frac{3720.1\left(\frac{kg}{MSm^3}\right)}{\rho_{MeOH}} = \frac{3720.1\left(\frac{kg}{MSm^3}\right)}{791.8\left(\frac{kg}{Sm^3}\right)} = 4.70\left(\frac{Sm^3}{MSm^3}\right)$$

Calculation 23

$$Q_{INJECTION,MeOH} = Q_{gas} \times 3720.1\left(\frac{kg}{MSm^3}\right) = 35MSm^3 \times 3720.1\left(\frac{kg}{MSm^3}\right) = 1.30E5\left(\frac{kg}{D}\right)$$

Calculation 24

$$Q_{INJECTION,MeOH} = Q_{gas} \times 4.70\left(\frac{Sm^3}{MSm^3}\right) = 35MSm^3 \times 4.70\left(\frac{Sm^3}{MSm^3}\right) = 164.44\left(\frac{Sm^3}{D}\right)$$

Calculation 25

8.2 Hydrate Calculations Ormen Lange

Normal Operation

For the base case for Ormen Lange, the average ocean temperature has been estimated to be 2.5 ° C. The overall heat transfer coefficient (U) for has been assumed to be 20 W/m².C. The seabed temperature is taken from a previous project (Heskestad, 2004). U is a standard heat transfer coefficient for carbon steel pipelines (Gudmundsson, 2012) and is usually between 15 W/m².C and 25 W/m².C.

The base case temperature and pressure development with increasing distance from the inlet of the pipeline is showed in Figure 21. The temperature and pressure profile is calculated using HYSYS. In addition, the equilibrium curves of the system with 0, 20, 30 wt% MeOH and MEG in the aqueous phase are plotted. These hydrate curves are calculated using Hydoff.

The base case for the Ormen Lange field was made with average values for the variables that had to be assumed. The overall heat transfer coefficient was the most decisive factor. How the hydrocarbons in one of the two 30” pipelines transport moves past several hydrate curves from the seabed to the onshore facility is illustrated in Figure 21.

The system starts on the right, outside the hydrate region, and moves to the left as primarily the temperature drops. After about 26.1 km the pipeline enters the hydrate region for the Ormen Lange gas. It is then a potential for hydrate formation in the water phase, if there is enough water present at this point. From the figure one can see that the system crosses several equilibrium lines for different concentrations of inhibitor in the water phase.

The temperature drops steadily until about 99 km. From there it begins to increase, this is because of changes in the seabed topography. The pipeline goes down in a valley and the gas is compressed, so the temperature increases slightly. At 99 km the temperature in the pipeline is below the seabed temperature. Heat exchange with the surroundings can then lead to heating of the hydrocarbons. As the pipeline reaches the slug catcher, the temperature is at its lowest. This is also where the temperature and pressure graph protrudes deepest into the hydrate region.

Since the middle value of the heat transfer coefficient interval was chosen as the base case, it was interesting to see what the consequences of inhibition would be if a U outermost in the interval was selected. It was made a case for U = 15 W/m².C and U =2 5 W/m².C. The results for all three cases are presented in Table 13.

The amount of inhibitor required for each system is very similar. But it is possible to observe a trend. As the outlet temperature is lower than the sea temperature, the gas flow will experience heat transfer from the surroundings. Higher U means increased heat exchange with the surroundings and it is reflected in that the outlet temperature is the highest for U = 25 W/m².C. This also means that a lower U will bring the system further into the hydrate region, and then more inhibitor is needed.

Figure 22 shows the temperature and pressure development of hydrocarbons being transported through one of the major flowlines at Ormen Lange. It is also plotted equilibrium curves of the system with several different inhibitor concentrations in the water phase. The reason why the curve that is at the bottom is the one that represents overall heat transfer coefficient equal 15, is because this stream cools slowest. That is, it has higher temperature at lower pressures.

The hump in the curves at around 100 bars is caused by the pipeline plunging down in a valley. From there, the temperature and the pressure drop while the pipeline rises to the onshore facility. In line with the results of Table 13 we see that it is U = 15 W/m².C, which sinks to the lowest temperature, thus creating the need for maximum inhibition of normal operations.

In the case of Ormen Lange, none of the cases were so extreme that it would be wise to calculate the inhibitor injection on the basis of them. At its deepest, down at the wellhead, the ocean temperatures reach -1.2 °C. And during an emergency shut-in this can cause major problems.

It is worth noting that the inhibitor injection led to increased pressure loss in the pipeline and thus the temperature fell slightly at the outlet. But as these conditions were not limiting conditions, it is not discussed further.

Extreme Case: Emergency Shut-in.

In the area where the Ormen Lange wells are located, there are ocean currents that can reach -1.2 °C. The equilibrium pressure for this temperature and 33.63 wt% MeOH, was in Hydoff found to be 124.324 bars. This means that the system is under-inhibited at an emergency shut-in. To determine the amount of inhibitor that was needed, it was necessary to determine the wellhead pressure during a production stop.

During a shut-in the fluids in the pipeline will cool down to ambient temperature. The shut-in temperature development at Ormen Lange is illustrated in Figure 23. The profile has been made by using average hydrocarbon properties, found in HYSYS, in Equation 6. It does not take long before the fluids inside the pipeline have the same temperature as the sea water. The cooling rate is dependent on the heat exchange between the sea water and the hydrocarbons.

In Equation 6: T_2 = the temperature after a given time period, Δt = time period in seconds, T_u = ambient temperature [°C], T_1 = initial temperature [°C], U = total pipeline heat transfer coefficient [W/m².°C], ρ = average fluid density [kg/m³], C_p = [J/kg.°C]

Figure 24 shows the combinations of pressure and temperature for two different cases at emergency shut-in. In addition, the equilibrium curves of methanol and MEG are plotted to

provide a picture of how much inhibitor is required at these conditions. The most extreme case is Norwegian Hydro's estimate (Røsdal, 2008). It is also included an estimate that has been done on the basis of the Ormen Lange HYSYS model and the well pressure iteration process is described below and in Figure 25. The numerical values are presented in Table 13. There is also included an estimate that includes a safety factor of 5% (Li, 2012), such as Statoil uses at Snøhvit.

The equation for a compressible fluid was used to determine the well pressure (Equation 7). The friction component is zero when there is no flow in the pipe and falls away. The equation is reduced to one paragraph, and is then only dependent on the gas properties under given temperature and pressure. The problem is that the gas properties change continuously upward in the well because of reduced pressure and temperature. Components condense and the molecular weight changes. The compressibility changes with pressure.

To make a linear average value of the properties of the gas at reservoir and wellhead conditions are the easiest solution. A more accurate way would be to perform multiple iterations and use the average value of smaller intervals in the well. The Ormen Lange well is divided into four parts with different slopes. Thus it was natural to create four segments for the iterations. A excel sheet (Worksheets for wells and pipelines) that can be found on the homepage of the Processing of Petroleum (Gudmundsson, 2012) was modified for the calculation procedure.

To read the values at each segment the well model in HYSYS was modified. The well was divided into four parts, one part for each well segment. Since I did not manage to run dynamic modeling in HYSYS and shut the well to read the values directly, the model had to be modified. The temperature profile of a well filled with gas is equal to the formation which it is enclosed by. Based on the linear temperature profile that was created for the Ormen Lange model, the temperature at each segment bottom and top was found.

The procedure is described in Figure 25. With the initial values I could find the pressure at the top of the segment that gave the right starting pressure. This provided the basis for calculating the average value between the bottom and top of segment 1. A new pressure was calculated from the average values. Based on this the new pressure values could be read

from HYSYS and a new pressure could be calculated. When the difference in pressure between the iterations was small enough, I went on to the next segment and repeated the process. The criterion was that the initial the pressure would be equal to two decimal places when the pressure was adjusted at the top.

By looking closer at the elevation profile (Røsdal, 2008) for Ormen Lange, it is pointed out two locations where it is more likely for the formation of hydrates. Right at the start of the pipeline, two points are highlighted as particularly detrimental to avoid hydrates. The reasons why hydrates can be formed, including the location is presented in Table 14.

8.3 Hydrate Calculation Snøhvit

It was made a base case where U = 20 W/m².C for the Snøhvit as well. Seabed temperature was assumed to be 4 °C, and the overall heat transfer coefficient, U, for the pipeline was assumed to be 20 W/m².C (Figure 27). To the right of the curves, the system is outside the hydrate region, while to the left of the curve it is inside the hydrate region. The distance where all the equilibrium curve intersections are, is noted in the figure. In addition the distance where major temperature changes occur is noted. The temperature changes at the end of the pipeline are caused by a very hilly terrain that can cause pressure increase and pressure reduction.

The base case temperature and pressure development with increasing distance from the inlet to the pipeline is showed in Figure 27. The temperature and pressure profile are calculated using HYSYS. In addition, the equilibrium curves of the system with 0, 20, 30 wt% MeOH and MEG in the aqueous phase is plotted. These hydrate curves are found using Hydoff. It turns out that the combination of the most extreme pressure and temperature does not take place at the end of the pipeline, but after the 96.7 km from the inlet.

The base case for the Snøhvit field was made with average values for the variables that had to be assumed. Of these the overall heat transfer coefficient was the most decisive factor. How the hydrocarbons in the 26” large pipeline moves past several hydrate curves on its way from the seabed to the onshore facility is illustrated in Figure 27.

The system starts right outside the hydrate region and moves to the left when the temperature decreases. After about 13.4 km the pipeline enters the hydrate region. It is

then a potential for hydrate formation in the water phase (if there is enough water present at this point). From the figure it can be seen that the system crosses several equilibrium lines for different concentrations of inhibitor in the water phase.

The temperature drops steadily to about 96.7 km. Here, the pipeline reaches the top of a 330 meters climb. The pressure loss here may have led to the expansion of the gas in the pipeline and thus caused the gas to be cooled (Joule-Thomson effect). This is where the base case model protrudes deepest inside the hydrate region. Data for all the inflection points and extreme points are presented in Table 15.

After passing that point the temperature begins to increase because of changes in the seafloor topography. The pipeline goes down in a valley and the gas is compressed, so the temperature increases slightly. At 96.7 km the temperature in the pipeline is below the seabed temperature. Heat exchange with the surroundings can then lead to heating of the hydrocarbons.

From the figure it can be seen that one needs in excess of 30 wt% methanol, or about 49 wt% MEG the water phase at 96.7 km. This will thus be the conditions which require the most inhibition in the base case. Yet my models are not close to the conditions Statoil themselves have stated that they relate to, which is 60 wt% MEG in the water phase. The wt% inhibitor in the water phase when the safety factor is accounted for is listed in Table 17.

Three scenarios with three different values of U (U = 15, U = 20 and U = 25) W/m².C was made for Snøhvit as well. The results are listed in Table 16 and illustrated in Figure 28. The same trend that was seen in the Ormen Lange model is visible in this model. The outlet temperature increases when the value of U increases. This happens, as previously mentioned, due to larger heat exchange with the surroundings.

For both the case where U=20 W/m².°C and U=25 W/m².°C the extreme point is at the same location. This is after 96.7 km because the gas cools when the pipeline reaches the top of a steep climb of about 330 m. For the case where U=15 W/m².°C the curve follows the same trend as for the other two cases , but because of reduced heat exchange with the surroundings the outlet conditions are deepest inside the hydrate region.

It could also been done cases where a change in the seabed temperature. This would most likely give the greatest effect during an emergency shut-in. With negative seabed temperature the need for inhibitor would be greater than what is estimated with the simulations in HYSYS.

The gas cross section in a tube that slopes down where liquid and gas flows, are greater than for a tube that slopes upwards. In upward-facing tubes the liquid occupies a larger volume. A liquid column which grows until the pipe inclination ends can be formed. This is the basis for slugging.

Slugging does not occur in steady-state systems, because it is a transient phenomenon. But the gas is still getting compressed in the bottom of the v-shaped pipe segment. The analogy could be made to a reverse Joule-Thomson effect where the gas volume decreases, which causes the temperature to increase. The temperature increase is also due to heating from the surroundings if the previous cooling has led the gas temperature below the seabed temperature.

The curves for the gas hydrate composition at Snøhvit are illustrated in Figure 29. The comparisons of 20, 30, and 40 wt% of each inhibitor are included. In addition, the equilibrium curve without inhibitor and a variety of other wt% are included. It is evident that the pure inhibitory effect of methanol is much stronger than for MEG. It requires larger injection pipes for MEG than for MeOH because the high viscosity leads to larger frictional pressure losses. If the injection pipeline is not designed for MEG injection, larger injection pumps are needed for MEG compared to MeOH.

In models with inhibitor injection the increased amount of fluid led to an increased pressure drop in the pipeline, which led to some extra cooling of the system. In Table 18 we can see how much the outlet temperature changed. The changes were small, and did not require additional inhibition. With a safety margin of 5%, the effect of the extra amount of fluid in the system will not be visible.

Emergency Shut-in

For Snøhvit, there was no information about whether or not the seabed temperature was particularly low. Hence it was assumed to be 4 °C. Compared with the lowest temperature in

the system during production, the Snøhvit shut-in temperature is quite high. A quick check with Hydoff showed that the equilibrium pressure at 4 °C and 31.7 wt% MeOH was 274 bar. It is not likely to have such high pressures the system. Thus, an emergency shut-in could be dismissed as extreme case at Snøhvit.

Volume Calculations

After the injection rate was calculated and the HYSYS models for inhibitor injection were completed, everything was ready for calculating the volume of inhibitor in the system. The plan was to use the fluid velocity from each increment in each pipeline to calculate the time it spent from the injection pump to the slug catcher.

The time was calculated by the simple relationship: time = distance / velocity. HYSYS can divide the pipeline up in many parts, and provide the fluid velocity along with the length of each section. Afterwards the time the liquid used could be calculate for each segment and then added to get the time for the whole pipeline.

The MEG at Snøhvit uses about 7 days from the injection pump down to the wellheads. And from the well heads and up to the slug catcher it uses 4 to 5 days. Total retention time at full production is about 12 days. During some turndown it may take considerably longer because fluid is accumulated in the system. These figures were attained through private communication with a Statoil representative (Svenning, 2012).

Estimates made from the HYSYS-model indicated that the MEG used between 7 and 8 days to reach the wellheads. A bit longer to reach the wellheads located furthest away. The big discrepancy came during the calculation of the retention time from the wellheads to the slug catcher. The figures from HYSYS suggested that the MEG used about 23 days on this trip. Total retention time calculated from HYSYS was over 31 days.

To be able estimate the needed inhibitor storage capacity on a field of Snøhvit's size, the inhibitor's retention time in the system should be known. By multiplying the injection rate with retention time, the amount of inhibitor that is in the upstream system could be calculated. The regeneration capacity would be useful to know if one were to calculate the minimum storage capacity of inhibitor.

Via mail correspondence Baard Kaasa, Specialist Upstream Gas Production Systems Statoil ASA, informed me of the storage capacities for inhibitor and the regeneration of MEG at Snøhvit (Kaasa, 2012). Storage space is not as critical for onshore facilities as for offshore platforms where there is limited surface space.

At Snøhvit, there are four storage tanks. Two for rich MEG and two for lean MEG. For rich MEG there is one storage tank of 3500 m^3 and one of 1500 m^3, where the smallest is for dirty rich MEG. For lean MEG lean one of the storage tanks is 2000 m^3 and the other is 1000 m^3. The latter is for MEG containing salt. It can be assumed that the storage tanks at Ormen Lange are at least equally large, because the injection rate is much larger.

The recovery of MEG is very efficient and in practice it is almost 100%. The water removed in the regeneration process (distillation) may contain about 100 ppm MEG, so the losses are small. Sometimes there are shut-ins for cleaning, and then there will be some losses. At Snøhvit, they have also some loss of MEG in connection with the salt treatment. This only happens when formation water is produced, but this is not the case yet. MEG loss is therefore in the range from 0 to for example 1 m3 per day.

The calculations of inhibitor volume in the system together with the costs of the injection rate and the cost to fill up the entire system once are given in Table 19. They are based on Statoil's own figures since the figures from HYSYS model were almost three times as large. The costs are stated in thousands of dollars, and can be located completely to left in the table when viewed from the front. The figures are significantly greater for MEG than for MeOH. But for both inhibitors the costs are so great that it is necessary for regeneration to reduce the expenditures. Inhibitors in these volumes are too large to dump in the ocean anyways.

9 Methanol versus MEG

Introduction

Every gas/oil field development needs to take into account the possibility of hydrate formation and have a plan for preventing and managing the hydrates. Both in the normal production scenario and during planned/un-planned shut-ins. The consequence of pipeline and/or process equipment blocking can be devastating for the projects economy, the environment and the health and safety of the workers.

There are several different hydrate managing strategies. For short-medium ranged tie-backs the most common strategy is to avoid the pipeline temperature to sink, into the hydrate formation area, in combination with depressurization.

Insulation reduces the heat transfer between the pipeline flow and the ambient. Proper insulation can be achieved either by burying the pipeline, or by adding an insulating layer on the pipe's outside. When we have cold well fluids, or a restart of a well where there is difficult to depressurize, that is in deep waters, direct heating has proven to be a successful method.

Already and in the future, the developments of remote fields are in high focus to sustain the gas and oil production all over the world. Many of the fields are too small to justify a platform development, and with higher cost of recovery subsea development is preferred. Subsea separation is still not developed which results in long distance multiphase pipeline transport. In the case of long distance tie-backs pipeline insulation and/or heating may not be economical and chemical inhibition is the preferred alternative.

Many of the remote developments are far away from existing infrastructure and the consumer marked. It may not be economically feasible to build a pipeline to export the gas. The preferred alternative is to convert the produced gas to LNG, like Statoil is doing at Snøhvit in Hammerfest. Specially designed ships transports LNG to terminals in Europe and USA where LNG is converted into sales gas.

There are two groups of chemical inhibitors: Thermodynamic Hydrate Inhibitors (THI) and Low Dosage Hydrate Inhibitors (LDHI). LDHI, like Anti Agglomerates (AA) and Kinetic Hydrate

Inhibitors (KHI) are popular in some places in GoM and on the UK sector. But they have limitations which make them unsuitable for long distance, high pressure multiphase transport. AAs must have certain amount of condensate to function, and KHIs give only limited hydrate formation temperature suppression.

In the situation of long distance multiphase tie-backs the cost of burying or insulating the pipeline becomes very large and carbon steel pipes are favored. With the technology of today THIs are the only robust choice. The two most common types are MEG (mono ethylene glycol) and MeOH (methanol), but there are various other types available (Table 20). Huge amounts of inhibitor are needed for these types of projects and a thorough investigation of the system has to be conducted prior to deciding on the inhibitor of choice.

Important factors like storage capacity, regeneration plant have to be evaluated and also forecasted production rates, water rates, production of LNG or not and many other factors have to be included in the analysis.

9.1 Comparison Based on Literature

Comparison

MEG has higher molecular weight than MeOH and is therefore not as effective inhibitor. A larger weight percent inhibitor in the aqueous phase is needed. But MEG has low solubility in the vapor phase and only a diminutive part is lost to condensate. This means that only a small amount of the injected MEG is lost in the production system. Another good property is that MEG is a corrosion inhibitor which reduces the overall operation cost of the corrosion program. However MEG injection is seldom enough to provide total corrosion inhibition for the whole system.

MEG is easier to reclaim than MeOH because it has lower vapor pressure. Compared to MeOH a smaller high temperature-recovery column can be used for MEG regeneration. Methanol is being regenerated on some locations in Asia and the GoM like the Shell Malampaya onshore facility in the Philippines and the Williams Canyon Station platform (part of the Canyon Express system) in the GoM. But because regeneration of a volatile like MeOH is complicated there are limited records of its economical benefits. MEG has higher

flash temperature (111 °C) than MeOH which makes it safer to store and handle, especially offshore with limited space.

A company performed some experiments where KHI was mixed into the THI to suppress the hydrate formation temperature at peak water production. And it was reported that MEG was the preferred choice of mixing inhibitor. In some places in the GoM, MEG is used as a combined hydrate inhibitor and dehydrator to prepare the produced gas for the export pipeline.

On the down side MEG regeneration can lead to increased salt concentration in the waste water which then has to be cleaned before disposal or re-injection. I addition common problems associated with closed MEG loops containing salt- and water removal are "*carbonate scale deposits, accumulation of corrosion products and other small particles and carry-over/foaming*"(Brustad, et al., 2005). Due to its low viscosity, larger diameter injection pipelines and/or larger injection pumps are needed compared with injection of MeOH.

MeOH is much cheaper than MEG. From Sloan Hydrate Engineering we can see that it is only a third of the price of MEG (Table 21). It has low viscosity which makes it easy to inject, even over long distances. But one of the heaviest arguments against the use of MeOH is the major loss to the gas phase.

Rule-of-thumb 4 from Hydrate Engineering states that at 4 °C and pressure above 70 bar, 16 kg MeOH is lost per MSm3 gas production per wt% in the water phase (Sloan, 2000). For Ormen Lange with a production of 70 MSm3/D and the equivalent amount of inhibitor of approximately 40 wt% MeOH in the water phase, roughly 70×16×40=448000 kg of MeOH is lost every day. For higher temperatures the loss is even more severe. Compared to the total injection rate of MeOH in the region of 17 % is lost to the gas phase.

A polluted gas phase may result in a price penalty of the sales gas, or a large investment in a cleaning plant to prepare the gas for sale and/or LNG production. On Snøhvit MeOH is excluded as an alternative because the MeOH will freeze in the cryogenic "Cold Box". Due to Methanol's low flash temperature of 11 °C, it is dangerous to handle and store. Especially

offshore where there is limited space. And because it burns with an invisible flame it makes the potential disaster harder to spot.

MeOH has been used around the world for a long time as a hydrate inhibitor. It has been the cheapest alternative on the marked. But the fact is that it is very flammable, pollutes the sales gas, is expensive to regenerate and is impractical to use related to LNG production makes it a poor alternative to MEG for long distance gas-condensate tie-backs.

"*Surveying the choices made by the operators for recently built and planned gas condensate tie-backs, it is evident that MEG seems to be the preferred inhibitor. The list of MEG-based developments includes record-breaking developments like Ormen Lange (Norsk Hydro - Norway), Snøhvit (Statoil - Norway), KG D6 (Reliance Industries – India), Scarab-Safron (Burullus – Egypt), South Pars (Total Iran), Shah Deniz (BP - Azerbaijan), Britannia Satellites (ConocoPhillips – UK), Gorgon (Chevron Texaco – Australia) and finally the ultimate Subsea to Beach concept: Shtokman (Gazprom - Russian Barents Sea).*"(Brustad, et al., 2005)

9.2 Comparison Based on Own Calculations

The results from both of the HYSYS-models are presented in Table 22. Both Shell and Statoil have stated that they use 60 wt% MEG to inhibit Ormen Lange and Snøhvit. Based on these data the HYSYS-models have been adapted to provide values to be used to calculate the inhibitor injection rate. To compare methanol and MEG a correlation mentioned earlier (Equation 2) have been used to find the corresponding methanol wt%.

The pump data are found from the injection models in HYSYS. Pump-inlet conditions are standard conditions (15 °C and 1 atm). The wt% in the aqueous phase was found with Hydoff, and the rest was calculated by the use of a method ("The most accurate method") from Hydrate Engineering, presented earlier in this thesis. No reasonable data was acquired for the volume of inhibitor in the pipelines for Ormen Lange.

The first thing we notice is that the wt% in the aqueous phase is smaller for methanol than for MEG. This is because methanol has lower mole weight than MEG, and thus is a more effective inhibitor. It can be seen that the total injection rate is not very different for the two inhibitors from Table 22. Even though the rates are quite similar, there is much less methanol kg/MSm³ than MEG kg/MSm³. The reason is due to the fact that methanol is much

more volatile than MEG, and a large part is lost into the gas phase. A significant amount of MeOH is dissolved in the condensate. The results from each inhibitor calculation are found in tables 23-29.

The reason why the MEG injection rate is lower than that of methanol, which has a lower wt%, in two of the cases is because of the correlation between inhibitors is a cubic function. MEG is less effective when the concentration in the aqueous phase reaches a certain value. After this more MEG is required for each additional degree of temperature suppression. The correlation of methanol and MEG are illustrated in Figure 30.

Since MEG has greater viscosity than methanol the frictional pressure loss in the injection pipeline will be somewhat larger for MEG. However, MEG has greater density than methanol, and will thus have larger static pressure contribution during the injection. As long as the injection rate is not too large for the injection pipe diameter, the static contribution will compensate for the added viscosity in terms of ΔP in the injection pump.

The pump effect is larger at Ormen Lange compared to Snøhvit even if ΔP is almost twice as high on Snøhvit. The reason why ΔP is smaller at Ormen Lange is because it is much more static pressure support from the inhibitor due to the fact that the wells are located at larger depth. However, the injection rate is greater at Ormen Lange. This compensates for ΔP. Well head pressure is quite similar for both fields. The relationship between rate and pressure drop is shown in Equation 10. If the fields have been designed for MeOH injection the injection pipelines would most likely have a smaller diameter.

In Equation 10: P is the pump power in [W], q is the rate in [Sm^3/s], ΔP [Pa] is pressure the pump needs to induce and ŋ is efficiency constant when comparing with an ideal pump where ŋ = 1.0.

10 Discussion

Hydrates are formed in the water phase, in the transition between water and hydrocarbons. Hydrates are formed in different places and in different ways in gas-dominated and oil-dominated systems. This is dependent on where the water is located in each of the cases.

In oil-dominated systems it is often produced formation water in addition. The liquid is accumulated in geometry changes in the pipeline. Water is emulsified in the oil and it starts growing hydrate shells around the water droplets. Capillary forces lead hydrate droplets together. When many droplets come together the mixture's apparent viscosity increases, and it flows more slowly. After a while, the lump grows so large that it gets stuck in the pipeline and a plug is formed.

The HYSYS models are probably the largest source of uncertainty in this thesis. First, there were made some assumptions about input data where the specific values for each field were not found. The assumptions have been made after best efforts. It has always been the aim that they came from reputable sources, such as my professor.

The models have also been simplified compared to the real conditions. For example, there is no distance between the wells at each template. Inflow losses are calculated based on a completely theoretical model, and not adapted directly to the real conditions.

Field models are steady state at full production. They are intended to simulate average conditions in the field, except from when there is made specific special cases. An example of this is the shut-in case at Ormen Lange.

The HYSYS license at NTNU only provides access to the simplest fluid packages and offers no additional software, such as Olga. Olga is a recognized multiphase flow simulator that can be linked to HYSYS to make the multiphase data calculations more accurate.

Input values that can vary greatly from location to location and in time, are seabed temperature and the total heat transfer coefficient to the pipelines. In the case of Ormen Lange a worst case seabed temperature that is far below the normal temperature of 4 °C was given. It was not found a value for the overall heat transfer coefficient, U, for any of the transport pipelines. The effect of different values of U was investigated in the thesis. There

are some crucial differences between if the U=15 W/m².°C or U=25 W/m².°C, as illustrated in Figure 22 and Figure 28.

The MEG requirement at Ormen Lange and Snøhvit is stated to be 60 wt% in water phase. This corresponds respectively to 402 Sm^3/D and 122 Sm^3/D. The need at Ormen Lange is much larger than that at Snøhvit, but so is also the gas production. The inhibitor demand was calculated based on data from HYSYS models and are presented in Table 22. These calculations are made under the assumption that there is only condensed water, not formation water in the pipeline.

In the case study concerning Ormen Lange, Sloan has a reference that claims that the injection rate at the most can be as high as 750 Sm^3/D. That is a lot more than what my calculations for 60 wt% MEG estimates, which is 402 Sm^3/D. The reason for this discrepancy may be that the expected amount of produced water volume is much larger than in the HYSYS model and / or that the wt% of MEG is higher than stated in the lectures.

In the interpretation of the temperature development of the hydrocarbons along the pipeline, it has been assumed that the cooling below the seabed temperature is a result of the Joule-Thomson expansion. At the same time, midway heating of the gas flow from below the seabed temperature is explained by that the gas heats up when it is compressed at the bottom of a valley. And the sea will help to heat the gas up to its own temperature.

The inhibitor injection leads to greater pressure losses in the pipeline because the liquid phase volume increases. Increased pressure can lead to greater cooling of the gas, and thus require more inhibition. This was examined in HYSYS, and the results are presented in Table 18. The temperature difference was so small that a safety factor of five percent would account for the change in the concentration of inhibitor in the water phase.

During the volume calculations of inhibitor in the system, it was discovered that HYSYS did not provide numbers that were close to the numbers from reality. It was investigated whether the pipe flow correlation that was chosen was the origin of the deviation. Several types of pipe flow correlations as Beggs and Brill (1979), HTFS liquid slip and other pipe flow correlations was tested. All gave retention times close to each other, but not in near real values.

The size of the inhibitor storage tanks at Snøhvit is several thousand cubic meters and there are four of them. This indicates that a field in need of inhibition on this scale also needs plenty of space to store the inhibitor. Ormen Lange has an even greater consumption of inhibitor, and probably need even more storage space. It will require a very large offshore development, and it may not be economical to implement.

Because of the methanol's volatility, much disappear into in gas phase after injection. It is not straight forward to recover a volatile like MeOH. For these reasons, knowledge of the cost effectiveness of methanol recovery processes is limited. This means methanol is not recovered, which is a must for projects with large consumption of inhibitor.

The low flash temperature also makes it difficult to store / treat the methanol. In addition, the methanol is easily-combustible and burns with an invisible flame. It is also difficult to recover the methanol from the gas phase. On Snøhvit methanol is not an option because it freezes in the cryogenic “cold box”. Based on all of these reasons, methanol is not suitable for projects that require continuous injection of large amounts of inhibitor. At least not if the gas is going to be frozen for LNG production.

There are several interesting newer technologies and strategies to ensure flow assurance available on the market. Anti agglomerates and kinetic hydrate inhibitors are not suitable for long multi-phase tie-backs. AAs must have certainties amount of condensate in order to function, and the KHIs only provide limited hydrate formation temperature suppression. They are also toxic, and are not permitted to use on the Norwgian Continental Shelf.

A technology that has the potential to make flow assurance to a yesterday's problem is something called subsea factories. A subsea factory usually consists of a single processing facility that can separate gas, oil and water. This will lead to a very limited need for hydrate inhibition and increase the pipeline transportation range of hydrocarbons.

In a subsea factory unit there are also pumps, or compressors which can contribute to increase the recovery from the reservoirs. Statoil has just given a contract to Framo Engineering which involves that they will deliver subsea wet gas compressors to the Gullfaks field. This is an initiative that aims to increase the recovery rate from 60% to 70% on the entire field.

Volume calculations were only conducted for Snøhvit. I only had access to real data from that field. The figures from the HYSYS models were unrealistically large. At Snøhvit, there are four storage tanks. Two for rich MEG and two for lean MEG. For rich MEG there is one storage tank of 3500 m^3 and one of 1500 m^3, where the smallest is for dirty rich MEG. For lean MEG there is one storage tank of 2000 m^3 and another one of 1000 m^3. The latter is for MEG containing salt. Although it was not done calculations for Ormen Lange's storage volume it can be assumed that the plant has at least as much storage capacity because it has a larger injection rate.

11 Conclusion

Hydrates are formed at the pipe wall in gas-dominated systems. Once hydrates have collapsed from the wall into the liquid hydrocarbon phase, the hydrate lump may build up to block the pipeline.

Hydrates are formed around the water droplets that are emulsified in the oil phase. Capillary forces pull hydrate particles together and they can form a hydrate mass that eventually may block the pipeline.

MeOH has been used around the world for a long time as hydrate inhibitor. It has been the cheapest alternative on the marked. But the fact is that it is very flammable, pollutes the sales gas, is expensive to regenerate and is impractical to use related to LNG production makes it a pour alternative to MEG for long distance gas-condensate tie-backs, especially in remote locations.

The MEG requirement for Ormen Lange and Snøhvit is stated to be 60 wt% in water phase. This corresponds, respectively, 402 Sm^3/D and 122 Sm^3/D. The inhibitor need at Ormen Lange is much larger than it is at Snøhvit, but so is also the gas production from Ormen Lange.

The inhibition effect of 39.8 wt% MeOH equals that of 60 wt% MEG. At Ormen Lange with 39.8 wt% inhibitor in the aqueous phase the MeOH injection rate is 329 Sm^3/D. Of the total rate 79.4 Sm^3/D are lost to the vapor phase and 0.021 Sm^3/D are lost to the condensate. Only 249.6 Sm^3/D are dissolved in the aqueous phase and contributes to inhibition of hydrates.

At Ormen Lange with 60 wt% MEG in the aqueous phase the MEG injection rate is 402 Sm^3/D. Of the total rate 0.0037 Sm^3/D are lost to the vapor phase and 0.00014 Sm^3/D are lost to the condensate. Thus, virtually everything that is injected contributes to the inhibition of hydrates.

At Snøhvit with 39.8 wt% MeOH in the aqueous phase the MeOH injection rate is 104.5 Sm^3/D. Of the total rate 25.9 Sm^3/D are lost to the vapor phase and 3.2 Sm^3/D are lost to the

condensate. Only 75.4 Sm^3/D are dissolved in the aqueous phase and contributes to inhibition of hydrates.

At Snøhvit with 60 wt% MEG in the aqueous phase the MEG injection rate is 121.6 Sm^3/D. Of the total rate 0.0012 Sm^3/D are lost to the vapor phase and 0.021 Sm^3/D are lost to the condensate. Thus, virtually everything that is injected contributes to the inhibition of hydrates.

At Snøhvit, there are four storage tanks. Two for rich MEG and two lean MEG. For rich MEG there is one storage tank of 3500 m^3 and one of 1500 m^3, where the smallest one is for dirty rich MEG. For lean MEG lean one of the storage tanks is 2000 m^3 and the other is 1000 m^3. The latter is for MEG containing salt. It can be assumed that the storage tanks at Ormen Lange are at least equally large, because the injection rate is much larger.

12 Nomenclature

Symbol	Explanation	Unit
Wt%	Weight Percent in the Water Phase	-
GoM	Gulf of Mexico	-
P_{wf}	Well Flow Pressure	[bar]
P_R	Reservoir Pressure	[bar]
q	Gas Rate	[Sm³/D]
MEG	Mono Ethylene Glycol	-
MeOH	Methanol	-
K_{MeOH}^{V}	Distribution Coefficient	-
$\mathrm{T}(^{\circ}\mathrm{R})$	Cold Temperature	[°R]
K_{MeOH}^{L}	Distribution Coefficient	-
K_{MEG}^{L}	Distribution Coefficient	-
T_2	Next Temperature	[°C]
T_u	Ambient Temperature	[°C]
T_1	Current Temperature	[°C]
U	Overall Heat Transfer Coefficient	[W/m².°C]
Δt	Time Step	[s]
ρ	Average Density	[kg/m³]
C_p	Specific Heat Capacity	[J/kg.°C]
d	Diameter	[m]
M	Mole Weight	[kg/kmole]
z	Z-factor	-

R	Universal Gas Constant	[J/kmole.K]
T	Temperature	[K]
P	Effect	[W]
ΔP	Pressure Difference	[Pa]
η	Pump Efficiency Coefficient	-
q	Injection Pump Flow	[Sm³/s]
Ppm	Parts Per Million	-

13 References

Austvik, T., Hustvedt, E., Gjertsen, L. & Urdahl, O., 1997. s.l., s.n., p. 205.

Berge, L., Gjertsen, L. & Lysne, D., 1998. 1631. 53(9).

Biørnstad, O. C., 2006. *Ormen Lange og Langeled,* Trondheim: s.n.

Brustad, S., Løken, K.-P. & Waalmann, J., 2005. *Hydrate Prevention using MEG instead of MeOH: Impact of experience from major Norwegian developments on technology selection for injection and recovery of MEG.* Houston, Aker Kværner Engineering and Technology, p. 2.

Brustad, S., Løken, K.-P. & Waalmann, J., 2005. *Hydrate Prevention using MEG instead of MeOH: Impact of experience from major Norwegian developments on technology selection for injection and recovery of MEG.* Houston, Aker Kværner Engineering and Technology.

Carroll, J. J., 2003. Natural Gas Hydrates. In: *Natural Gas Hydrates.* s.l.:s.n., p. 115.

Carroll, J. J., 2003. Natural Gas Hydrates. In: *Natural Gas Hydrates.* s.l.:s.n., p. 18.

Carroll, J. J., 2003. Natural Gas Hydrates. In: *Natural Gas Hydrates.* s.l.:s.n., p. 8.

Carroll, J. J., 2003. Natural Gas Hydrates. In: *Natural Gas Hydrates.* s.l.:s.n., p. 22.

Carroll, J. J., 2003. Natural Gas Hydrates. In: *Natural Gas Hydrates.* s.l.:s.n., pp. 25-27.

Carroll, J. J., 2003. Natural Gas Hydrates. In: *Natural Gas Hydrates.* s.l.:s.n., pp. 41-42.

Carroll, J. J., 2003. Natural Gas Hydrates. In: *Natural Gas Hydrates.* s.l.:s.n., p. 31.

Carroll, J. J., 2003. Natural Gas Hydrates. In: *Natural Gas Hydrates.* s.l.:s.n., p. 1.

Carroll, J. J., 2003. Natural Gas Hydrates. In: *Natural Gas Hydrates.* s.l.:s.n., p. 40.

Carroll, J. J., 2003. Natural Gas Hydrates. In: *Natural Gas Hydrates.* s.l.:s.n., p. 17.

Chitwood, J., 2003. *Personal Communication.* s.l.:s.n.

Davies, S. et al., 2006. Hydrate Plug Dissociation. *AIChE J.*, 52(12), p. 4016–4027.

Freitas, A., Lobao, D., Anselmo, C. & Cardoso, C., 2002. *Hydrate Blockages in Flowlines and Subsea Equipment in Campos Basin.* Houston, TX, s.n.

Geerts, B., 2012. *www.waterencyclopedia.com.* [Online]
Available at: http://www.waterencyclopedia.com/Re-St/Sea-Water-Freezing-of.html

Granger, P. J., n.d. *H20 - The Mystery, Art, and Science of Water.* [Online]
Available at: http://witcombe.sbc.edu/water/chemistrystructure.html

Gudmundsson, J. S., 2010. *TPG 4140 - Natural Gas.* [Online]
Available at:
http://www.ipt.ntnu.no/~jsg/undervisning/naturgass/lysark/LysarkGudmundssonAlphaField2010.pdf
[Accessed April 2012].

Gudmundsson, J. S., 2011. *TPG 4140 - Natural Gas.* [Online]
Available at:
http://www.ipt.ntnu.no/~jsg/undervisning/naturgass/lysark/LysarkGudmundssonFlowAssurance2011.pdf
[Accessed 8 June 2012].

Gudmundsson, J. S., 2012. *Home page.* [Online]
Available at: http://www.ipt.ntnu.no/~jsg/
[Accessed 2012].

Gudmundsson, J. S., 2012. *Private conversation with professor.* Trondheim: s.n.

Gudmundsson, J. S., 2012. *Processing of Petroleum.* [Online]
Available at: http://www.ipt.ntnu.no/~jsg/undervisning/prosessering/Ovinger/ovinger.html

Gudmundsson, J. S., 2012. *Snøhvit information.* Trondheim: s.n.

Gudmundsson, J. S., 2012. *TPG 4140 - Natural Gas.* [Online]
Available at: http://www.ipt.ntnu.no/~jsg/undervisning/naturgass/TPG4140.html
[Accessed 2012].

Gupta, N., 2011. *TPG 4140 - Natural Gas.* [Online]
Available at: http://www.ipt.ntnu.no/~jsg/undervisning/naturgass/TPG4140.html
[Accessed 2012].

Heiersted, R. S., 2004. *TPG 4140.* [Online]
Available at:
http://www.ipt.ntnu.no/~jsg/undervisning/naturgass/lysark/LysarkDel2Heiersted2004.pdf
[Accessed 8 June 2012].

Henriksson, A., Wilhelmsen, A. & Karlsen, T., 2004. Pipelines in harsh environment.

Heskestad, K. L., 2004. *DEPOSITS DETECTION USING PRESSURE PULSE TECHNOLOGY,* Trondheim: NTNU.

Holder, G. & Hand, J., 1982. Multi-phase equilibria in hydrates from methane, ethane, propane, and water mixtures .. *AIChE J,* Issue 28, p. 440 – 47.

JR., E. D. S., 2000. *HYDRATE ENGINEERING.* Richardson, Texas: Henry L. Doherty Memorial Fund of AIME. Society of Petroleum Engineers Inc..

Kaasa, B., 2012. *Mail.* Trondheim: s.n.

Kelland, M. A., 2000. *"Chemicals for Gas Hydrate Control.* Trondheim, NTNU.

King, R., Sharples, T., Stewart, J. & S.Sortland, 1994. *Canadian Association of Petroleum Producers Hydrate Guidelines,* Calgary, Alberta, Canada: Canadian Association of Petroleum Producers.

Lingelem, M., Majeed, A. & Stange, E., 1994. *Industrial Experience in Evaluation of Hydrate Formation, Inhibition, and Dissociation in Pipeline Design and Operation.* New York, Annals of the New York Academy of Sciences, pp. 75-93.

Li, X., 2012. *Private conversation by mail.* Trondheim: Mail.

Li, X., 2012. *Private conversation by mail.* s.l.:s.n.

Macintosh, N., 2000. *FlowAssurance Still Leading Concern Among Producers.* s.l.:Offshore.

Ng, H.-J. & Robinson, D., 1983. *Equilibriumphasecomposition and hydratingconditions in systemscontainingmethanol, lighthydrocarbons, carbondioxide and hydrogensulfide,* s.l.: GPA Research Report RR-66.

Peters, D., 1999. *A Study of Hydrate Dissociation in Flowlines by the Method of Two-Sided Depressurization: Experiment and Model,* Golden, CO: Colorado School of Mines.

Pettersen, J., 2011. *Snøhvit field development,* Trondheim: Statoil.

Ree, M., 2012. Nærmer seg industridrømmen. *Teknisk Ukeblad,* 159(19), pp. 8-9.

Røsdal, A. M., 2008. [Online]
Available at:
http://www.ipt.ntnu.no/~jsg/undervisning/naturgass/lysark/LysarkRoesdal2008.pdf

Schnitker, D., 1980. Quaternary deep-sea benthic foraminifers and bottom water masses. Issue 8.

Shuker, M. T., Firas, B. & Ismail, C. U., 2011. *Onepetro.* [Online]
Available at: http://www.onepetro.org/mslib/servlet/onepetropreview?id=IPTC-15492-MS

Sloan, E., 1998. *Clathrate Hydrates of Natural Gases.* 2nd ed. New York(New York): Marcel Dekker.

Sloan, E. D. J., 2000. *HYDRATE ENGINEERING.* Richardson, Texas: Henry L. Doherty Memorial Fund of AIME. Society of Petroleum Engineers Inc..

Sloan, E. D. J., 2000. *HYDRATE ENGINEERING.* Richardson, Texas: Henry L. Doherty Memorial Fund of AIME. Society of Petroleum Engineers Inc..

Sloan, E. D. & Koh, C. A., 2008. Clathrate Hydrates of Natural Gases. In: *Clathrate Hydrates of Natural Gases.* Golden(Colorado): Taylor & Francis Group, LLC.

Sloan, E. D. & Koh, C. A., 2008. Clathrate Hydrates of Natural Gases. In: *Clathrate Hydrates of Natural Gases.* Golden(Colorado): Taylor & Francis Group, LLC, p. 651.

Sloan, E. D. & Koh, C. A., 2008. Clathrate Hydrates of Natural Gases. In: *Clathrate Hydrates of Natural Gases.* Golden(Colorado): Taylor & Francis Group, LLC, p. 657.

Sloan, E. D. & Koh, C. A., 2008. Clathrate Hydrates of Natural Gases. In: *Clathrate Hydrates of Natural Gases.* Golden(Colorado): Taylor & Francis Group, LLC, p. 653.

Sloan, E. D. & Koh, C. A., 2008. Clathrate Hydrates of Natural Gases. In: *Clathrate Hydrates of Natural Gases.* Golden(Colorado): Taylor & Francis Group, LLC, p. 655.

Sloan, E. D. & Koh, C. A., 2008. Clathrate Hydrates of Natural Gases. In: *Clathrate Hydrates of Natural Gases.* Golden(Colorado): Taylor & Francis Group, LLC, p. 672.

Sloan, E. D. & Koh, C. A., 2008. Clathrate Hydrates of Natural Gases. In: *Clathrate Hydrates of Natural Gases.* Golden(Colorado): Taylor & Francis Group, LLC, p. 676.

Sloan, E. D. & Koh, C. A., 2008. Clathrate Hydrates of Natural Gases. In: *Clathrate Hydrates of Natural Gases.* Golden(Colorado): Taylor & Francis Group, LLC, p. 652.

Svenning, M., 2012. *Private conversation by mail.* Trondheim: Statoil.

Taylor, C., 2006. *Adhesion Force between Hydrate Particles and Macroscopic Investigation of Hydrate Film Growth at the Hydrocarbon/Water Interface,* Golden, CO: Colorado School of Mines.

Valberg, T., 2005. *Temperature calculations in production and injection,* Trondheim: NTNU.

von Stackelberg, M., 1949. Feste gashydrate. In: *Naturwissenschaften.* s.l.:s.n., p. 327 – 33.

Wilson, A., Overaa, S. & Holm, H., 2004. *Ormen Lange - Flow assurance challenges.* Houston, Offshore Technology Conference.

Xiaoyun, L., 2012. *Hydrate Plugs – Still a Major Flow Assurance Challenge,* Trondheim: s.n.

Yousif, M., Li, P., Selim, M. & Sloan, E., 1990. J. Inclus. Phenom. Mol. 8(71).

14 Tables

Table 1: Comparison of Type 1, Type 2 and Type H Hydrates (Carroll, 2003)

	Type I	Type II	Type H
Water Molecules per Unit Cell	46	136	34
Cages per Unit Cell			
Small	6	16	3
Medium	–	–	2
Large	2	8	1
Theoretical Formula[†]			
All cages filled	X . 5 3/4 H_2O	X . 5 2/3 H_2O	5X . Y . 34 H_2O
Mole fraction hydrate former	0.1481	0.1500	0.1500
Only large cages filled	X . 7 2/3 H_2O	X . 17 H_2O	–
Mole fraction hydrate former	0.1154	0.0556	–
Cavity Diameter (Å)			
Small	7.9	7.8	7.8
Medium	–	–	8.1
Large	8.6	9.5	11.2
Volume of Unit Cell (m^3)	1.728×10^{-27}	5.178×10^{-27}	
Typical Formers	CH_4, C_2H_6, H_2S, CO_2	N_2, C_3H_8, i-C_4H_{10},	See text

[†] *Where X is the hydrate former and Y is a Type H former.*

Table 2: Hydrate Forming Conditions Methane

Temp. (°C)	Press. (MPa)	Phases	Composition (mol %)		
			Aqueous	Vapor	Hydrate
0.0	2.60	L_A-H-V	0.10	0.027	14.1
2.5	3.31	L_A-H-V	0.12	0.026	14.2
5.0	4.26	L_A-H-V	0.14	0.026	14.3
7.5	5.53	L_A-H-V	0.16	0.025	14.4
10.0	7.25	L_A-H-V	0.18	0.024	14.4
12.5	9.59	L_A-H-V	0.21	0.024	14.5
15.0	12.79	L_A-H-V	0.24	0.025	14.5
17.5	17.22	L_A-H-V	0.27	0.025	14.5
20.0	23.4	L_A-H-V	0.30	0.027	14.6
22.5	32.0	L_A-H-V	0.34	0.028	14.6
25.0	44.1	L_A-H-V	0.37	0.029	14.7
27.5	61.3	L_A-H-V	0.41	0.029	14.7
30.0	85.9	L_A-H-V	0.45	0.029	14.7

***Notes**: Composition for aqueous phase and for the hydrate is the mole percent of the hydrate former (CH_4). For the vapor, the composition is the mole percent water.*

Table 3: Physical Properties and Hydrate Formation of Some Common Natural Gas Components (Carroll, 2003)

	Hydrate Structure	Molar Mass (g/mol)	Hydrate Press. at 0°C (MPa)	Normal Boil. Point (K)	Density (kg/m³)	Solubility (mol frac $\times 10^4$)
methane	Type I	16.043	2.603	111.6	19.62	0.46
ethane	Type I	30.070	0.491	184.6	6.85	0.80
propane	Type II	44.094	0.173	231.1	3.49	0.74
isobutane	Type II	58.124	0.113	261.4	3.01	0.31
acetylene	Type I	26.038	0.557	188.4	6.70	14.1
ethylene	Type I	28.054	0.551	169.3	7.11	1.68
propylene	Type II	42.081	0.480	225.5	9.86	3.52
c-propane	Type II	42.081	0.0626	240.3	1.175	2.81
CO_2	Type I	44.010	1.208	194.7[2]	25.56	13.8
N_2	Type II	28.013	16.220	77.4	196.6	0.19
H_2S	Type I	34.080	0.099	213.5	1.50	38.1

Table 4: Properties of Common Chemical Inhibitors (Carroll, 2003)

	methanol	ethanol	EG	TEG
empirical formula	CH_4O	C_2H_6O	$C_2H_6O_2$	$C_6H_{14}O_4$
molar mass, g/mol	32.042	46.07	62.07	150.17
boiling point, °C	64.7	78.4	198	288
vapor press. (at 20°C), kPa	12.5	5.7	0.011	<0.001
melting point, °C	−98	−112	−13	−4.3
density (at 20°C), kg/m³	792	789	1116	1126
viscosity (at 20°C), cp	0.59	1.2	21	49

EG= ethylene glycol, HO-CH_2-CH_2-OH
TEG= triethylene glycol, HO-CH_2-CH_2-O-CH_2-CH_2-O-CH_2-CH_2-OH

Table 5: Ormen Lange Well Temperature Profile

Reservoir temperature	96,0	**[°C]**
Sea bottom temperature	-1,2	**[°C]**
Depth	2013	**[m]**
Temp gradient	0,048	**[°C/m]**

Segment No	Increment [m]	Depth [m] Bottom	Depth [m] Top	Temperature [°C] Bottom	Temperature [°C] Top	Average Temperature [°C]
1	100	2013	1913	96,0	91,2	93,6
2	800	1913	1113	91,2	52,5	71,9
3	400	1113	713	52,5	33,2	42,9
4	713	713	0	33,2	-1,2	16,0

Table 6: Gas Composition Ormen Lange (Valberg, 2005)

Component	Mole Fractions
N2	0.003411
CO2	0.00408
H2O	0.005931
Methane	0.930927
Ethane	0.034719
Propane	0.012177
i-Butane	0.002717
n-Butane	0.00322
i-Pentane	0.00151
n-Pentane	0.001308

Table 7: HYSYS Model Data

HYSYS model data	Ormen Lange	Snøhvit	UNITS
Pipeline:			
Pipeline outer diameter	762	680,7	**[mm]**
Pipeline inner diameter	690	655	**[mm]**
Pipeline vertical distance	875	339	**[m]**
Pipeline length	121	143	**[m]**
Overall heat transfer coefficient	20	20	**[W/m²·°C]**
Roughness	35	35	**[µm]**
Well:			
Well length	4213	2200	**[m]**
Well depth	2013	2200	**[m]**
Production tubing outer diameter	244,5	219,1	**[mm]**
Production tubing inner diameter	215,9	193,7	**[mm]**
Overall heat transfer coefficient	4	4	**[W/m²·°C]**
Roughness	53	35	**[µm]**
Temperatures:			
Reservoir temperature	96	92	**[°C]**
Ambient temperature	2,5	4	**[°C]**
Extreme temperature	-1,2	-	**[°C]**
Pressures:			
Arrival pressure	90	75	**[bar]**
Reservoir pressure	290	267	**[bar]**
Production:			
Field gas rate	70	20,8	**[MSm³/day]**
Number of wells	8	9	
Well gas rate	8,75	2,31	**[MSm³/day]**

Table 8: HYSYS Model Data Reference Table

References		
HYSYS model data	**Ormen Lange**	**Snøhvit**
Pipeline:		
Pipeline outer diameter	(Heskestad, 2004)	(Gudmundsson, 2012)
Pipeline inner diameter	(Henriksson, et al., 2004)	(Gudmundsson, 2012)
Pipeline vertical distance	(Gupta, 2011)	(Pettersen, 2011)
Pipeline length	(Gupta, 2011)	(Pettersen, 2011)
Overall heat transfer coefficient	(Gudmundsson, 2012)	(Gudmundsson, 2012)
Roughness	(Gudmundsson, 2012)	(Gudmundsson, 2012)
Well:		
Well length	(Heskestad, 2004)	(Gudmundsson, 2012)
Well depth	(Heskestad, 2004)	(Gudmundsson, 2012)
Production tubing outer diameter	(Valberg, 2005)	Assumed
Production tubing inner diameter	(Valberg, 2005)	Assumed
Overall heat transfer coefficient	(Gudmundsson, 2012)	(Gudmundsson, 2012)
Roughness	(Gudmundsson, 2012)	(Gudmundsson, 2012)
Temperatures:		
Reservoir temperature	(Heskestad, 2004)	(Gudmundsson, 2012)
Ambient temperature	(Heskestad, 2004)	Assumed
Extreme temperature	(Heskestad, 2004)	Assumed
Pressures:		
Arrival pressure	(Gupta, 2011)	(Heiersted, 2004)
Reservoir pressure	(Heskestad, 2004)	(Gudmundsson, 2012)
Production:		
Field gas rate	(Gupta, 2011)	(Pettersen, 2011)
Number of wells	(Gudmundsson, 2012)	(Pettersen, 2011)
Well gas rate	Calculated	Calculated

Table 9: Pipeline Diameter Table

Pipeline Type	Pipe diameter [mm]	Design Pressure/ Reference Height [bara@m]	Design Temp. (min/ max) [°C]	Medium Density [kg/m^3]	Design life [years]	Material
30" Multiphase PL-A	ID = 690.0	255 / 200 @ -890m	-20 / 80	80-200	50	X65 Carbon steel
30" Multiphase PL-B	ID = 690.0	255 / 200 @ -890m	-20 / 80	80-200	50	X65 Carbon steel
6 5/8" MEG-A	OD = 168.3	345 @ -890m	-10 / 50	1125	50	X65 Carbon steel
6 5/8" MEG-B	OD = 168.3	345 @ -890m	-10 / 50	1125	50	65 Carbon steel
6 5/8" MEG Cross-over A-B	OD = 168.3	345 @ 30m	-10 / 50	1125	50	X65 Carbon steel
20" Multiphase Cross-over spool	OD = 508.0	255 /200 @ -890m	-20 / 80	80-200	50	X65 Carbon steel

Table 10: Snøhvit Well Temperature Profile

Reservoir temperature	92	**[°C]**
Sea bottom temperature	4	**[°C]**
Depth	2200	**[m]**
Temp gradient	0,04	**[°C/m]**

Segment No	Increment [m]	Depth [m] Bottom	Depth [m] Top	Temperature [°C] Bottom	Temperature [°C] Top	Average Temperature [°C]
1	300	2200	1900	92,0	80,0	86
2	300	1900	1600	80,0	68,0	74
3	300	1600	1300	68,0	56,0	62
4	300	1300	1000	56,0	44,0	50
5	300	1000	700	44,0	32,0	38
6	300	700	400	32,0	20,0	26
7	300	400	100	20,0	8,0	14
8	100	100	0	8,0	4,0	6

Table 11: Gas Composition Snøhvit (Gudmundsson, 2012)

Component	Mole Fraction
Nitrogen	0.0253
CO2	0.0526
Methane	0.8102
Ethane	0.0503
Propane	0.0253
i-Butane	0.0040
n-Butane	0.0083
i-Pentane	0.0021
n-Pentane	0.0031
C6*	0.0035
C7*	0.0039
C8*	0.0032
C9*	0.0014
Benzene	0.0008
Toluene	0.0009
p-Xylene	0.0006
C10*	0.0014
C11*	0.0006
C12*	0.0006
C13*	0.0005
C14*	0.0003
C15*	0.0003
C16*	0.0002
C17*	0.0002
C18*	0.0001
C19*	0.0001
C20+*	0.0002
H2S	5.E-06
Phenol	2.E-06
Helium	0.0002

Table 12: The Summary of the Most Accurate Method

THE SUMMARIZE OF THE MOST ACCURATE METHOD		
PR 30" PIPELINE!!	MeOH	MEG
In water, kg/MSm3	2822,3	6403,1
In gas, kg/MSm3	898,26	5,9E-02
In condensate, kg/MSm3	2,4E-01	2,1E-03
Total, kg/MSm3	3720,8	6403,2
Total, Sm3/MSm3	4,7	5,8
Total kg/D	**1,3E+05**	**2,2E+05**
Total Sm3/D	**164,5**	**201,3**
FIELD TOTAL kg/D	**2,6E+05**	**4,5E+05**
FIELD TOTAL Sm3/D	**328,9**	**402,6**
In water, lbm/MMscf	176,1	399,5
In gas, lbm/MMscf	56,0	3,7E-03
In condensate, lbm/MMscf	1,5E-02	1,3E-04
Total, lbm/MMscf	**232,1**	**399,5**
Total, gal/MMscf	**35,2**	**43,0**

Table 13: Ormen Lange Case Comparison

SF=5%	Table for case comparison					
	U=15 [W/m²·°C]	U=20 [W/m²·°C]	U=25 [W/m²·°C]	Shut-in	Shut-in with SF	Norsk Hydro
Tmin [°C]	-2,29	-2,14	-1,72	-1,20	-1,26	-5,00
Tmin[°K]	270,86	271,01	271,43	271,95	271,89	268,15
wt% MeOH	33,63	33,43	32,82	37,04	38,89	41,75
wt% MEG	49,10	48,79	47,86	54,78	57,52	64,07

Table 14: Why Hydrate Plugs may Form, and Where

Why hydrate plugs may form	
Flowing conditions, storegga slide edge	No- flowing conditions, deepest sea bottom
MEG-injection failure	Commissioning in new in-field flowlines
Undetected formation water break through	Cooled by cold sea water or commissioning fluid

Table 15: Inflection Point Data from Base Case Snøhvit

	Inflection point data from base case Snøhvit									
	No inhibitor	**MEG**			**MeOH**		**Extreme point**	**Inflection points**		**End point**
	0 wt%	**20 wt%**	**30 w%**	**40 wt%**	**20 wt%**	**30 wt%**	**30,2 wt% MeOH**			
Distance from PLEM [m]	13403	21076	30022	65702	32342	95785	96716	121343	138806	143284
Temperature [°C]	19,45	13,37	8,95	3,37	8,10	1,16	0,99	3,20	1,82	0,52
Pressure [bar]	114,4	112,6	110,3	102,4	109,7	91,2	90,6	86,0	78,5	75,0

Table 16: Snøhvit Case Comparison

U=[W/m²·°C]	Table for case comparison		
	U=15	U=20	U=25
Toutlet [°C]	-0,15	0,51	0,96
Toutlet [°K]	273,00	273,66	274,11
wt% MeOH	30,73	29,75	29,09
wt% MEG	44,81	43,45	42,55

Table 17: Snøhvit Base Case Extreme Point with SF

Extreme point wt% with safety factor of 5%		
MeOH	31,7	wt%
MEG	46,3	wt%

Table 18: Effects of Inhibitor Injection on Outlet Temperature

U=[W/m²·°C]	No inhibitor injection		
	Table for case comparison		
	U=15	U=20	U=25
Toutlet [°C]	-0,15	0,51	0,96
Toutlet [°K]	273,00	273,66	274,11
wt% MeOH	30,73	29,75	29,09
wt% MEG	44,81	43,45	42,55
U=[W/m²·°C]	MEG injection		
	Table for case comparison		
	U=15	U=20	U=25
Toutlet [°C]	-0,17	0,52	0,95
Toutlet [°K]	272,98	273,67	274,10
wt% MeOH	30,73	29,77	29,09
wt% MEG	44,81	43,47	42,55
U=[W/m²·°C]	MeOH injection		
	Table for case comparison		
	U=15	U=20	U=25
Toutlet [°C]	-0,16	0,50	0,94
Toutlet [°K]	272,99	273,65	274,09
wt% MeOH	30,73	29,76	29,09
wt% MEG	44,81	43,46	42,55

Table 19: Upstream Field Volume Inhibitor Snøhvit

	Snøhvit		MeOH	MEG	MeOH	MEG
Inhibitor retention time:			**Weight [kg]**		**Costs [1000US$]**	
Injecion pipeline	7					
From wellhead to slugcatcher	5					
Total	12					
Base Case	**MeOH**	**MEG**	**Base Case**		**Base Case**	
Injection rate [Sm³/D]	70,4	63,9	55733,0	71090,0	16,7	64,0
Upstream field volume [Sm³]	844,7	766,3	668796,0	853080,1	200,6	767,8
Base Case with SF=5%	**MeOH**	**MEG**	**Base Case with SF=5%**		**Base Case with SF=5%**	
Injection rate [Sm³/D]	75,2	69,8	59560,5	77688,2	17,9	69,9
Upstream field volume [Sm³]	902,7	837,5	714725,9	932257,9	214,4	839,0
Corresponding to 60 wt% MEG	**MeOH**	**MEG**	**Corresponding to 60 wt% MEG**		**Corresponding to 60 wt% MEG**	
Injection rate [Sm³/D]	104,5	121,6	82706,1	135338,4	24,8	121,8
Upstream field volume [Sm³]	1253,4	1458,9	992473,3	1624060,7	297,7	1461,7

Table 20: Calculated Values of Depression of Hydrate Point (°C) For Various Thermodynamic Inhibitors (Kelland, 2000)

Depression of hydrate point [°C]						
Concentration of inhibitor [wt%]	MeOH	EtOH	MEG	DEG	TEG	NaCl
5	2.0	1.4	1.05	0.63	0.46	1.96
10	4.2	3.0	2.25	1.4	1.05	4.3
20	9.3	6.6	5.2	3.3	2.7	10.7
30	15.3	10.7	9.0	5.9	5.0	15.0
35	18.6	13.0	11.35	7.5	6.5	-
40	22.2	15.4	14.0	9.3	8.2	-

Table 21: Rough Costs for Common Thermodynamic Inhibitors (Brustad, et al., 2005)

Chemical	Cost USD/Metric Tonne
MeOH	300
MEG	900

Offshore shipping cost is approximately 150-200 USD/tonne of chemical.

Table 22: Summary of Inhibitor Comparison from Ormen Lange and Snøhvit

60 wt%	Ormen Lange		Snøhvit	
	MeOH	MEG	MeOH	MEG
Wt% in aqueous phase	39,8	60,0	39,8	60,0
Inhibitor Volume In The Pipelines [Sm³]			1253,4	1458,9
Injection rate [Sm3/D]	329	402	104,5	121,6
Pump ΔP [bar]	108,3	86	196,6	230,1
Pump effect [kW] @ ŋ=0,75	54,7	53,2	31,5	42,9
Amount lost to condensate [Sm3/D]	2,1E-02	1,5E-04	3,2	2,1E-02
Amount lost to vapor [Sm3/D]	79,4	3,7E-03	25,9	1,2E-03

From my calculations	Ormen Lange		Snøhvit	
	MeOH	MEG	MeOH	MEG
Wt% in aqueous phase	37,0	54,8	30,2	44,1
Inhibitor Volume In The Pipelines [Sm³]			844,7	766,3
Injection rate [Sm3/D]	295	325	70,4	63,9
Pump ΔP [bar]	107,8	83,8	191,6	204,5
Pump effect [kW] @ ŋ=0,75	48,8	41,8	20,7	20,1
Amount lost to condensate [Sm3/D]	1,9E-02	1,1E-04	2,4	1,3E-02
Amount lost to vapor [Sm3/D]	72,8	3,7E-03	18,7	1,2E-03

From my calculations, included SF=5%	Ormen Lange		Snøhvit	
	MeOH	MEG	MeOH	MEG
Wt% in aqueous phase	38,9	57,5	31,7	46,3
Inhibitor Volume In The Pipelines [Sm³]			902,7	837,5
Injection rate [Sm3/D]	317	363	75,2	69,8
Pump ΔP [bar]	108,1	84,9	192,2	207,2
Pump effect [kW] @ ŋ=0,75	52,6	47,4	22,2	22,2
Amount lost to condensate [Sm3/D]	2,0E-02	1,2E-04	2,5	1,4E-02
Amount lost to vapor [Sm3/D]	77,2	3,7E-03	19,8	1,2E-03

Table 23: Snøhvit 60 wt% MEG

COMPARISON OF MeOH AND MEG REQUIRED		
	MeOH	**MEG**
In water, kg/MSm3	2868,0	6505,5
In gas, kg/MSm3	985,9	6,4E-02
In condensate, kg/MSm3	126,4	1,1E+00
Total, kg/MSm3	3980,3	6506,7
Total, Sm3/MSm3	5,03	5,85
Total kg/D	**8,3E+04**	**1,4E+05**
Total Sm3/D	**104,56**	**121,58**

Table 24: Snøhvit Base Case Including Safety Factor=5%

COMPARISON OF MeOH AND MEG REQUIRED		
	MeOH	**MEG**
In water, kg/MSm3	2013,8	3735,0
In gas, kg/MSm3	753,1	6,4E-02
In condensate, kg/MSm3	96,5	7,6E-01
Total, kg/MSm3	2863,5	3735,8
Total, Sm3/MSm3	3,62	3,36
Total kg/D	**6,0E+04**	**7,8E+04**
Total Sm3/D	**75,22**	**69,80**

Table 25: Snøhvit Base Case

COMPARISON OF MeOH AND MEG REQUIRED		
	MeOH	**MEG**
In water, kg/MSm3	1876,5	3417,0
In gas, kg/MSm3	711,8	6,4E-02
In condensate, kg/MSm3	91,2	7,0E-01
Total, kg/MSm3	2679,5	3417,8
Total, Sm3/MSm3	3,38	3,07
Total kg/D	**5,6E+04**	**7,1E+04**
Total Sm3/D	**70,39**	**63,86**

Table 26: Ormen Lange Shut-in Case (60 wt% MEG)

COMPARISON OF MeOH AND MEG REQUIRED		
PR 30" PIPELINE!!	MeOH	MEG
In water, kg/MSm3	2821,8	6400,5
In gas, kg/MSm3	898,1	5,9E-02
In condensate, kg/MSm3	2,4E-01	2,1E-03
Total, kg/MSm3	3720,1	6400,5
Total, Sm3/MSm3	4,7	5,7
Total kg/D	**1,3E+05**	**2,2E+05**
Total Sm3/D	**1,6E+02**	**2,0E+02**
FIELD TOTAL kg/D	**2,6E+05**	**4,5E+05**
FIELD TOTAL Sm3/D	**3,3E+02**	**4,0E+02**

Table 27: Ormen Lange Base Case Including Safety Factor=5%

COMPARISON OF MeOH AND MEG REQUIRED		
PR 30" PIPELINE!!	MeOH	MEG
In water, kg/MSm3	2715,8	5776,9
In gas, kg/MSm3	873,3	5,9E-02
In condensate, kg/MSm3	2,3E-01	1,9E-03
Total, kg/MSm3	3589,4	5777,0
Total, Sm3/MSm3	4,5	5,2
Total kg/D	**1,3E+05**	**2,0E+05**
Total Sm3/D	**1,6E+02**	**1,8E+02**
FIELD TOTAL kg/D	**2,5E+05**	**4,0E+05**
FIELD TOTAL Sm3/D	**3,2E+02**	**3,6E+02**

Table 28: Ormen Lange Base Case

COMPARISON OF MeOH AND MEG REQUIRED		
PR 30" PIPELINE!!	MeOH	MEG
In water, kg/MSm3	2510,4	5168,6
In gas, kg/MSm3	823,7	5,9E-02
In condensate, kg/MSm3	2,2E-01	1,8E-03
Total, kg/MSm3	3334,3	5168,7
Total, Sm3/MSm3	4,2	4,6
Total kg/D	**1,2E+05**	**1,8E+05**
Total Sm3/D	**1,5E+02**	**1,6E+02**
FIELD TOTAL kg/D	**2,3E+05**	**3,6E+05**
FIELD TOTAL Sm3/D	**2,9E+02**	**3,3E+02**

Table 29

COMPARISON OF MeOH AND MEG REQUIRED		
PR 30" PIPELINE!!	MeOH	MEG
In water, kg/MSm3	2821,8	6400,5
In gas, kg/MSm3	898,12	5,9E-02
In condensate, kg/MSm3	0,2359	2,1E-03
Total, kg/MSm3	3720,1	6400,5
Total, Sm3/MSm3	4,70	5,75
Total kg/D	**1,30E+05**	**2,24E+05**
Total Sm3/D	**164,44**	**201,24**
FIELD TOTAL kg/D	**2,60E+05**	**4,48E+05**
FIELD TOTAL kg/D	**328,88**	**402,48**
In water, lbm/MMscf	176,0	399,3
In gas, lbm/MMscf	56,0	3,7E-03
In condensate, lbm/MMscf	1,5E-02	1,3E-04
Total, lbm/MMscf	**232,1**	**399,3**
Total, gal/MMscf	**35,2**	**43,0**

15 Figures

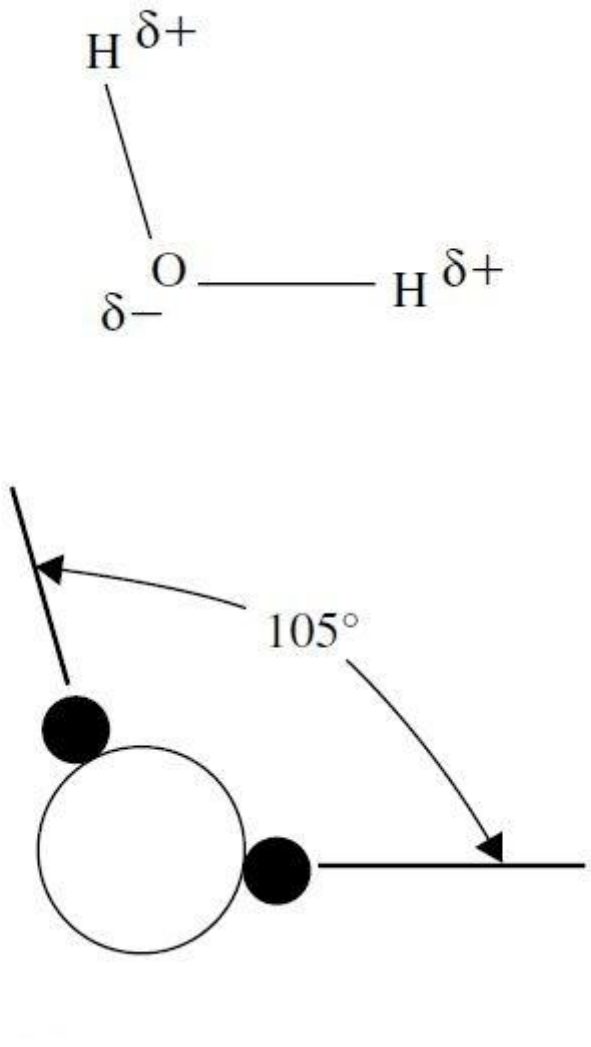

Figure 1: The Shape of the Water Molecule

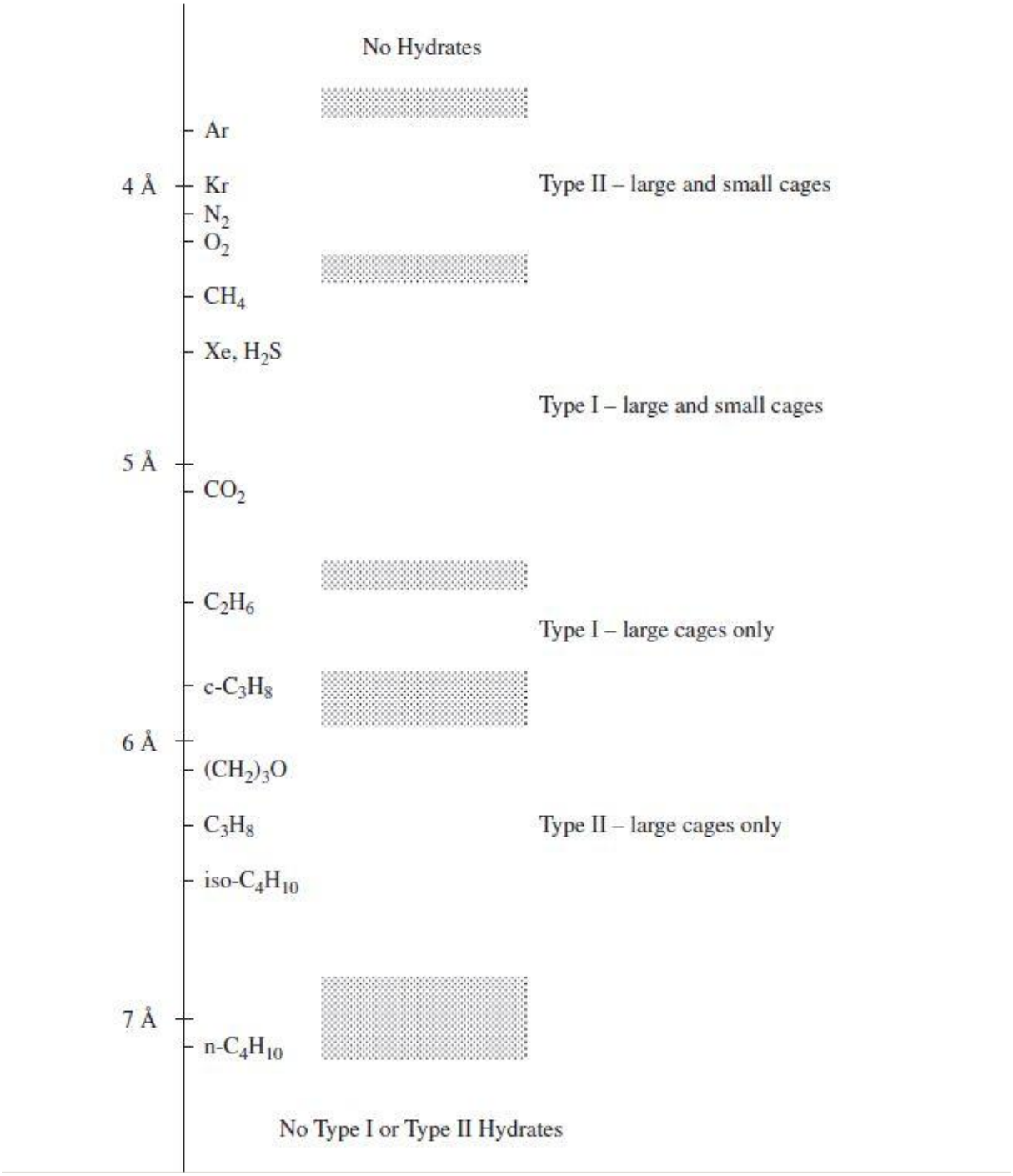

Figure 2: Comparison of Guest Size, Hydrate Type, and Cavities Occupied for Various Hydrate Formers (modified from the original by (von Stackelberg, 1949))

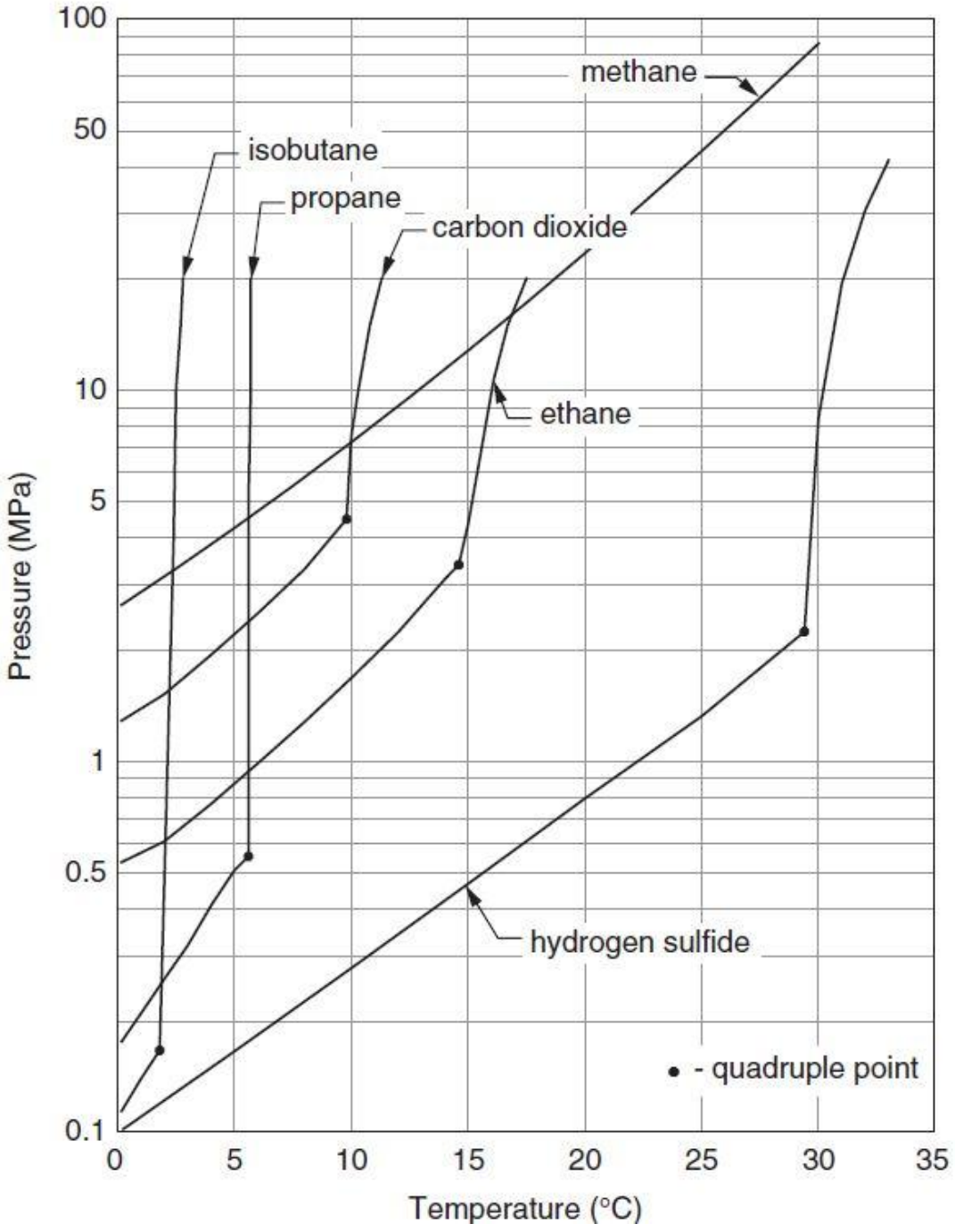

Figure 3: Hydrate Loci for Several Compounds Found in Natural Gas (Carroll, 2003)

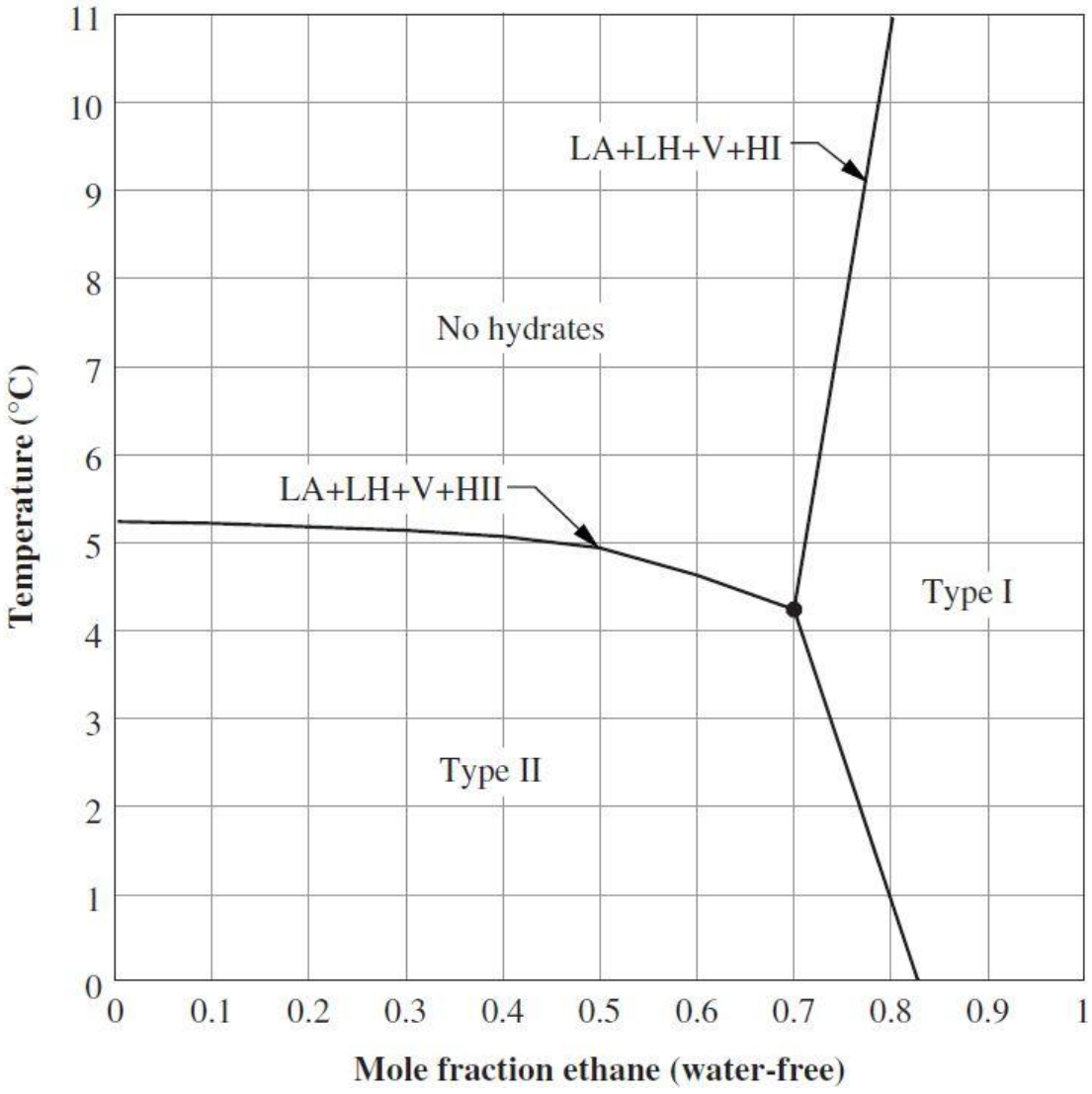

Figure 4: Hydrate Formation Map for A Mixture Of Ethane and Propane (base on Holder and Hands)(Holder & Hand, 1982)

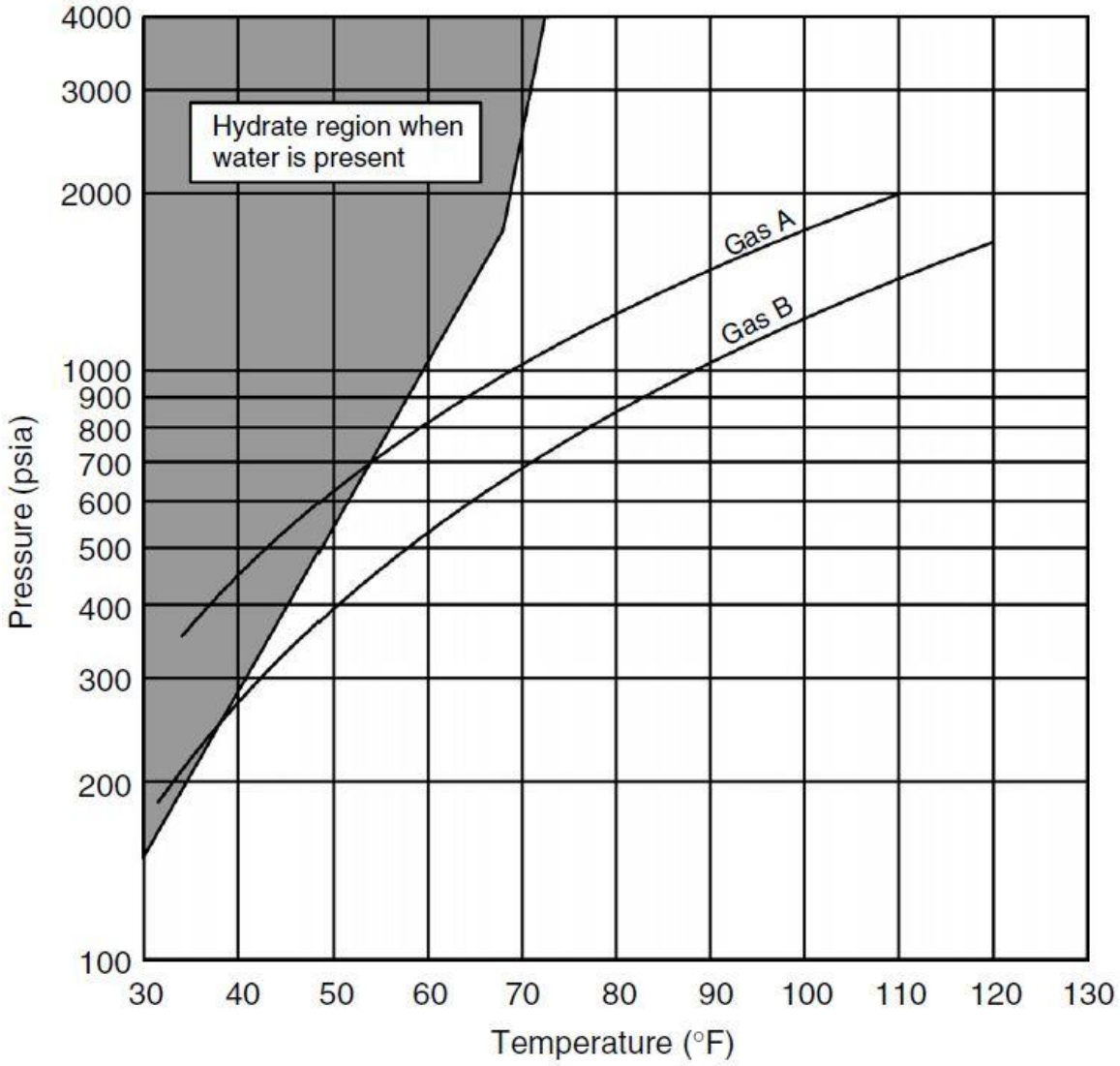

Figure 5: Expansion of Two Gases into Hydrate Formation Region (Sloan & Koh, 2008)

$$\Delta H = Q + W_S$$

Figure 6: 1st Law of Thermodynamics(Sloan & Koh, 2008)

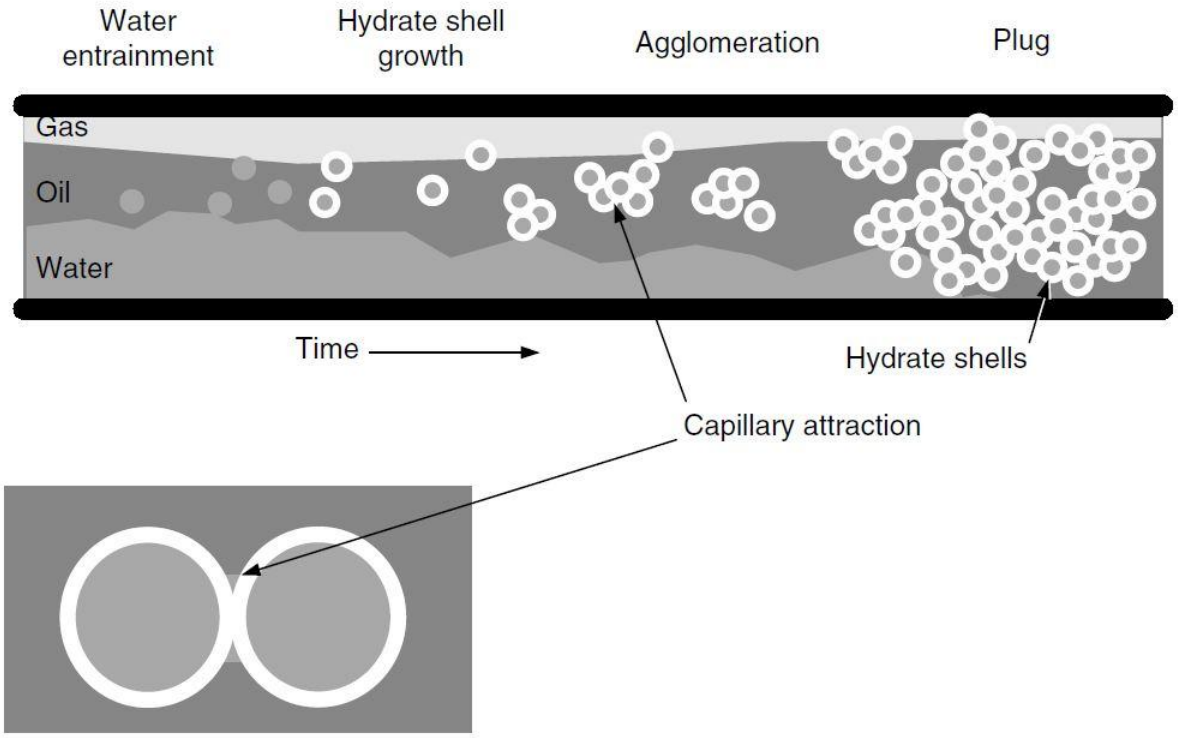

Figure 7: Conceptual Figure of Hydrate Formation in an Oil-Dominated System (Sloan & Koh, 2008)

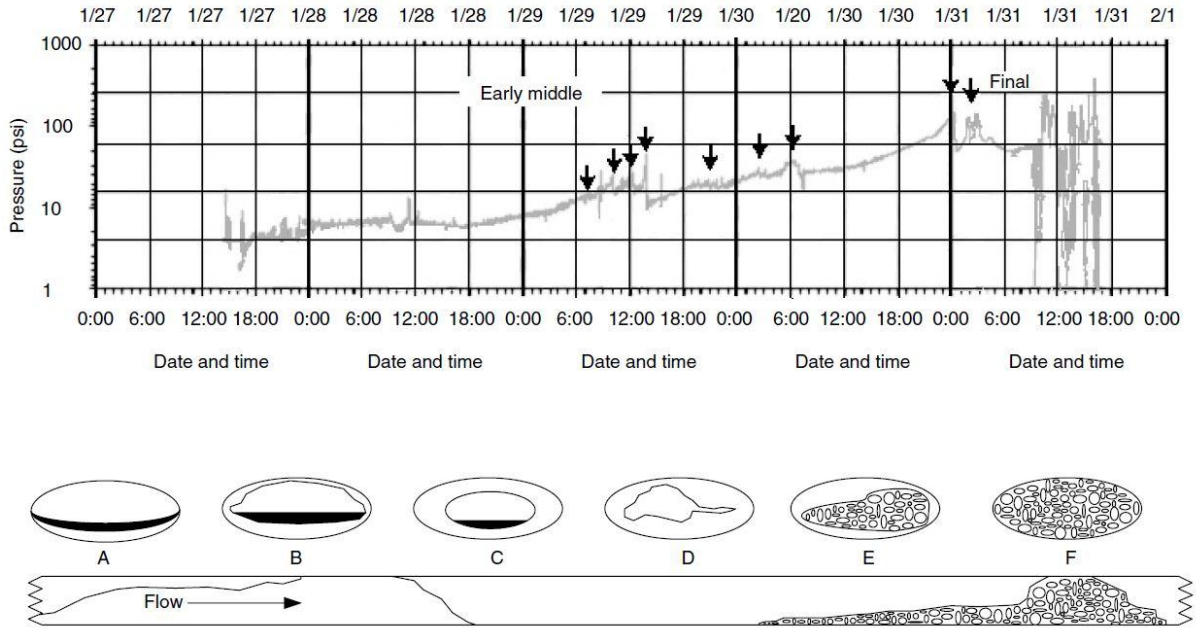

Figure 8: Hydrate Blockage Formation (bottom) and Corresponding Pressure Buildup (top) in A Gas-Dominated Pipeline (Sloan & Koh, 2008)

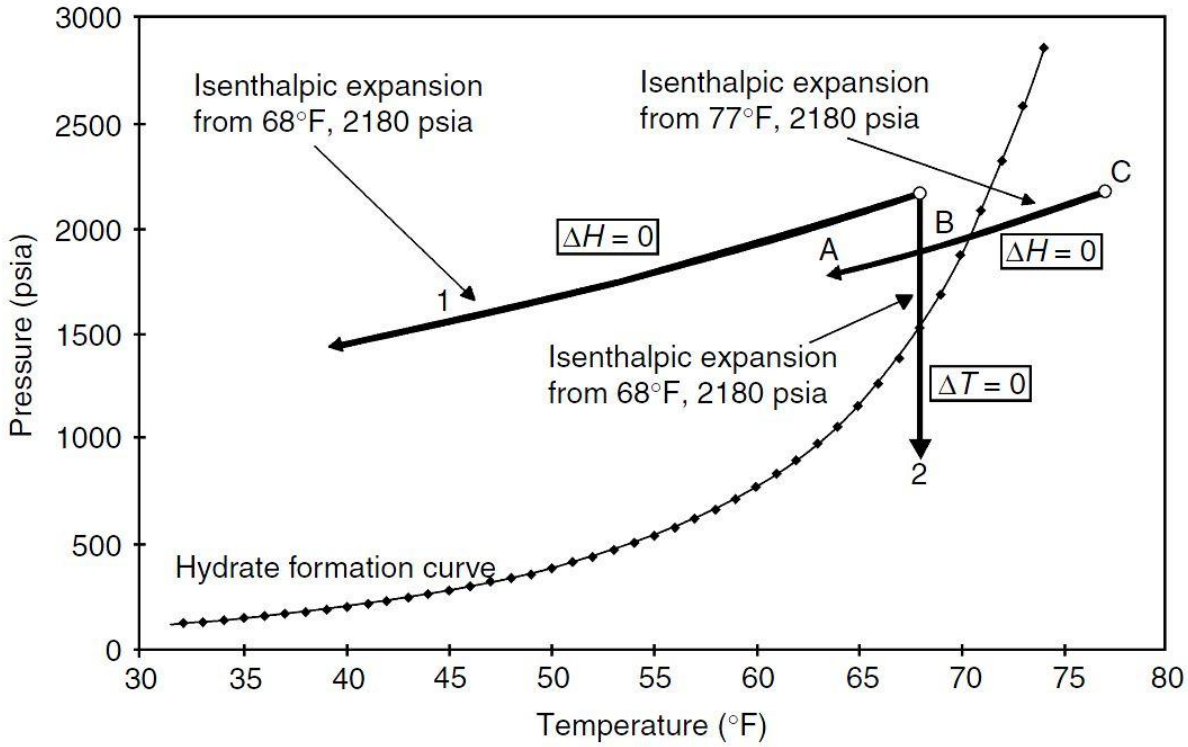

Figure 9: Pressure Dissociation (Sloan & Koh, 2008)

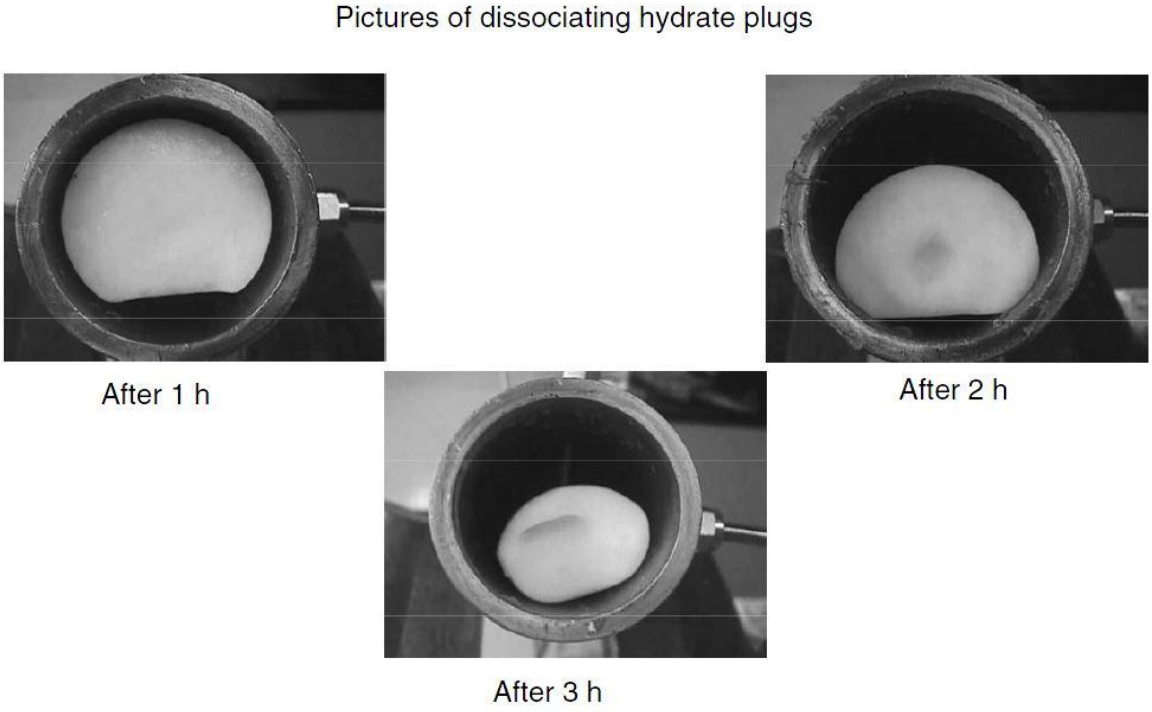

Figure 10: Radial Dissociation of Hydrate Plugs in Three Experiments (Peters, 1999)

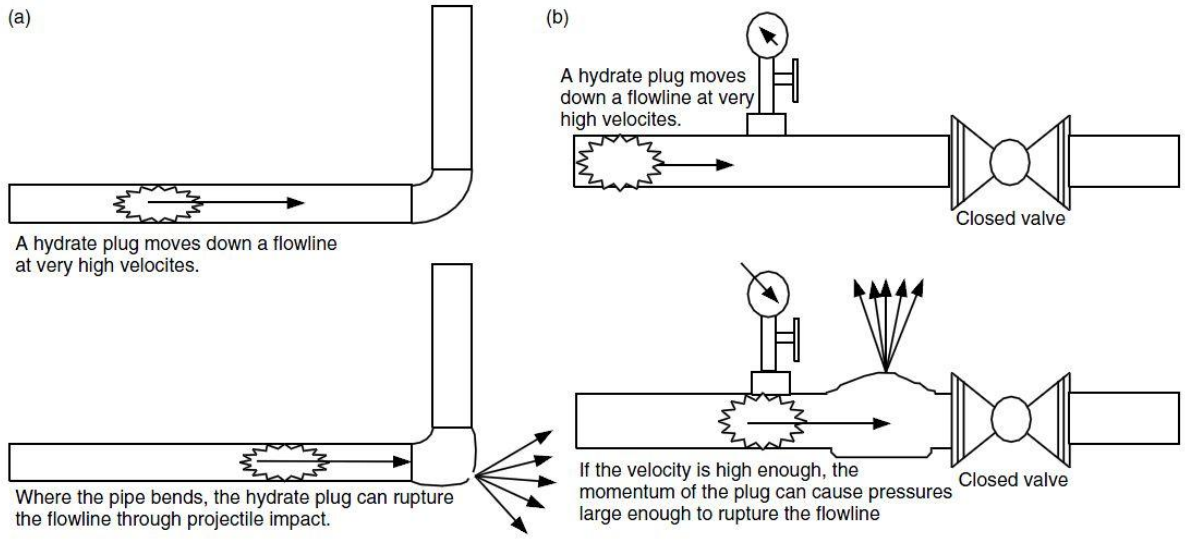

Figure 11: Two Ways a Hydrate Plug Can Rupture a Pipe (Sloan & Koh, 2008)

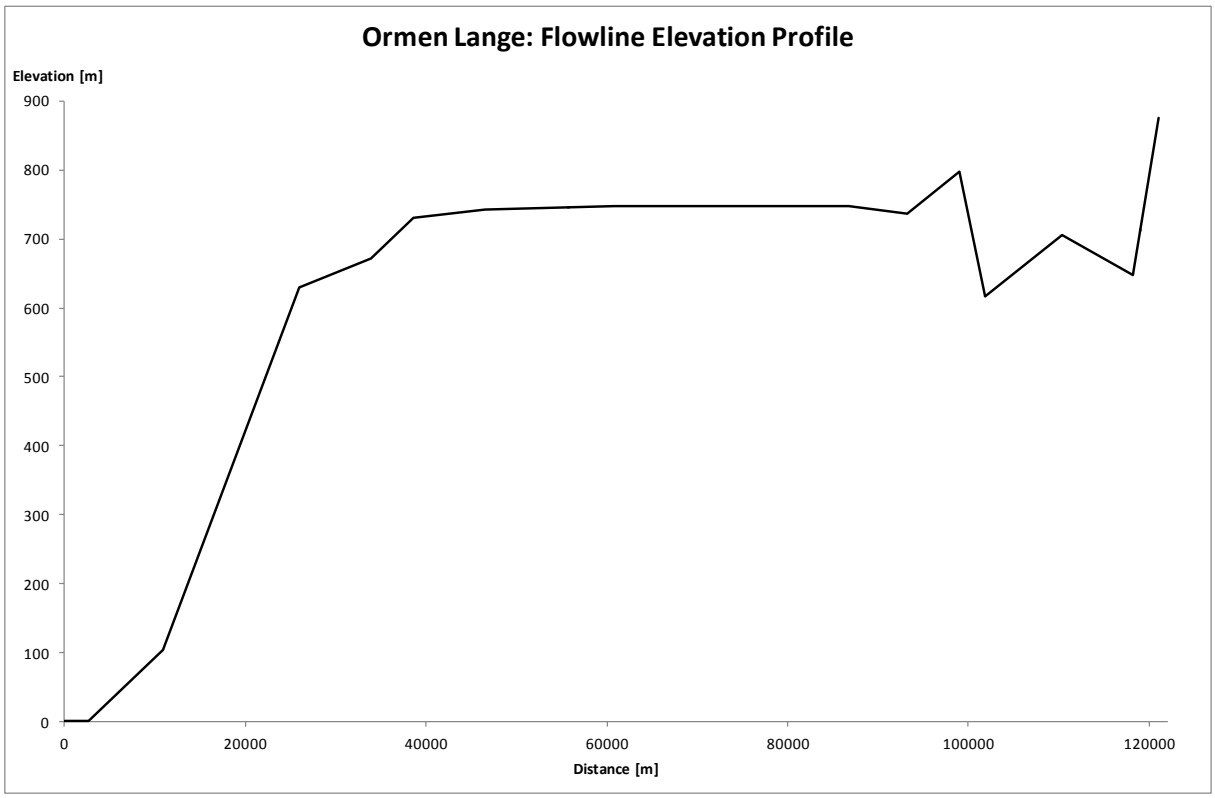

Figure 12: Ormen Lange Flowline Elevation Profile (Biørnstad, 2006)

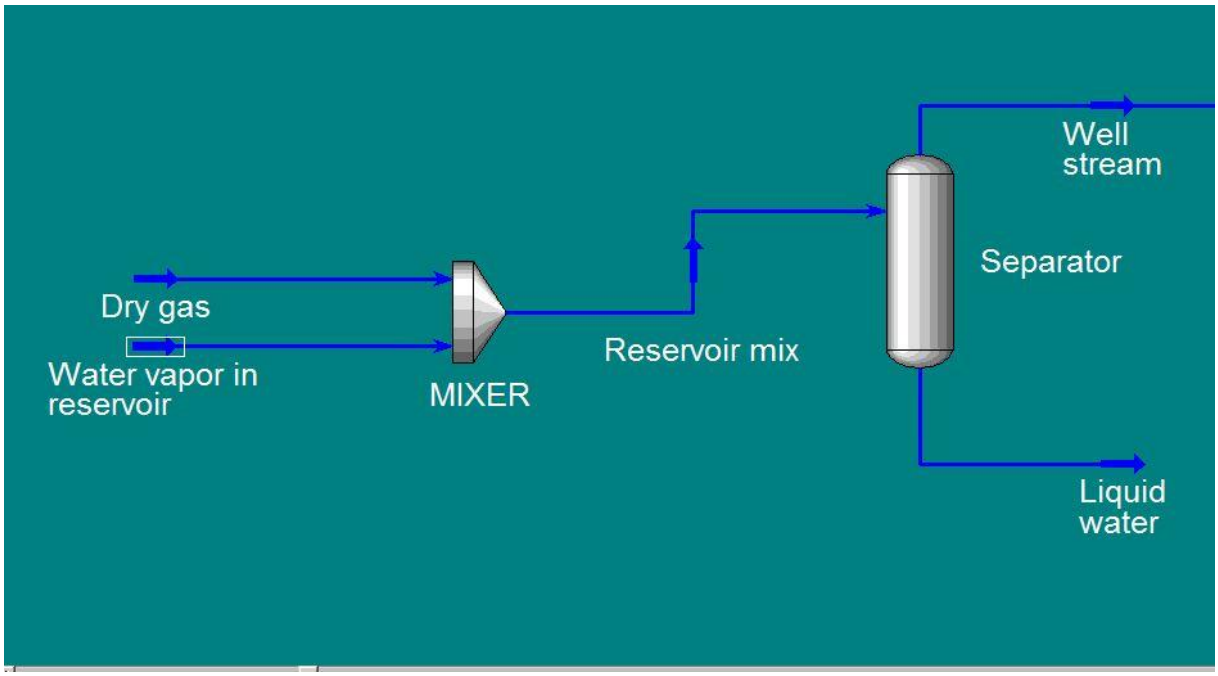

Figure 13: Reservoir Gas

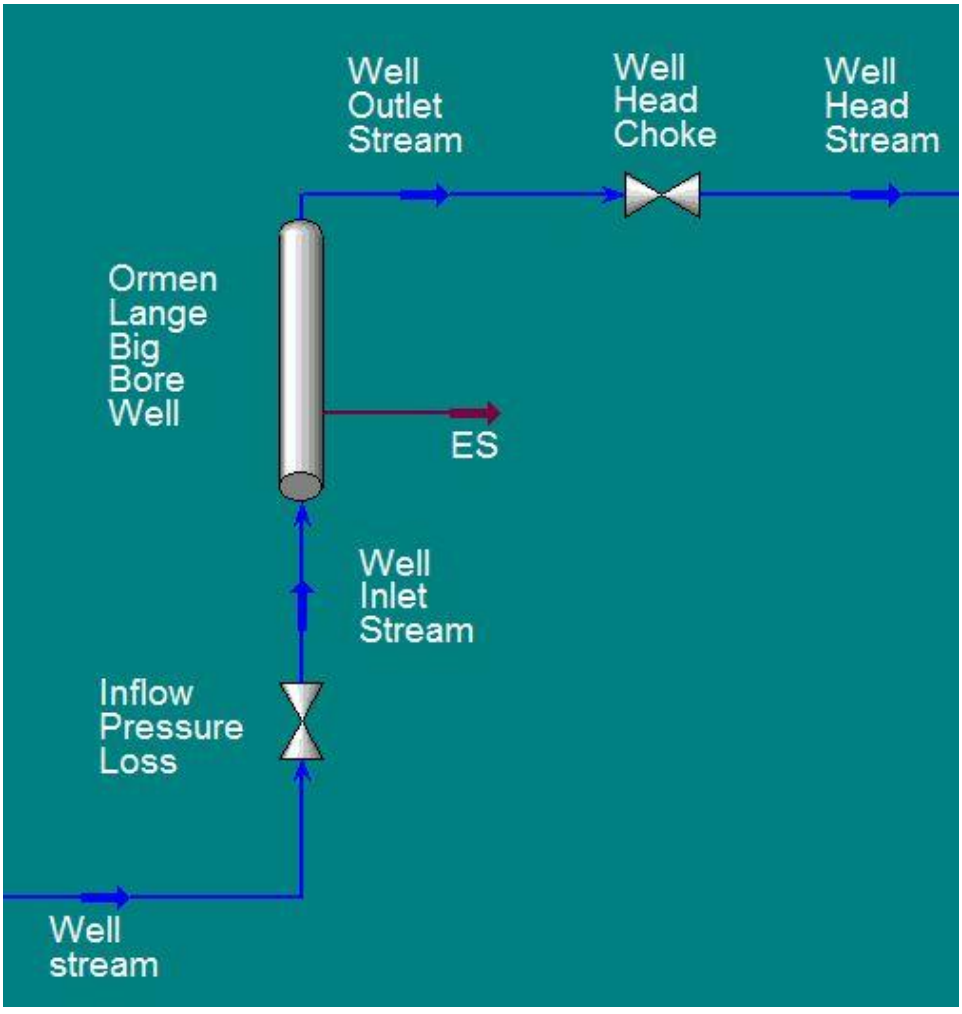

Figure 14: Ormen Lange Well

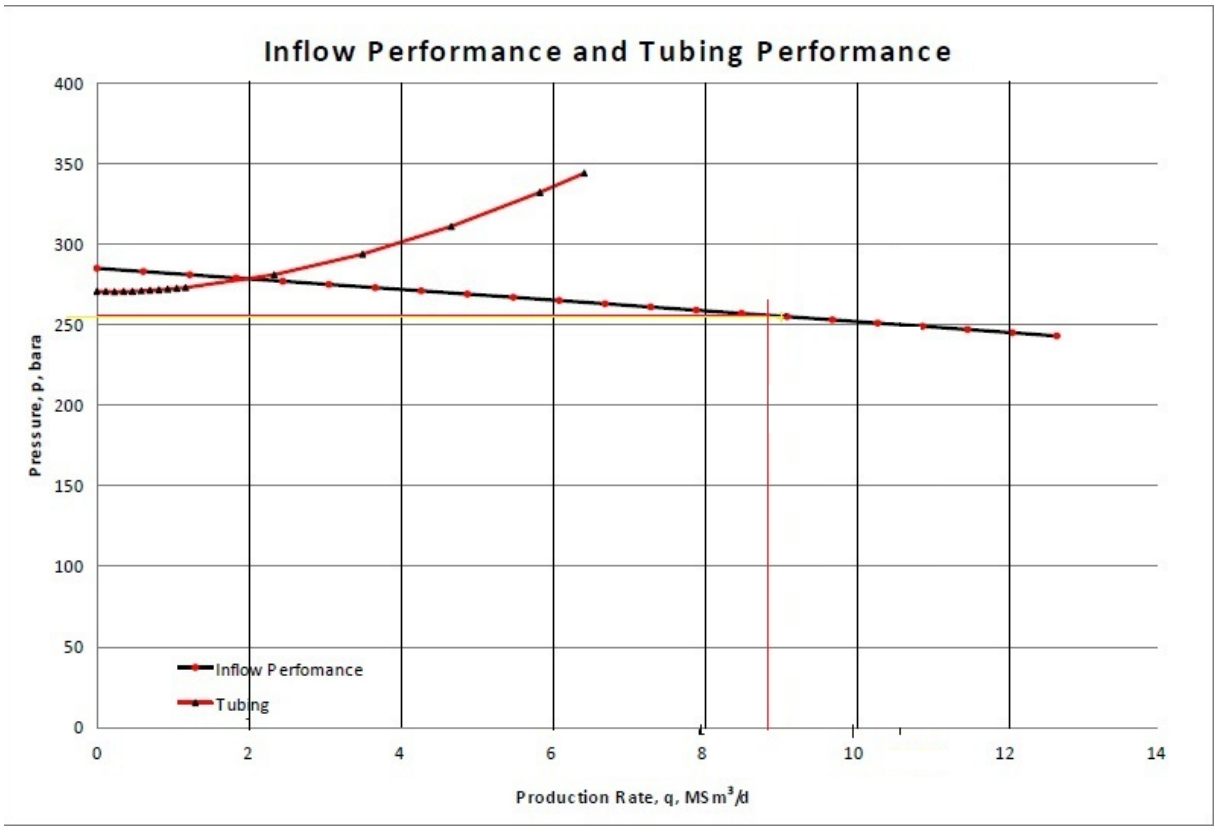

Figure 15: Inflow Performance and Tubing Performance

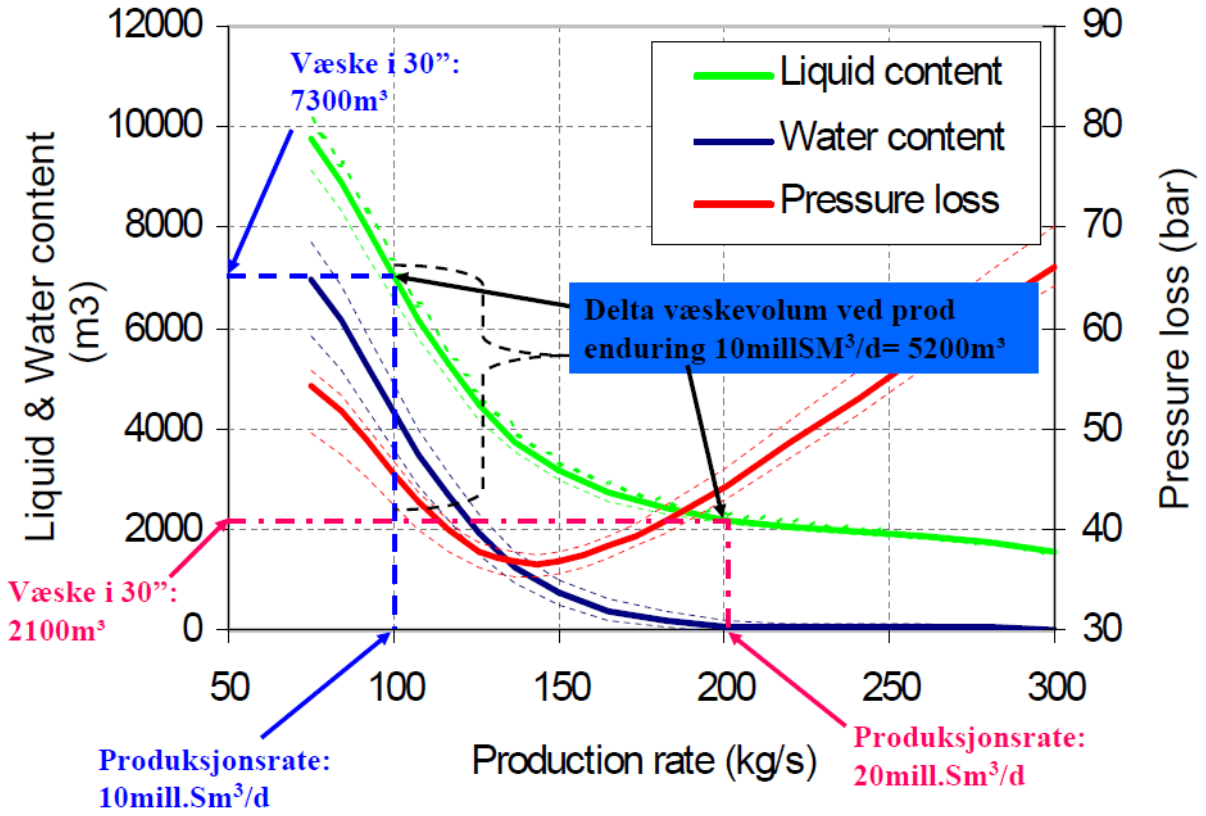

Figure 16: Liquid Loading vs Rate and Production Rate

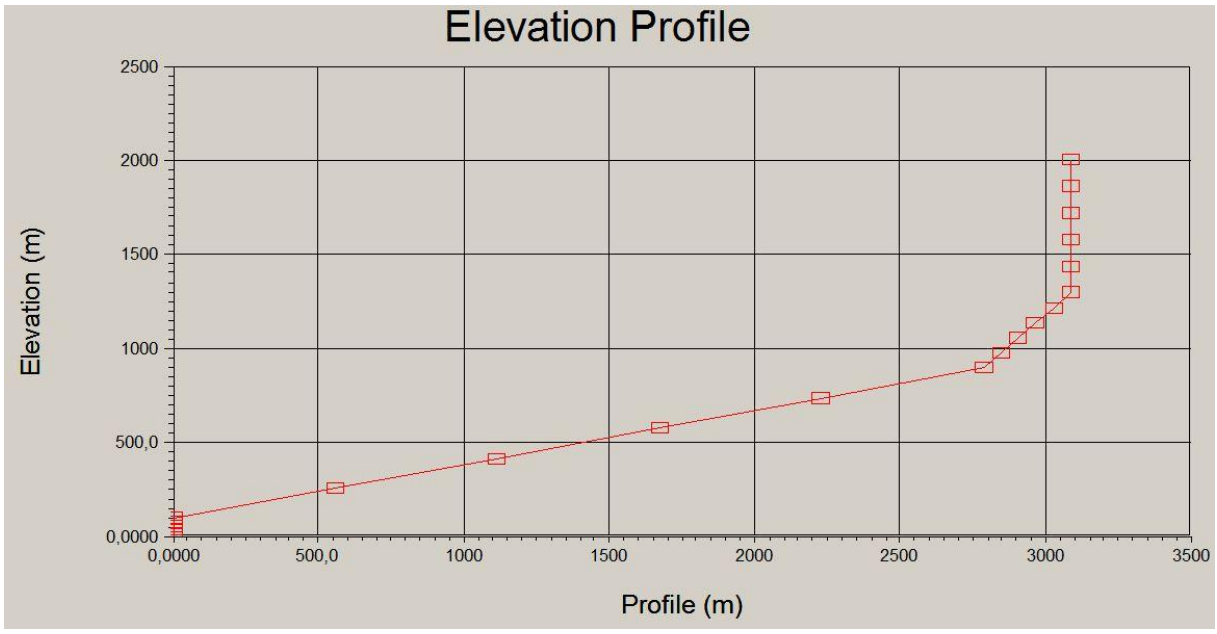

Figure 17: Ormen Lange Well Elevation Profile

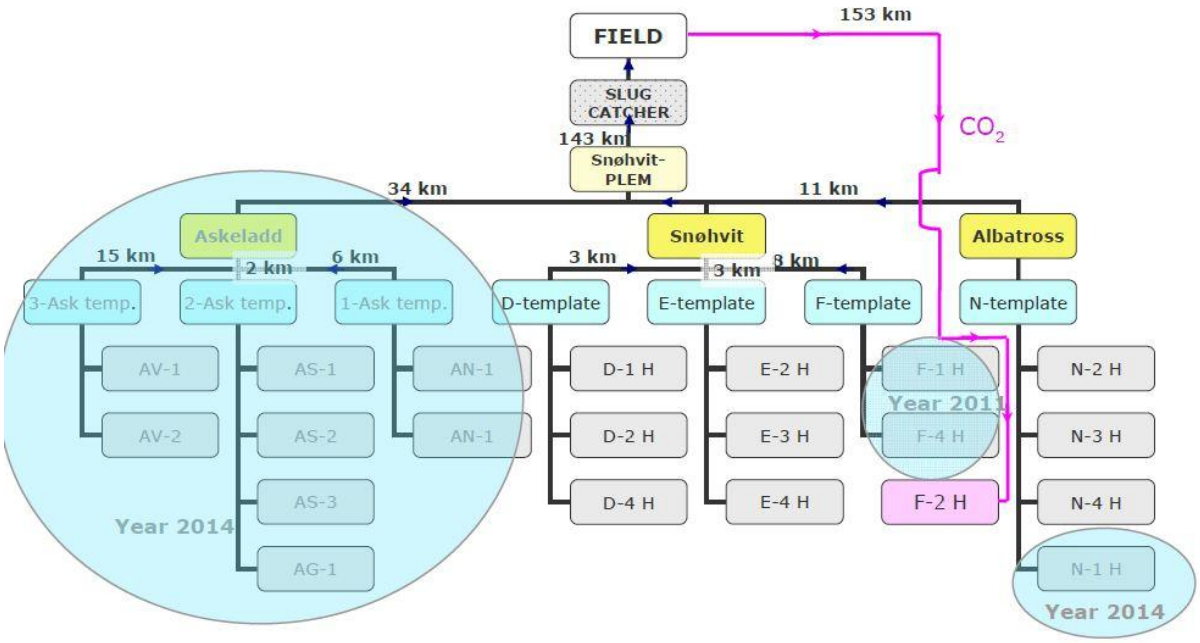

Figure 18: Network Hierarchy, Snøhvit Field Development (Pettersen, 2011)

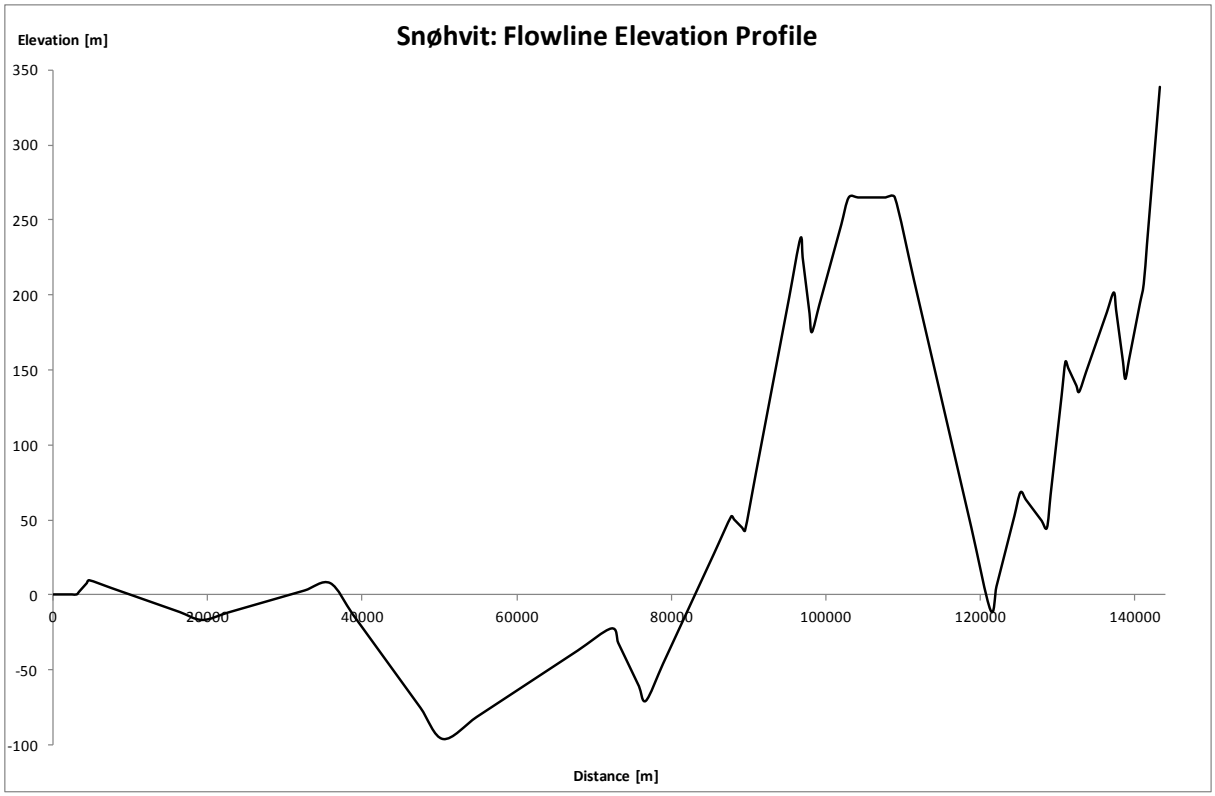

Figure 19: Snøhvit Flowline Elevation Profile

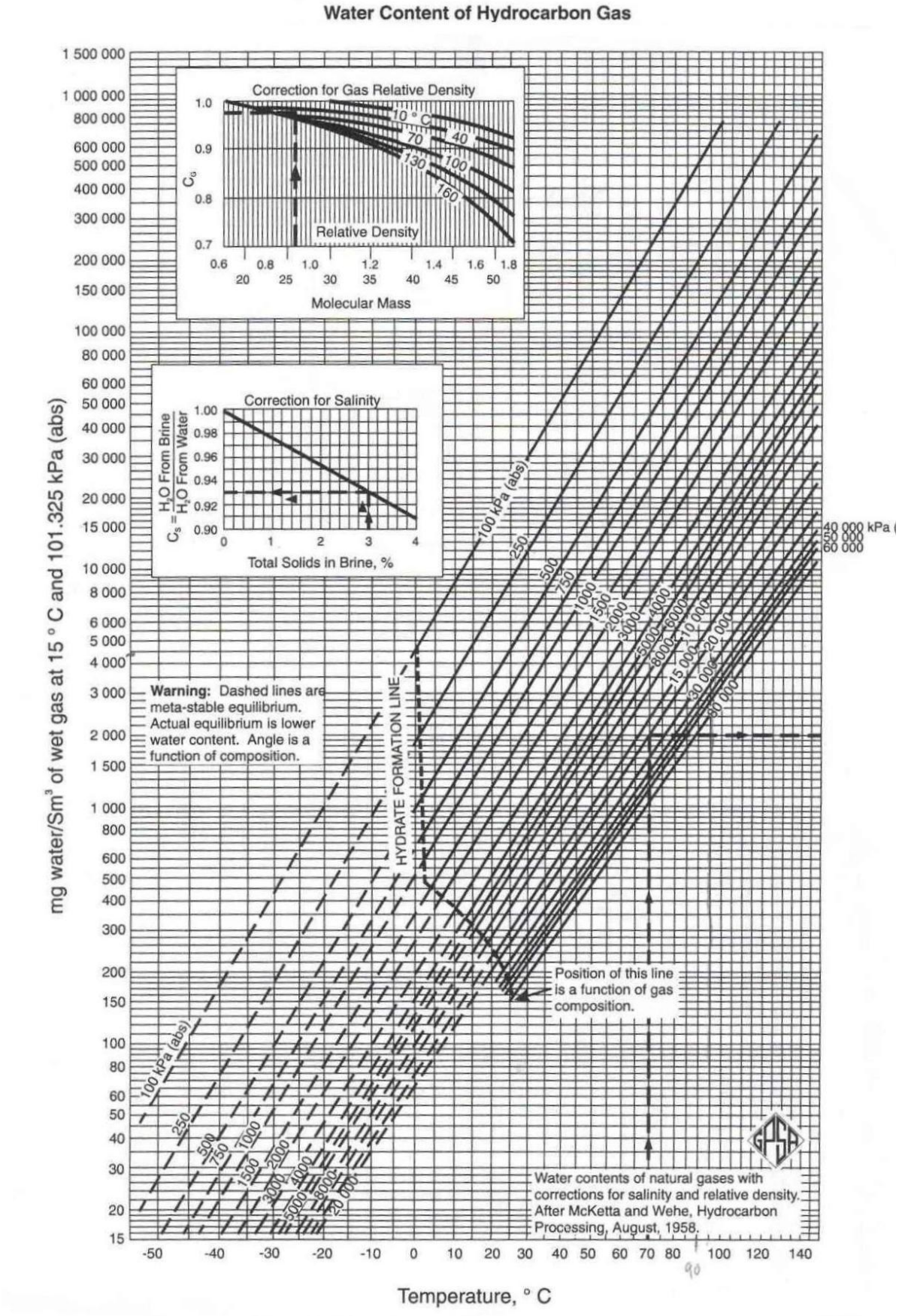

Figure 20: Water Content Chart (Heskestad, 2004)

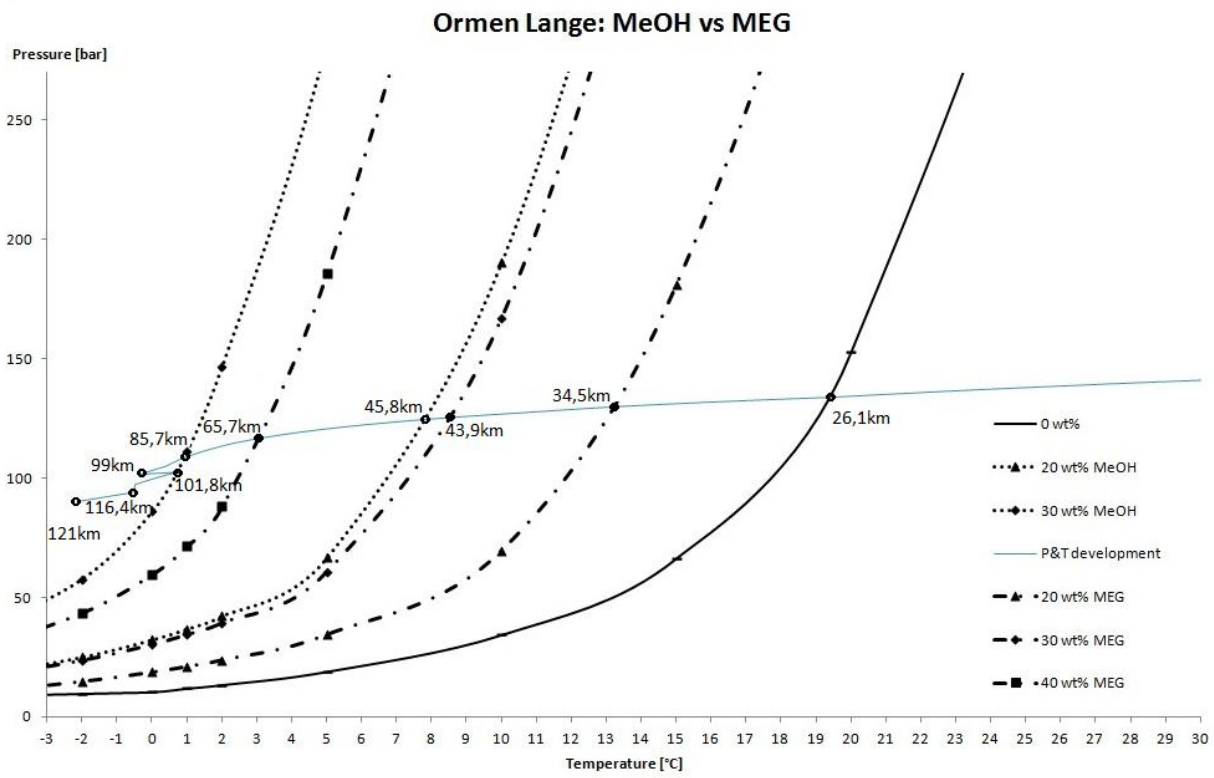

Figure 21: Ormen Lange Normal Operation U=20

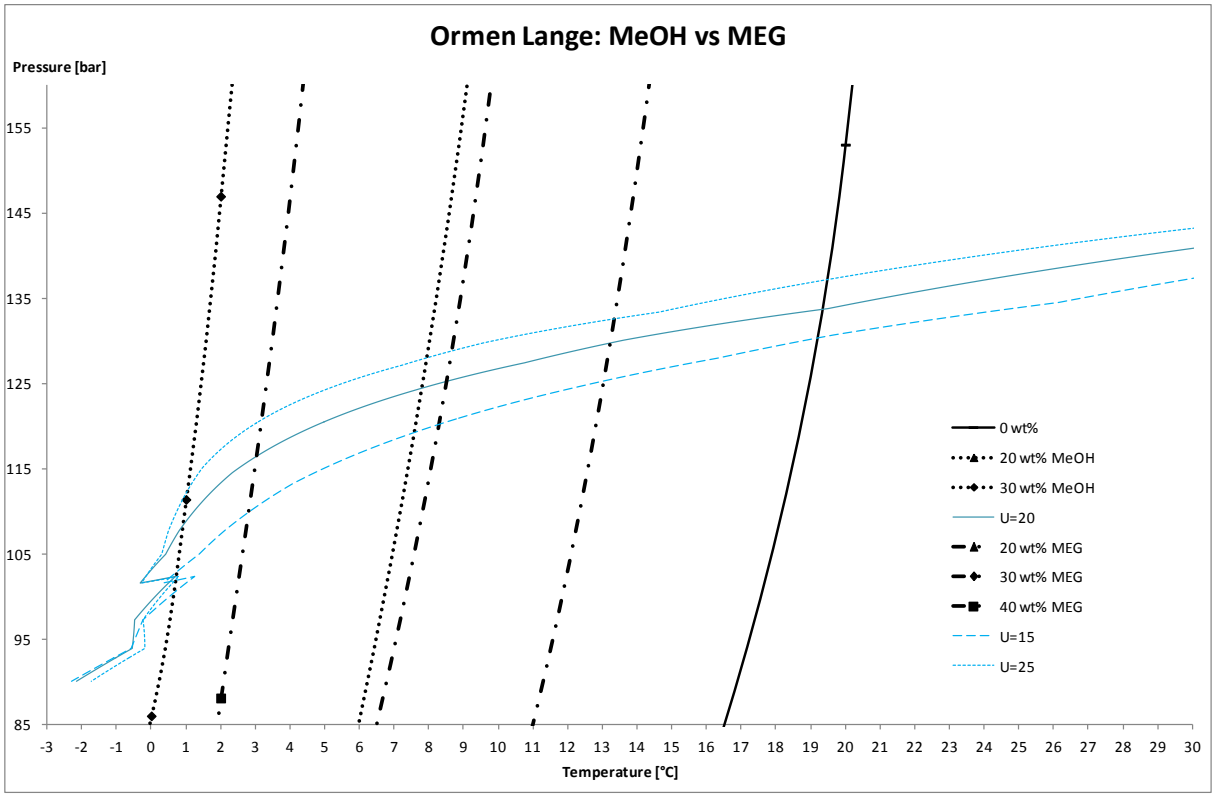

Figure 22: Ormen Lange Case Comparison

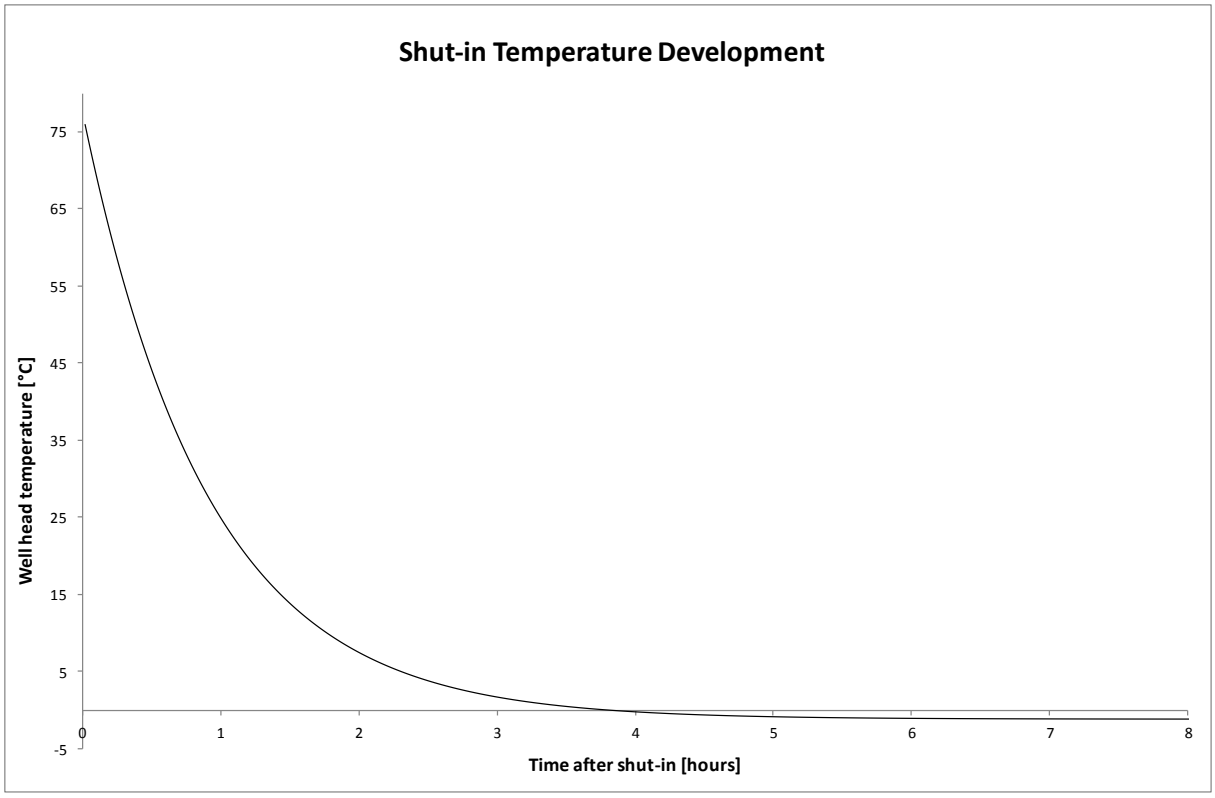

Figure 23: Ormen Lange Shut-in Temperature Development

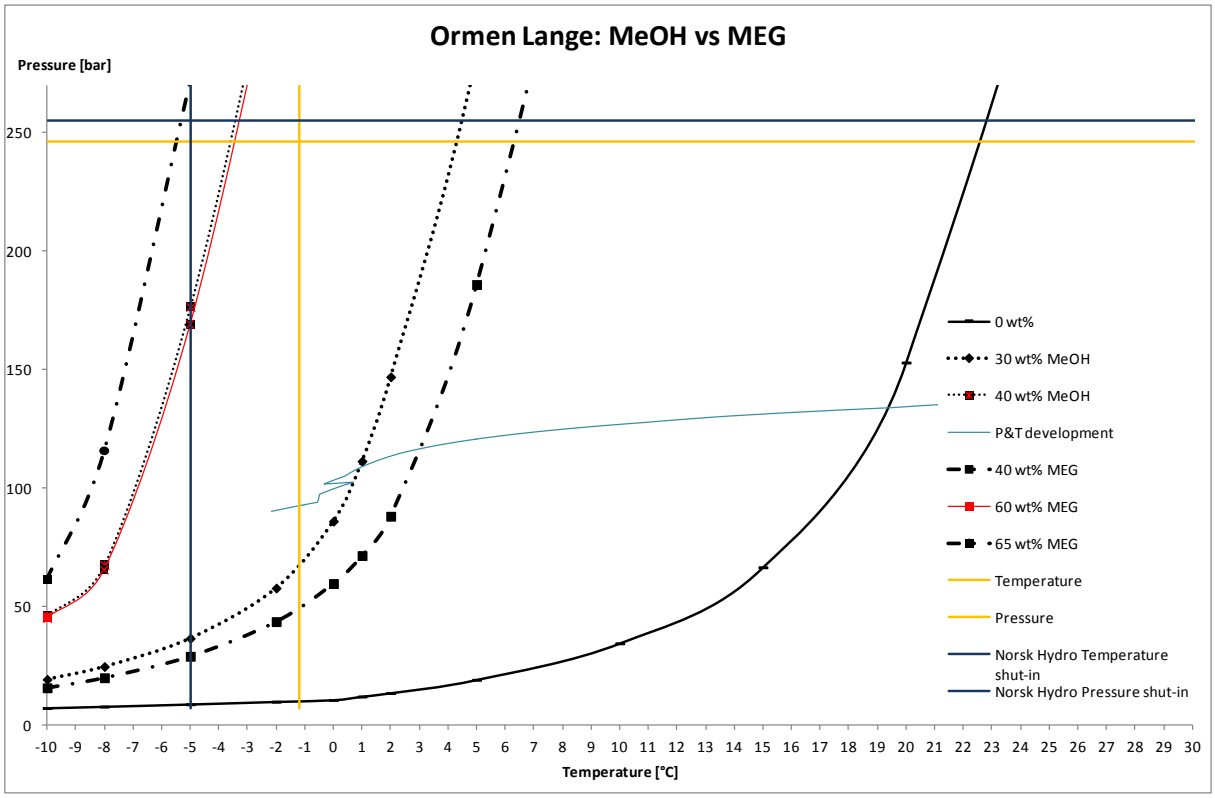

Figure 24: Ormen Lange Extreme Case

Iteration process for finding the well head pressure at shut-in conditions:

1. Read the molecular weight and the vapor phase z-factor at reservoir conditions from the HYSYS-model, and enter them in the excel sheet, n=1.
2. Adjust the downstream pressure in excel so that the upstream pressure equals the reservoir pressure.
3. Adjust the choke in the HYSYS-model to get the new pressure. Read and enter new values for molecular weight and z-factor.
4. Repeat step 2 and step 3 until the upstream pressure remains the same, use two decimals.
5. Copy downstream values from excel sheet n to sheet n+1. N=n+1.
6. Set upstream pressure equal to downstream pressure in the last sheet.
7. Adjust the HYSYS-model for well n, and read the molecular weight and the vapor phase z-factor downstream the well, and enter them in the excel sheet
8. Adjust the downstream pressure so that the upstream pressure equals the bottom segment's pressure.
9. Repeat step 7 and step 8 until the upstream pressure remains the same, use two decimals.
10. Repeat step 5-9 until N=4, them jump to step 11.
11. Use the same procedure for as 5-9, but now the molecular weight and z-factor has to be calculated with the z-factor excel sheet (all the gas have turned into liquid in HYSYS). The downstream pressure is the correct well head pressure.

Figure 25: Iteration Process for Finding the Well Head Pressure At Shut-in Conditions

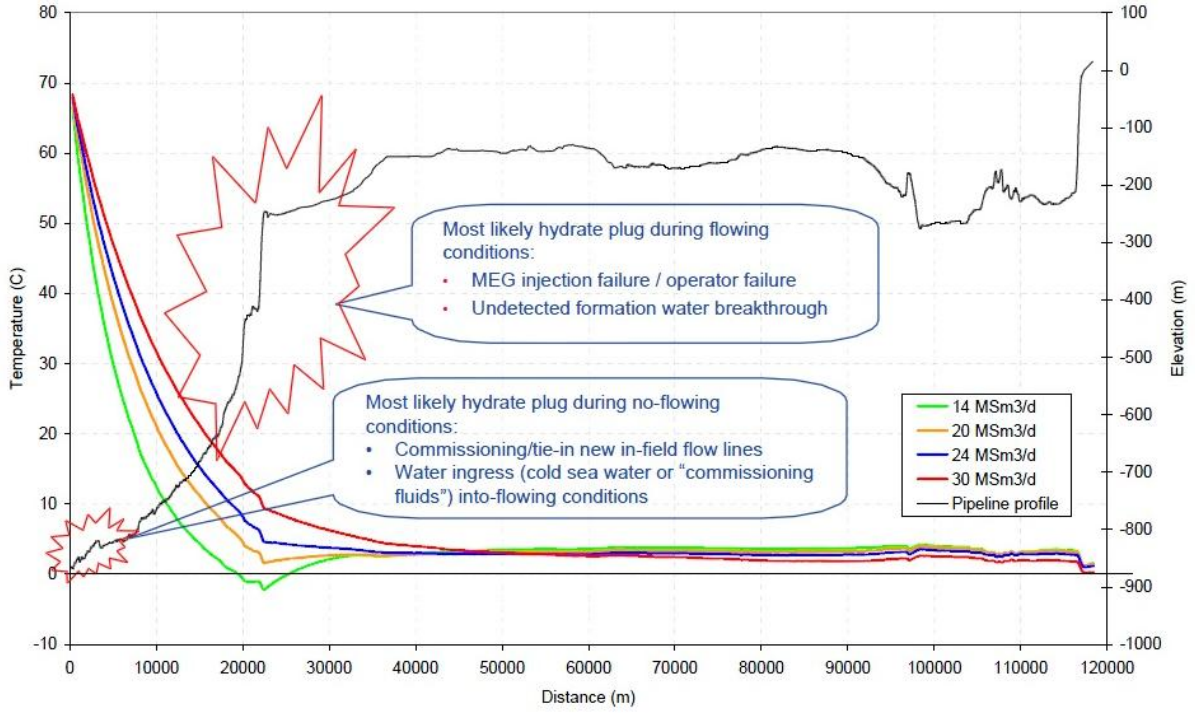

Figure 26: Most Likely Hydrate Formation Locations

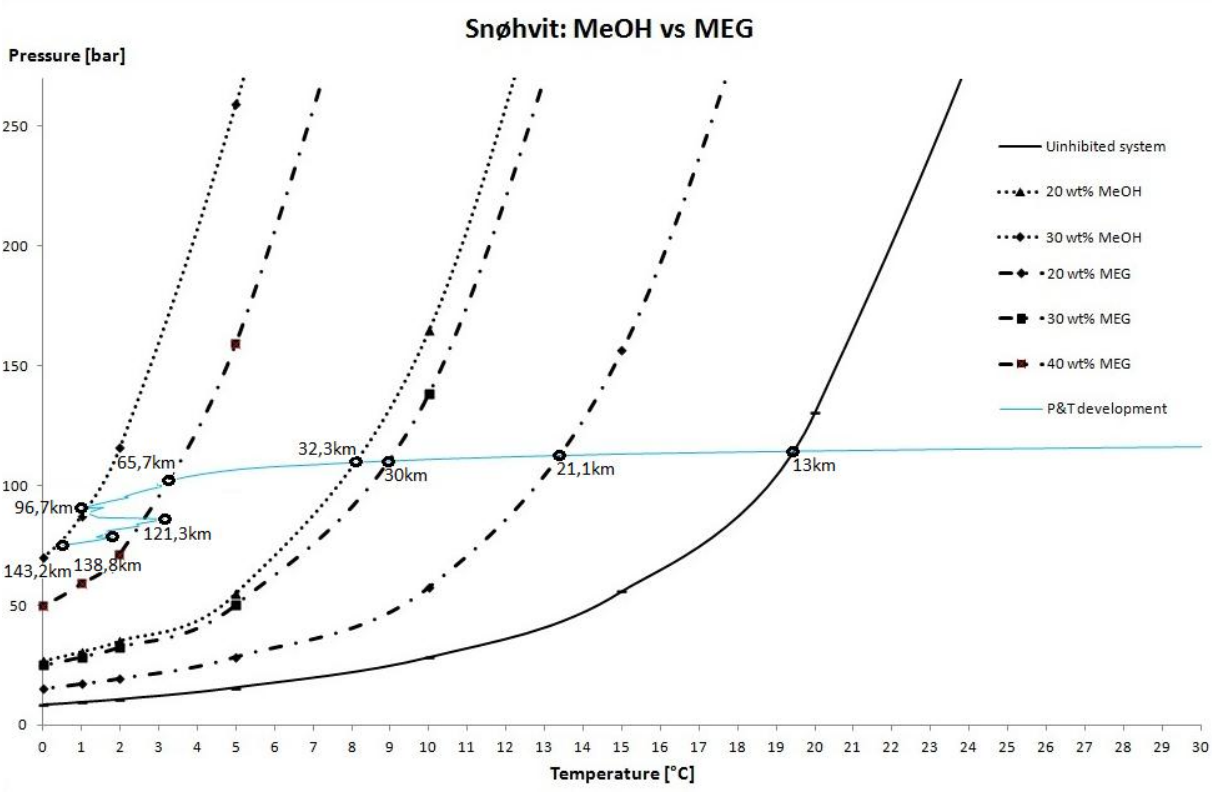

Figure 27: Snøhvit Normal Operation

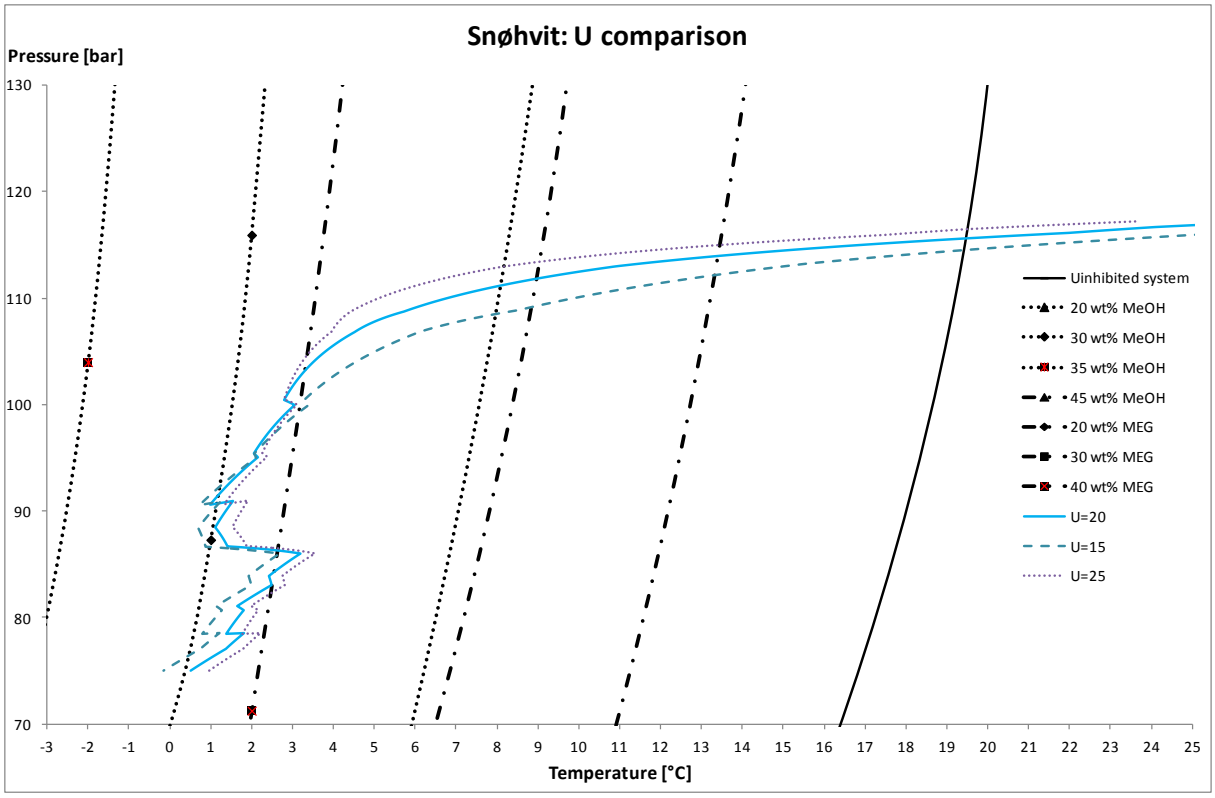

Figure 28: Snøhvit Case Comparison

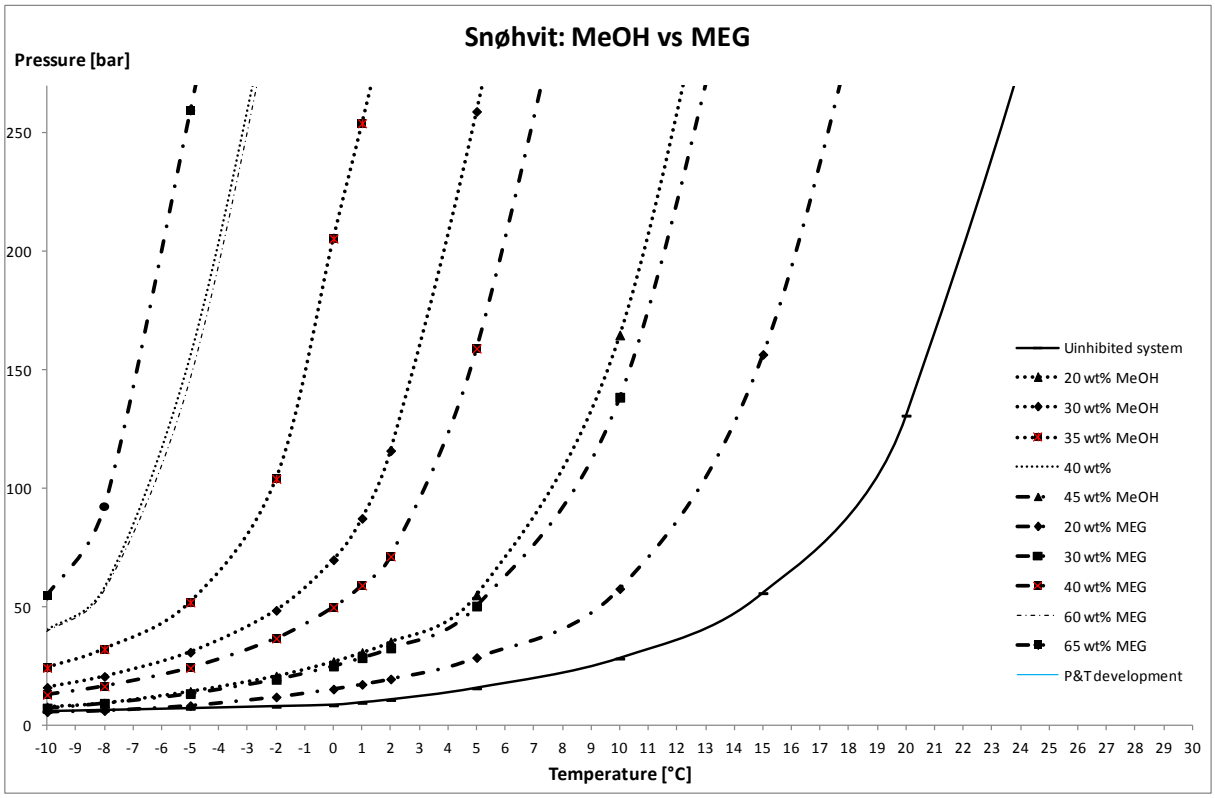

Figure 29: Snøhvit Hydrate Curves

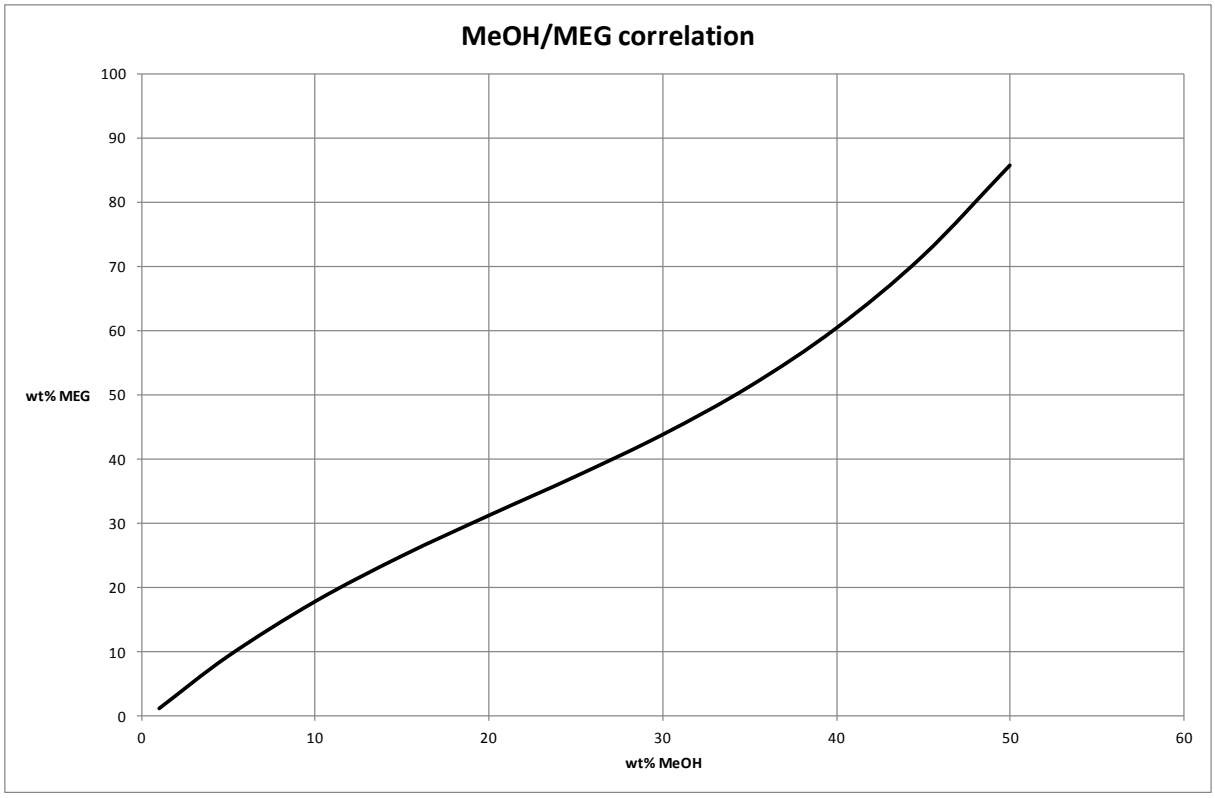

Figure 30: MeOH/MEG Correlation

16 Equations

$$P_{wf} = P_R - q - 1.11q^2$$

Equation 1: Inflow pressure equation

$$\text{wt\% MEG} = -1.209 + 2.34(\text{wt\% MeOH}) - 0.052(\text{wt\% MeOH})^2 + 0.0008(\text{wt\% MeoH})^3$$

Equation 2

MeOH: $$\mathrm{K}^{V}_{MeOH} = \exp\left[5.706 - 5738 \times \left\{\mathrm{T}(^{\circ}\mathrm{R})\right\}^{-1}\right]$$

Equation 3

MeOH: $$\mathrm{K}^{L}_{MeOH} = \exp\left[5.90 - 5404.5 \times \left\{\mathrm{T}(^{\circ}\mathrm{R})\right\}^{-1}\right]$$

Equation 4

MEG: $$\mathrm{K}^{L}_{MEG} = \exp\left[4.20 - 7266.4 \times \left\{\mathrm{T}(^{\circ}\mathrm{R})\right\}^{-1}\right]$$

Equation 5

$$T_2 = T_u + (T_1 - T_u)\exp\left(\frac{-4U\Delta t}{\rho C_p d}\right)$$

Equation 6: Shut-in Temperature Equation (Gudmundsson, 2011)

$$p_2^2 = p_1^2 \exp(-2ag\sin\alpha L) - \left(\frac{b}{a^2 g \sin\alpha}\right)\left[1 - \exp(2ag\sin\alpha L)\right]$$

Equation 7: Gas Well Pressure Equation

$$b = \frac{fm^2}{2A^2 d}$$

Equation 8: Gas Well Pressure Equation (well properties)

$$a = \frac{M}{zRT}$$

Equation 9: Gas Well Pressure Equation (gas properties)

$$P = \frac{q\Delta P}{\eta}$$

Equation 10: Pump Effect Equation